UNIVERSITY OF PARMA

Department of Genetics, Biology of Microorganisms, Anthropology, Evolution

Ph.D. in Biotechnologies
XXIV COURSE

Unraveling Mitochondrial Biogenesis in *Saccharomyces cerevisiae*: Genomics, Genetics and Biochemical Approaches

Coordinator of the Ph.D. Program:
Prof. Nelson Marmiroli

Mentor:
Prof. Claudia Donnini

Tutor:
Prof. Iliana Ferrero Fortunati

Ph.D. student:
Marco Tigano

To me and Bd.

“The most beautiful experience we can have is the mysterious-the fundamental emotion which stands at the cradle of true art and true science”

- A. Einstein -

“It is important that students bring a certain ragamuffin, barefoot irreverence to their studies; they are not here to worship what is known, but to question it.”

- J. Bronowski -

Table of Contents

Chapter 3: *Functional Characterization of YIR024C Gene Product, a Hypothetical Adrenodoxin Reductase Physical Interactor*

Preface: Aim of the Research

Mitochondria, besides their well-known role of “powerhouses” of the cell, is a central organelle in many others cellular processes as aging and apoptosis. An extensive interplay occurs between nuclear and mitochondrial genome, and allows cells to integrate mitochondrial metabolism in the cellular network. All the processes that concur to proper mitochondrial functionality and integration are collectively known as “mitochondrial biogenesis”. The yeast *S. cerevisiae* has been one of the most used model organism for mitochondrial research and many approaches have been used to identify nuclear genes involved in mitochondrial metabolism and in the last few years genome-scale approaches became very popular. However, the yeast mitochondrial proteome is still not totally covered.

In *Chapter 1* of this dissertation is described a genome-wide screening focused on identification of nuclear genes involved in mitochondrial biogenesis, performed at University of Parma, Department of Genetics in collaboration with Department of Biochemistry and Molecular Biology. Knowing that certain genes express mitochondrial phenotypes only in stressful conditions we carried out a genome-wide screening at 37˚C postulating that previous published results, obtained in experiments at 30˚C, could have underestimated the number of nuclear genes involved in such processes. Using complete ethanol media and analysing growth at 37˚C and 30˚C we identified 488 genes whose deletion led to a defect.

Through data mining and experimental confirmation we generated a list of 177 nuclear genes that were previously not linked to mitochondrial biogenesis or with a mitochondrial role still poorly understood. For the majority of those the mitochondrial phenotype was expressed only at 37˚C. Furthermore we gave a first characterization of the OXPHOS defect analysing cytochromes content and oxygen consumption, creating 4 phenotypical classes to depict the different impairments observed.

Interestingly several histone modifiers, transcriptional factor and cellular pathways were specifically enriched in our dataset at 37˚. Cytoplasmic tRNAs chemical modification, N-terminal protein acetylation and alkaline pH sensing were among the pathways identified. A functional importance of such processes in mitochondrial biogenesis under stress is for the first time discussed.

In *Chapter 2* particular attention has been given to one of the pathways identified in the described screening. Indeed enrichment in the pathway of chemical modification in

wobble bases of cytoplasmic tRNAs was very interesting since a relation between this process and mitochondrial biogenesis was never shown. We explored the possibility that tRNAs modified in this pathway could be essential for mitochondrial protein synthesis at 37˚C studying in particular the effects of three deletions in genes representative of the three different steps of the pathway. We were able to demonstrate clearly that under stress the mitochondrial protein synthesis is regulated by cytoplasmic tRNAs chemical modification, although the molecular mechanisms underlying are still uncertain.

In *Chapter 3* is described a single gene analysis carried out under the supervision of Prof. Antoni Barrientos at University of Miami Miller School of Medicine (Department of Neurology). We characterized functionally *YIR024C*, identified in the aforementioned screening as gene whose deletion caused OXPHOS defects at 37˚C. It codes for a mitochondrial protein of unknown function, a hypothetical interactor of Adrenodoxin Reductase (Arh1p).

Through extensive biochemical characterization a *yir024c* null mutant was found to have several mitochondrial respiratory chain defects. Mitochondrial encoded subunits of complex IV (Cox1p, Cox2p and Cox3p) and Cyt *b* were markedly decreased at 37˚C, along with corresponding enzymatic activities. Also mitochondrial heme profile showed impairments in the same conditions.

We obtained a strain expressing an epitope-tagged version of the protein, used to determine the mitochondrial localization, topology and the native size. These analyses confirmed that Yir024c is a mitochondrial protein, integral to the inner membrane and exposing a globular domain of 152 amino acids in the inter membrane space. The protein revealed a native size of about 250Kda, indicating that it resides in a complex. We failed in confirming the predicted physical interaction with Arh1p as this protein was not part of the same complex of Yir024cp and was not found to co-precipitate in affinity purification studies. To identify Yir024cp functional partners the 250Kda complex was purified and mass spectrometry analyses are in progress.

Chapter 1:

Genome-wide Screening Focused on Mitochondrial Biogenesis Under Stress Condition

1.1 Introduction

1.1.1 Mitochondria

1.1.2 Mitochondrial biogenesis: an overview

1.1.3 High-Throughput Approaches to Study Mitochondrial Biogenesis in S. cerevisiae

1.2 Results and Discussion

1.2.1 A Genome Wide Screening Focused on Mitochondrial Biogenesis Identifies 488 Strains

1.2.2 Data Filtering Allows Selection of 177 Genes

1.2.3 Functional Characterization of 177 Candidates

1.2.4 Gene Ontology Analysis and Comments about Identified Functions

1.3 References

1.1 Introduction

1.1.1 Mitochondria

Mitochondria are essential eukaryotic organelles evolved through an ancestral endosymbiotic event (Margulis 1975; Margulis *et al.* 1985). The most addressed mitochondrial role is to be “the powerhouse” of the cell being pivotal sites of fatty acids metabolism, tri-carboxylic cycle (TCA, Krebs Cycle) and oxidative phosphorylation. Nevertheless mitochondria play recognized roles in many other essential cellular processes such as calcium homeostasis, apoptosis, ageing and are major production sites of oxygen reactive species (ROS). With their metabolic capabilities mitochondria take part also in Fe/S cluster assembly, heme biosynthesis, metabolism of amino acids and nucleotides. These organelles are integrated in the cellular network in a very complex fashion and many aspects of this relationship are still partially unknown. Furthermore malfunction in mitochondria have been extensively associated with numerous neurodegenerative disorders in *Homo* sapiens (Wallace 2001; DiMauro *et al.* 2003; Diaz *et al.* 2008; Duffy *et al.* 2011) and many other pathological conditions (Kamp *et al.* 2011). Indeed mitochondrial malfunctions with consequent energy failure target moreover tissues where energy demand is high, such as brain, nervous tissue and muscles.

Mitochondria are elliptic organelles with a variable diameter of 0.2-1μm and length of 3-4μm. From structural point of view are quite complex organelles, with a double system of lipid membranes (outer and inner) that creates two distinct compartments: the soluble core matrix and the inter-membrane space (IMS). The outer membrane is lipid rich and contains high number of β-barrel proteins forming pore complexes that regulates permeability in a size-dependent manner. Outer membrane is also the site were nuclear encoded mitochondrial proteins are recognized and imported in mitochondria.

The inner membrane is much more complex and contains the highest protein content among the biological membranes (Herrmann 2011). It is folded in the matrix in several invaginations (*cristae*) that allow the extension of inner membrane length, site of all respiratory complexes used in the oxidative phosphorylation and ATP synthesis. Each *crista* is connected to external portions of the inner membrane, the “inner membrane boundaries”. The junctions between *cristae* and boundaries are called “contact sites”, dynamic protein rich structures with crucial role in the mitochondrial inner organization (Harner *et al.* 2011; Hoppins *et al.* 2011; Alkhaja *et al.* 2012). The IM boundaries, being

close to the outer membrane, are site of metabolite transporters and protein import and insertion systems for the matrix and the inner membrane.

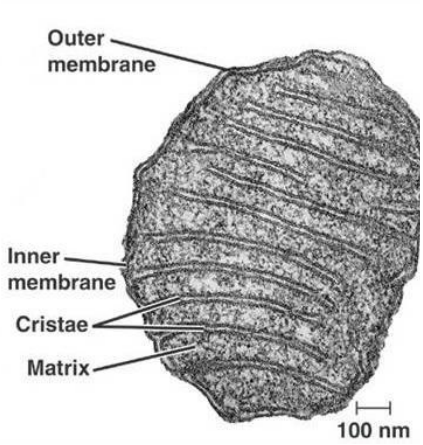

FIG 1.1: Mitochondria ultrastructure (electronic microscopy). Copyright Pearson Education Inc.

Mitochondria are not single cytoplasmic units but highly dynamic organelles heavily interconnected and forming a reticulum. This structure is continuously regulated in response to cellular environment in a complex process known as "mitochondrial dynamic" with distinct and coordinated processes of fusion and fission (Dimmer 2002; McBride *et al.* 2006).

As pointed out before mitochondria are principal site of energy production. Principal energy sources for the cells are sugars and fatty acids. Sugars are catabolized through glycolysis, which occurs in cytosol, allowing production of 2 ATP, 2 NADH and 2 pyruvate molecules for each glucose molecule processed. In anaerobiosis pyruvate is converted to lactate during lactic fermentation or, in yeasts, also to ethanol in alcoholic fermentation. These processes, which again occur in the cytosol, recycle NADH back to NAD+ to allow glycolysis to continue. In presence of oxygen pyruvate can be totally oxidized with higher net ATP production in a process called cellular respiration.

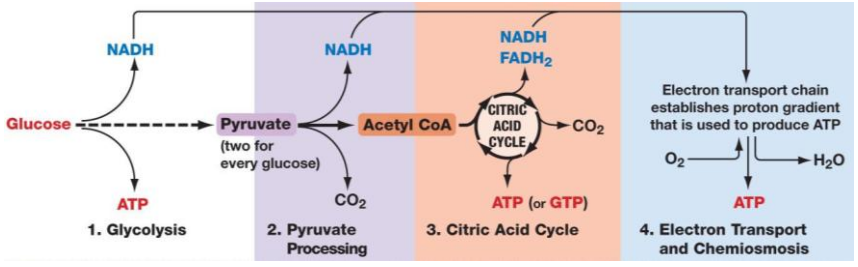

FIG 1.2: General overview of cellular respiration. Reducing equivalents produced in glycolysis, pyruvate processing and Krebs cycle are used in mitochondria during oxidative phosphorylation. Copyright Pearson Education Inc.

Pyruvate is imported in mitochondria and converted by pyruvate dehydrogenase in acetyl-CoA that is in turn shuttled in Krebs cycle. Also fatty acids are totally converted in mitochondria in acetyl-CoA units in a process known as β-oxidation. In *S. cerevisiae* (and in yeast in general) this process takes place in peroxisomes producing acetyl-CoA units later imported in mitochondria through an acetyl-carnitine carrier.

Krebs cycle (tri-carboxylic acids cycle, TCA cycle), a set of eight reactions occurring in the mitochondrial matrix, converts acetyl-CoA in CO_2 with production of reductive equivalents in form of NADH and $FADH_2$. Stoichiometrically 1 molecule of acetyl-CoA is converted in 2 CO_2 with production of 3 NADH, 1 $FADH_2$ and an additional high energy GTP molecule. The final product of the cycle, oxaloacetate, is used in the first reaction, a condensation with acetyl-CoA catalyzed by citrate synthase. Krebs cycle is also a pivotal amphibolic pathway; indeed intermediates such as α-ketoglutarate and oxaloacetate are common precursors for biosynthesis of aminoacids, nucleotides and other molecules. All the enzymes of Krebs cycle are soluble proteins of mitochondrial matrix with the only exception of succinate dehydrogenase, which is anchored to inner membrane *via* two integral membrane subunits (Sdh3p and Sdh4p in yeast) while the catalytic core (Sdh1p and Sdh2p in yeast) is facing the matrix. This enzyme represents a physical connection between Krebs cycle and oxidative phosphorylation. Indeed SDH complex is also the second respiratory complex (complex II) of mitochondrial respiratory chain (MRC).

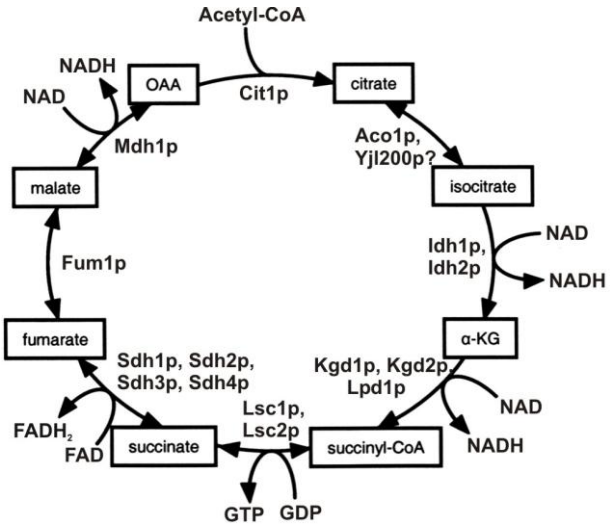

FIG 1.3: Eight steps of Krebs cycle (TCA cycle).

MRC is the latest metabolic step that uses the reductive equivalents produced in the other metabolic pathways to generate an electron flow along the mitochondrial inner membrane. This flow is used to reduce oxygen in H_2O and is coupled to proton pumping from matrix to IMS generating an electrochemical gradient across the inner membrane.

Four enzymatic complexes across the inner membrane compose MRC and use different electron transport centers that are cyclically reduced and oxidized: Fe/S clusters, heme centers, heme binding proteins (cytochromes) and the soluble factor coenzyme Q10.

Complex I is the biggest respiratory complex of the chain. It shuttles electrons from NADH to coenzyme Q10 *via* flavin mononucleotide center (FMN) and several Fe/S clusters. The process is coupled to the expulsion of $4H^+$ in the IMS. *S. cerevisiae* is one of the few eukaryotes lacking complex I even if the same reaction is performed by NADH dehydrogenase (Nde1p/Nde2p and Ndi1) without proton pumping.

Complex II is the aforementioned Krebs cycle enzyme that couples oxidation of succinate to fumarate with the reduction of coenzyme Q10. The same complex can also oxidize $FADH_2$ and shuttle the electrons in the respiratory chain. Two catalytic subunits (Sdh1p and Sdh2p in yeast) transfer electrons from succinate to a flavin adenine dinucleotide cofactor (FAD) and sequentially to three Fe/S cluster before reducing a covalently bound heme b moiety found in the membrane domain of the complex (Sdh3p and Sdh4p in yeast). Electrons are finally flow to coenzyme Q10. No proton pumping is associated to this respiratory complex.

Complex III (cytochrome bc_1 complex) is an integral membrane complex that faces both mitochondrial matrix and IMS. Electrons flow from reduced Q10 to cytochrome *b,* an embedded protein with a covalently bound heme b moiety. This in turn shuttles the electrons to a Fe/S protein (Rieske protein) and eventually to cytochrome c_1 on the IMS side. The process is completed with the oxidation of cytochrome c_1 and reduction of soluble IMS protein cytochrome *c.* Complex III couples the electron flow to pumping of two protons.

Complex IV is the last respiratory complex and is deputed to the oxidation of soluble cytochrome *c* and final reduction of oxygen to H_2O concomitantly to expulsion of four H^+. The complex COX structure contains two cytochromes (*a* and a_3) and copper centers for electron transport.

A last non-respiratory complex is involved in energy production in mitochondria: ATPase or complex V. This enzymatic complex dissipates the electrochemical proton gradient produced across inner membrane to synthetize ATP starting from ADP and inorganic phosphate. It is formed by two discrete units: F_0 and F_1. The first consists of a proton

channel in the inner membrane where $3H^+$ flow back inside the matrix. The second unit (F_1) is connected to the first one generating a rotary motor that perform a 120° rotation every imported proton. With a rotational catalysis mechanism ADP and P_i are bound together with ATP release. Produced ATP that is needed in the cytosol is exported *via* ATP/ADP carrier that concomitantly imports ADP in the matrix to be recycled.

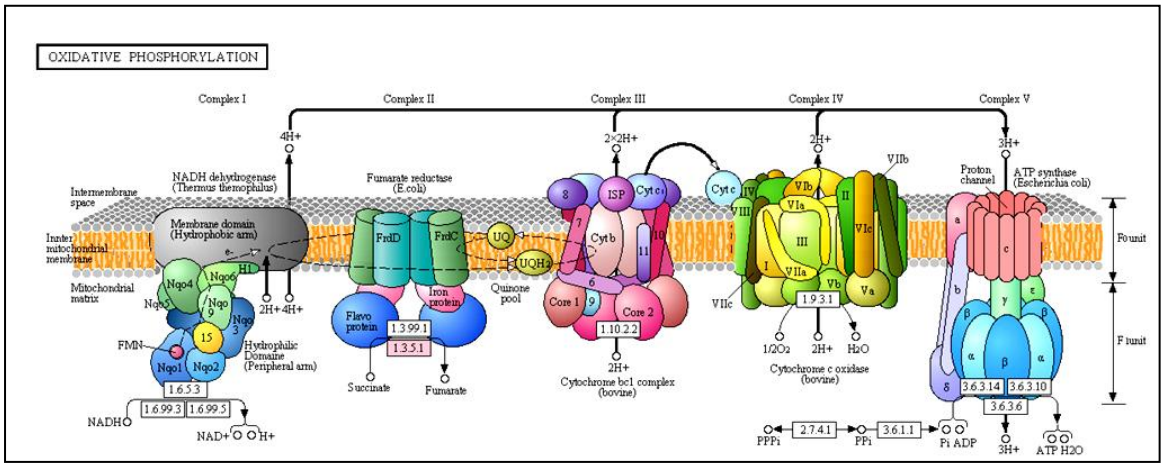

FIG 1.4: MRC complexes across the inner membrane. Image taken from KEGG pathways database. Yeast *S. cerevisiae* lacks complex I.

S. cerevisiae is a facultative aerobe/anaerobe that harbors some peculiarities from metabolic point of view. Metabolic life is regulated in accordance to oxygen availability and carbon source provided. Indeed when glucose is provided in aerobic environment and respiratory metabolism would be the most convenient, *S. cerevisiae* relies its energy production exclusively on glycolysis and fermentation. When glucose is provided in limiting amounts or in batch cultures when glucose levels are decreasing, respiratory metabolism is de-repressed. Yeast has the capability to use also alternative carbon sources then glucose. Disaccharides like maltose, sucrose and melibiose can be broken in monosaccharides like glucose and fructose, and then normally used. Galactose is an epimer of glucose that is directly phosphorylated by galactokinase and converted to galactose-1-phosphate. This product is in turn converted to glucose-1-phosphate by galactose-1p-urydiltransferase. In this reaction galactose is shuffled with the glucose bound in UDP-glucose with resulting glucose-1-phosphate and UDP-galactose. Glucose-1-phospate is used in normal glycolysis whilst UDP-galactose is converted to UDP-glucose by an epimerase. Galactose has the particularity to be a sugar totally processed in glycolysis without any glucose-repressing effects on mitochondrial function.

Yeast can also use other carbon sources that are not fermentable (oxidative) like glycerol, ethanol, acetate and lactate. All these metabolites require a proper mitochondrial functionality to be used as sole carbon sources and are commonly used in mitochondria-related research to highlight mitochondrial dysfunctions.

The use of yeast like *S. cerevisiae* in this research field comes from the ability to survive with respiratory deficient mitochondria if a fermentable carbon source is available, showing a growth defect only in presence of respiratory carbon sources. Impairments in each of the processes that directly or indirectly affect mitochondrial metabolic function (collectively called “mitochondrial biogenesis”) will therefore be highlighted in presence of oxidative carbon sources, but not in presence of fermentable ones. However some mitochondrial functions are essential for life regardless of the carbon source, such as Fe/S cluster biosynthesis. This exceptional ability, unique among eukaryotes and restricted to only some yeast genus (Bulder 1964), made *S. cerevisiae* one of the most used model organisms in mitochondrial research.

1.1.2 Mitochondrial Biogenesis: an Overview

Mitochondrial biogenesis is a complex event that comprises a great variety of different cellular processes. Every single aspect of cellular life that can influence and regulate mitochondrial function can be mentioned in “mitochondrial biogenesis processes”. These events can be directly or indirectly connected to mitochondria. For instance every process that takes place in mitochondria, played by the members of mitochondrial proteome, is concurring directly to a correct functionality of the organelle. Processes physically residing in mitochondria can range from respiratory functions, assembly of protein complexes, organization of mitochondrial ultrastructure or mitochondrial DNA expression and maintenance. On the other hand to ensure a correct mitochondrial biogenesis is necessary to integrate mitochondria in the cellular network and to regulate mitochondria function in response to environment and external stimuli, process that requires also other cellular compartments. Thus giving a proper definition of “mitochondrial biogenesis” is quite challenging.

Mitochondria possess the peculiarity of having a mitochondrial genome (mtDNA) with a size of 68Kb (in *short strains*) or 86Kb (in *long strains*). This genome is the product of more than a billion years of evolution in which an original independent genome (after the endosymbiosis event) was extensively reduced in a mechanism known as Müller ratchet (Muller H. J. 1964). This size reducing was coupled with either loss or transfer of genes to the nuclear DNA. The coding capacities of mitochondrial genome are thus limited to seven essential protein components of mitochondrial respiratory complexes (Cox1p, Cox2p, Cox3p, Cyt *b*, Atp6, Atp8 and Atp9) and a protein of the small subunit of mitochondrial ribosome, Var1p. *S. cerevisiae* mtDNA also encodes for a complete set of 24 tRNAs and 2 rRNAs. Up to 13 introns are present in 3 genes (*COX1, COB* and 21sRNA) and different intronic ORFs have been characterized. These ORFs code for maturases that assist splicing, endonucleases, reverse transcriptases and additional unknown/putative proteins (Foury *et al.* 1998).

Although the coding potential is limited compared to the total mitochondrial proteome, these mtDNA encoded proteins are essential in mitochondrial biogenesis. Furthermore mitochondria need active processes of packaging, replication, transcription and translation essential for proper mitochondrial DNA expression. All the proteins necessary for these processes are nuclear encoded and thus participate to mitochondrial biogenesis. For instance more then 22 proteins were found to be part of the nucleoids, dynamic nucleo-protein structures anchored to inner membrane organizing more then 10 mtDNA molecules each (Chen *et al.* 2005; Kucej *et al.* 2008). Other 77 proteins (76

nuclear encoded) are part of the mito-ribosomes with additional initiation, elongation and termination factors (Mieszczak *et al.* 1988). Very interesting is to consider how expensive is to maintain such systems active. For a total 8 essential proteins, more then 200 nuclear encoded proteins are produced and imported in mitochondria only to allow a correct DNA metabolism and expression (Contamine *et al.* 2000; Lipinski *et al.* 2010). Many other proteins are used also to regulate the expression of these proteins, mainly residing on post-transcriptional events. For instance Cox1p, Cox2p and Cox3p translation is tightly regulated by assembly state of COX complex, environmental conditions such as oxygen availability or mitochondrial functionality (Soto *et al.* 2009; Soto *et al.* 2011). Just to mention, up to date six nuclear encoded translational activators are known to directly drive translation of *COX1* (Pet309p and Mss51p)*, COX2* (Pet111p) and *COX3* (Pet54p, Pet122p and Pet494p) mRNAs and a total of 25 different nuclear encoded proteins are known to work as trans-activating factors during mitochondrial genome translation.

Mitochondrial proteome is believed to count about 1000 (yeast) to 1500 (human) distinct members (Sickmann *et al.* 2003; Perocchi *et al.* 2006; Pagliarini *et al.* 2008). Being only 8 essential proteins encoded in mitochondrial DNA appears clear that one of the most important processes directly involved in mitochondrial biogenesis is the import of cytoplasmic translated proteins into mitochondria and their subsequent sorting to the correct site. Yeast evolved a complex machinery to recognize, process, import and sort proteins destined to mitochondria.

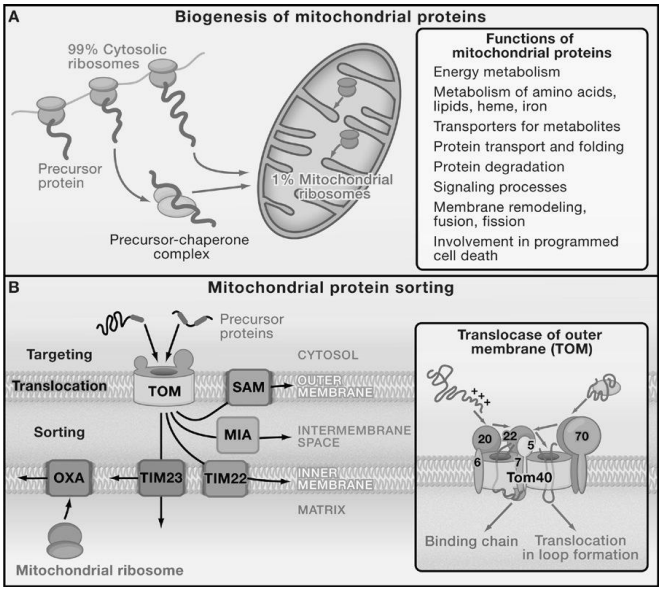

Fig 1.5: Mitochondrial protein biogenesis and (B) mitochondrial machinery for protein import. Image taken from Chacinska *et al.* 2009.

Firstly an outer membrane holocomplex representing a general entry gate recognizes cytosolic synthetized proteins that have to be imported. This complex, named TOM (Translocase Outer Membrane), forms a channel in the outer membrane, composed by the β-barrel protein Tom40p and other structural components (Tom5p, Tom6p and Tom7p). Associated receptors (Tom20p, Tom22p and Tom70p) are responsible of protein recognition and import. From here the fate of each protein depends on the mitochondrial sub-localization (Diaz *et al.* 2008; Chacinska *et al.* 2009). Matrix proteins are imported through a translocase of the inner membrane complex, TIM23, built of a structural and a motor component. In an ATP-dependent manner this complex import proteins from IMS to the matrix where they will be finally processed and folded. Common inner membrane proteins are imported in the matrix through TOM-TIM23 complexes and then inserted by Oxa1p, a mitochondrial matrix protein. Proteins with only one membrane helix are instead inserted laterally in the membrane directly by TIM23. Finally proteins with high hydrophobicity or even number of transmembrane helices are directly blocked in the IMS, recognized by small TIM proteins (Tim9p, Tim10p and Tim12p) and transferred to a different translocase of the inner membrane, the TIM22 complex, to be finally inserted. Outer membrane proteins usually contain a β-barrel domain and are imported through the classical TOM complex. Once in the IMS a set of small Tim proteins recognizes the polypeptide and drives it to an addition outer membrane translocase complex, called TOB/SAM. This complex finally mediates the insertion. A final essential component of protein import machinery has been evolved for IMS proteins that share particular disulfide bonds in their structure. The so called “disulfide relay system” based mainly on two essential IMS proteins, Erv1p and Mia40p, recognizes proteins with particular cysteine patterns (for instance twin C-X_9-C motifs) and directly drive an oxidative folding process creating the necessary disulfide bonds (Deponte *et al.* 2009).

Encoding organellar proteins in two different genomes require also a highly coordinated expression between the two compartments that relies on both nuclear-mitochondrial and mitochondrial-nuclear signaling. These pathways are known as anterograde and retrograde regulation and allow concomitantly to maintain mitochondria informed about cellular environment and to send to the nucleus signals about respiratory functions (Liu Z. *et al.* 2006; Woodson *et al.* 2008; Lipinski *et al.* 2010).

An excellent and extensively characterized signaling cascade is the one based on Rtg factors (Liu Z. *et al.* 2006). Rtg1p and Rtg3p are two helix-loop-helix leucine zippers transcriptional factors that form a heterodimer to bind promoter regions. Two positive

regulators (Rtg2p and Grr1p) and four negative regulators (Mks1p, Lst8p, Bmh1p and Bmh2p) create a signaling network that affects nuclear translocation of Rtg1/Rtg3 heterodimer. Many signals contribute to negative or positive Rtg regulation integrating mitochondrial function in the dynamic cellular environment. As yet not complete example Rtg1/Rtg3 is able to induce peroxisomes proliferation, β-oxidation and other anaplerotic pathways upon mitochondrial dysfunction in order to reconfigure cellular metabolic programs and ensure a correct supply of α-ketoglutarate (lacking in TCA defective mitochondria) used in biosynthesis of compounds like glutamate. On the other hand, when glutamate/glutamine levels are high due to mitochondria activity or environmental conditions a negative feedback signal downregulates Rtg1/Rtg3 nuclear translocation.

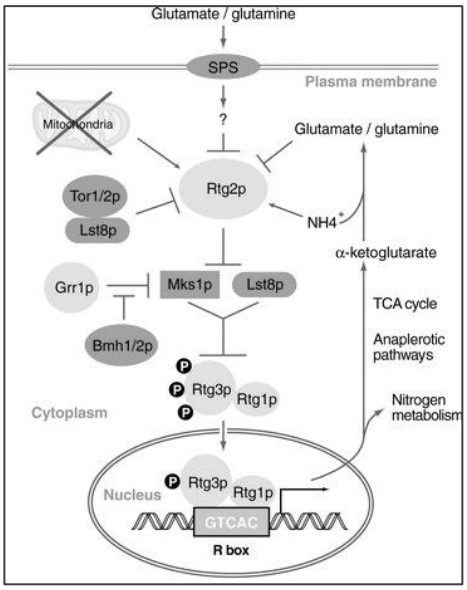

Fig 1.6: Mechanism and signals that Rtg retrograde pathway senses to integrate mitochondria in cellular network. Image taken from Liu and Butow 2006.

Mitochondrial biogenesis can be to this point considered as the sum of all functions that directly participate in generating a functional organelle, allowing expression of its genome, import of nuclear encoded proteins and assembly of all the mitochondrial complexes required for proper functionality. These direct processes are regulated through a coordinated expression of two distinct genomes that can also be target of environmental signals like ones sensed through Rtg pathway. However in the last years a great interest has been given to the highly dynamic behavior of these organelles in the cellular network. Since the first observation that mitochondria are not single units but rather form a complex network (Bereiter-Hahn 1990) three main processes have been characterize that contribute equally to mitochondrial dynamics: fusion, fission and selective degradation (mitophagy). These processes rather than contribute directly to

mitochondrial functions (such as TCA cycle or OXPHOS process) are involved in shape dynamics of mitochondrial network in response to environmental clues and mitochondrial functionality and recently they might mediate relationships between mitochondria and other organelles as ER and peroxisomes.

Two major GTPase complexes are associated with mitochondrial fusion: Fzo1p and Mgm1p complexes. This process allows mitochondria to fuse in a single structure, sharing then all the components and genomes. The GTPase Dnm1p as well as Fis1p and Mdv1p catalyze fission. Although molecular mechanisms of fission and fusion are quite understood, their regulation and biological functions are still poorly characterized. They are believed to control mitochondrial quality, on one hand allowing mitochondrial content mixing during fusion and thereby contribute to integrity and homogeneity. On the other hand fission could be used to isolate damaged mitochondria from the network, targeting them to clearance (Tatsuta *et al.* 2008). Interestingly mitochondrial dynamics and morphology were recently connected to bioenergetics state of mitochondria. Fusion complex Mgm1 is indeed influenced by reduced levels of ATP with consequent mitochondria fragmentation (Herlan *et al.* 2004). The same event was observed in upper eukaryotes, where OPA1 (human ortholog of Mgm1p) proteolysis was stimulated upon membrane potential dissipation with subsequently mitochondrial fragmentation (Duvezin-Caubet *et al.* 2006; Ishihara *et al.* 2006). Mitochondrial dynamics could indeed act as a mitochondrial modulator in order to adequate cellular response to physiological conditions (Westermann 2010).

A third process completes this scenario: the selective degradation of mitochondria. Autophagy is a specialized cellular process involving lysosomal/vacuolar clearance of long-lived proteins and organelles (Bhatia-Kissova *et al.* 2010). This non-selective process can be regulated and directed to specific purposes, like turnover of dysfunctional and damaged mitochondria. Such process is known as “mitophagy”. A key gene of the process was found to be *ATG32*, proposed to act as mitochondrial receptor interacting with the autophagy cascade member coded by *ATG11*. Atg32p thus is required to promote mitophagy recruiting to mitochondria the aspecific autophagy machinery (Kanki *et al.* 2009; Okamoto *et al.* 2009). In the last years became evident how mitophagy is not only a simple turnover mechanism but could be induced specifically in response to cellular environment. In this way cells would strictly regulate the quality and the quantity of mitochondria, eluding an accumulation of unproductive and harmful mitochondria (Kurihara *et al.* 2011). This process has therefore to integrate *stimuli* of different nature from nutrient availability and growth phase to redox imbalance,

ROS production and aging process (Bhatia-Kissova *et al.* 2010). Although molecular mechanisms nowadays are partially known, how this process is regulated and which are the molecular signals and the pathways involved remain unclear. Some indications exist, like role of independent regulators Uth1p and Aup1p and more recently the stress sensor Whi2p. The latter seems to link in yeast the general stress response that is activated reaching the stationary growth phase and the nutrient limitation to the activation of mitophagy and autophagy processes (Muller M. *et al.* 2011).

Concluding, also mitophagy process along with mitochondrial dynamics play an important role in integrating in the cellular environment the mitochondrial network, properly shaping it through fusion, fission and degradation processes. These three events could therefore be interconnected and together indirectly influence the mitochondrial function and thus mitochondrial biogenesis. Crucial importance of these processes is proven by the several pathologies related to impairments in such processes. For instance Parkinson's disease or autosomal optic atrophy type I are indeed severe neurodegenerative disorders associated to dysfunctions in both mitophagy and mitochondrial dynamics respectively (Schafer *et al.* 2009; Narendra *et al.* 2010).

Many experimental approaches can be used to assess and explore new roles and new members of mitochondrial biogenesis. Especially at this status of mitochondrial knowledge, when the scientific community is not so far from completion of mitochondrial proteome, a researcher should adopt a wider perspective when interpreting results and hypotheses, embracing also the "systems biology" point of view. Mitochondrial biogenesis definitely does not reside only in specific functions played by mitochondrial proteome but also on processes apparently unrelated that could act integrating mitochondria in the cellular network, event essential for proper mitochondrial functionality/cellular life.

1.1.3 High-Throughput Approaches to Study Mitochondrial Biogenesis in S. cerevisiae

More then 50 years of research on genetics and molecular biology of S. cerevisiae provided an exceptional set of research tools that can be used to dissect any aspect of cellular life. For sure in the last decades a great amount of data was obtained by high-throughput techniques that allowed analyses of thousands of different mutants, crossed strains or tagged proteins at the same time in any condition of interest. Mitochondria, given its pivotal role in eukaryotes life, made no exception. For sure one of the first high-throughput approach to study mitochondrial biogenesis worth of mentioning was the one described by Tzagoloff A. and Dieckmann C.L. (Tzagoloff *et al.* 1990). Authors divided all the nuclear mutants known by previous studies to harbor defects in mitochondrial function and hundreds of new ones obtained by mutagenesis in more then 200 complementation groups, thus creating a numerous collection. Mutants, identified by defects in oxidative growth, were organized in phenotypical classes on the base of mitochondrial phenotypes, such as defects in mitochondrial encoded cytochromes, in ATPase complex, or in other processes not involving MRC (TCA mutants for instance). For the first time was also precisely defined the term "*pet mutant"*, used to distinguish cytoplasmic petite mutants (harboring cytoplasmically inherited mutations) and mutants in nuclear genes with compromised mitochondrial function. Nowadays this term is still used to identify any nuclear mutant with a carbon-source dependent mitochondrial defect that could be also additionally affected by other environmental factors (as temperature).

Although the aforementioned collection contained several mutants, after the completion of *S. cerevisiae* genome sequencing a new powerful tool was introduced: the "knock-out" mutant collection. Several kinds of knock out collections are now available commercially and consist of thousand of yeast haploid or diploid strains carrying one single deletion in each non essential nuclear gene. Growth analyses using these collections were carried out in several conditions in order to study many different processes. These could range from nuclear DNA repair, virus replication, tolerance to salt and nutrient availability, tolerance to oxidative, heavy-metals, temperature and ethanol stresses (Winzeler *et al.* 1999; Giaever *et al.* 2002; Jazayeri *et al.* 2002; Scherens *et al.* 2004; Panavas *et al.* 2005; Ruotolo *et al.* 2008; Auesukaree *et al.* 2009; Teixeira *et al.* 2009; Yoshikawa *et al.* 2009).

Mitochondrial function was also extensively studied with high-throughput growth analysis of knock-out collections (Dimmer 2002; Steinmetz *et al.* 2002; Luban *et al.* 2005; Hess *et*

al. 2009; Merz *et al.* 2009). Some of these analyses produced extensive data reporting growth defects for hundreds of nuclear *pet* mutants, and are worth of further description.

Dimmer K.S. and colleagues described in 2002 a genome-wide screening performed on 4794 *S. cerevisiae* diploid strains carrying homozygous deletion in non essential genes. A first screening evaluated the growth performances of the entire collection on complete media supplied with oxidative carbon source glycerol at 30˚C. A total of 341 deletions caused a specific growth defect absent in the control condition (rich media with glucose). For the knowledge of that moment, more then half of the identified *pet* genes encoded known mitochondrial proteins. The remaining genes were relative to non-mitochondrial proteins with a total of 58 genes of unknown function. A second screening instead evaluated the mitochondrial morphology and distribution (MDM) looking for *mdm* mutants. If *mdm* mutant never displayed any wild-type mitochondria during analysis was defined as class I mutant and the corresponding gene was considered essential for mitochondrial morphology. A subset of *mdm* mutants was respiratory competent in the first screening and were referred as class II mutants. A last class was created, class III, relative to *mdm* mutants that instead showed also *pet* phenotype (Dimmer 2002).

In 2005 Cornelia Luban and colleagues presented a genome-wide screening focused on splicing metabolism of group II introns in mtDNA. A first screening was performed on complete media with glycerol at 30˚C using a complete knock out collection of 4878 viable haploid *S. cerevisiae* strains. A total of 355 mutants showed a *pet* phenotype on glycerol media. Authors compared results with those described by Dimmer in 2002 and found an overlap of 67.6%. A particular focus was given in nuclear genes possibly involved in splicing metabolism of group II introns of mtDNA. To this purpose in the preselected 355 strains loss of mtDNA was induced, replaced then by a rho^+ genome without group two introns and looking for complementation of foreseen *pet* phenotype. In this case phenotypes of 109 *pet* mutants were complemented by introduction of intronless mtDNA (Luban *et al.* 2005).

Merz S. and Westermann B. performed an interesting and exhaustive genome-wide screening, published in 2009. Analyzing a knock out collection of haploid strains for defects in growth on glycerol media at 30˚C, a total of 319 *pet* mutants were identified. The phenotype observed was checked also on different oxidative carbon sources, to confirm a general OXPHOS impairment rather then glycerol metabolism defects. A complex experimental flowchart (depicted in Figure 1.7) based on mitochondrial DNA maintenance analysis, cytoduction experiments to replenish mutants with fresh undamaged mtDNA, DAPI staining and mitochondrial translation analysis were used to

characterize the origin of *pet* phenotype. This allowed the identification of 88 genes required for mitochondrial translation, 10 genes for expression of specific mitochondrial products and 16 for mtDNA maintenance (Merz *et al.* 2009).

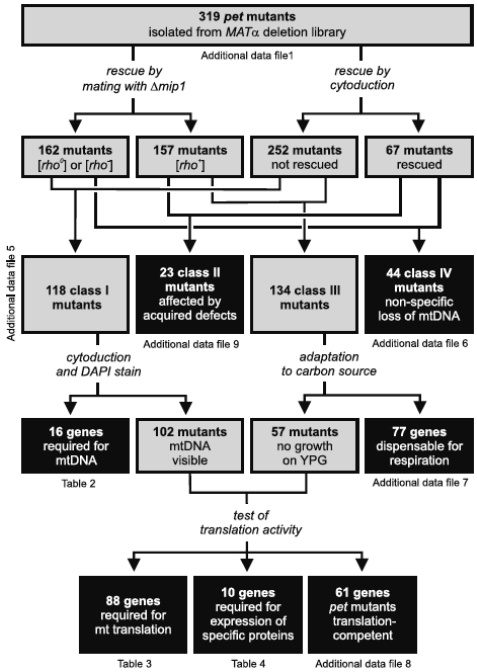

FIG 1.7: Experimental flowchart followed for functional characterization of 319 *pet* mutants identified on complete glycerol media at 30˚C. Image taken from Merz S. and Westermann B. 2009.

A last interesting dataset was produced by Hess D.C. and colleagues in 2009. In this case an algorithm was used to predict nuclear genes involved in mitochondrial biogenesis, rather than a direct phenotypical test on oxidative carbon sources. An ensemble of three different prediction algorithms, namely bioPIXIE, MEFIT and SPELL, was trained with data from numerous sources (expression profiling, sequencing, interactions ect.) and 106 genes curated by *Saccharomyces* Genome Database (Myers *et al.* 2005; Huttenhower *et al.* 2006; Hibbs *et al.* 2007; Myers *et al.* 2007). This ensemble ranked all genes from most likely to be involved in mitochondrial biogenesis to least likely. From the first round prediction 183 most confident genes were selected and in only 42 a relationship with mitochondrial function was already known. Prediction was then confirmed on experimental basis assaying *petite* mutants frequency, oxidative growth and mitochondrial morphology. The training set used for the first ensemble prediction was augmented with the experimentally confirmed prediction and a second iteration was performed. Additional 52 predictions were obtained, later confirmed experimentally. From a total of 193 total candidates authors demonstrated a functional role in mitochondrial biogenesis for 109 candidates. Among the confirmed genes only 42

were already known to be involved in mitochondrial biogenesis (Hess *et al.* 2009). These results demonstrated that also well trained computational predictions can be very effective in predict genes function, direct experimental approaches and extend knowledge about biological processes, with acceleration in the discovery rates (Hibbs *et al.* 2009).

In the present dissertation is presented a genome-wide screening focused on mitochondrial biogenesis, based on growth analysis of a *S. cerevisiae* knock out collection. Results and strategies will be described in the next section and compared with actual knowledge about mitochondrial biogenesis.

1.2 Results and discussion

1.2.1 A Genome Wide Screening Focused on Mitochondrial Biogenesis Identifies 488 Strains

In order to identify new nuclear genes possibly involved in mitochondrial biogenesis and metabolism, a genome-wide screening using *S. cerevisiae* null mutants collection was performed. A classical strategy to identify a respiratory dysfunction is a growth test in the presence of an oxidative carbon source. Optimal growth temperature for *S. cerevisiae* is 30˚C and deletions in genes essential for mitochondrial function show a strong phenotype already in this condition. However many references report for null mutants in genes involved in mitochondrial function a growth defect at temperatures above or below the optimal one (Phillips *et al.* 1993; Yang *et al.* 1994; Grandin *et al.* 1999; Shi *et al.* 2005; Medina-Silva *et al.* 2006; Polevoda *et al.* 2006; Spinazzola *et al.* 2006; Dallabona *et al.* 2010). Most likely 37˚C is a suitable condition to reveal phenotypes that would be subtle at 30˚C and possibly lost in high-throughput analysis. Interestingly, high temperature combined with oxidative carbon source could also be indicative for genes related to mitochondrial response in stress conditions. For these reasons the screening was performed at 37˚C, postulating that previous results, obtained in experiments at 30˚C, could have underestimated the number of nuclear genes involved in such processes.

S. cerevisiae knock out collection in BY4742 genetic contest was purchased at Open Biosystems and converted into 384-well plate format, for a total of 13 plates (see section 4.1.1 for details). A total of 4688 strains, not including 90 strains that failed quality control and 48 slow-growth strains (Yeast Deletion Mutant Database). Collection in this format was already used in a similar screening focused on metal tolerance (Ruotolo *et al.* 2008). The primary high-throughput screening was performed as described in section 4.2.1 at 37˚C in presence of ethanol 2% as sole carbon source. Mutant growth was then compared to performance in the same carbon source at 30˚C to check a possible temperature dependence of the phenotype. Media containing glucose at 30˚C and 37˚C were used as reference.

The strategy implemented was first of all validated using a control 384-plate. This dedicated plate contained strains known to be defective in the conditions of interest. Every strain selected was present four times in the plate and each condition was tested in four independent experiments (data not shown). Results reflected quite well the published data thus validating the strategy.

Each plate of the collection was then analyzed 4 times in each condition. To give semi-quantitative scores to the growth two controls were included in the analysis of each plate: a wild-type BY4742 strain as positive control and BY4742 ρ^0 (carrying no mitochondrial DNA, i.e. respiratory deficient) as negative one.

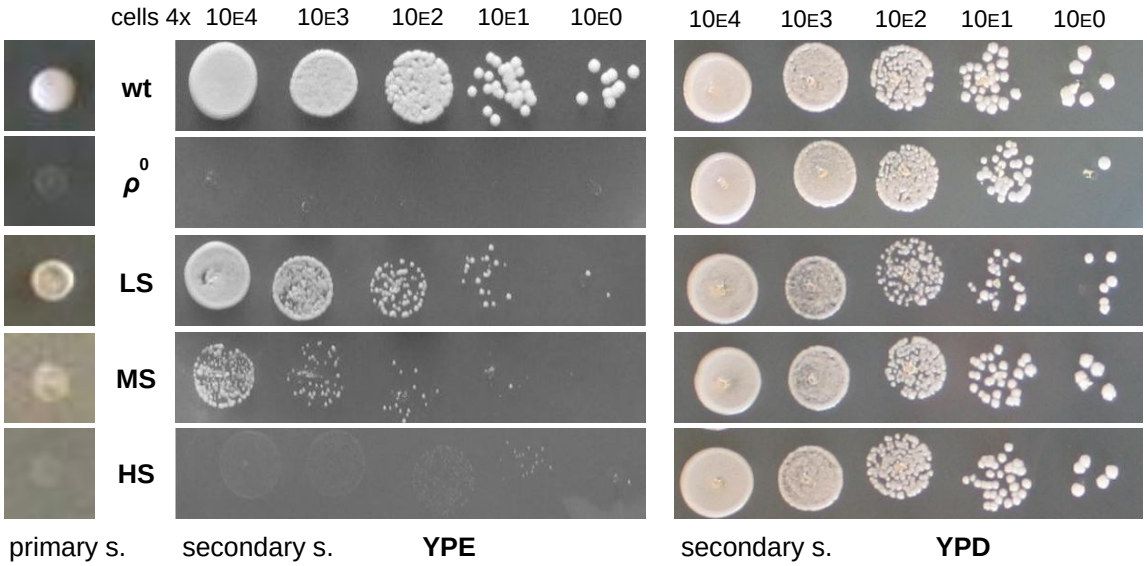

FIG 1.8: Image representative of strains growth in primary and secondary screening. HS (high sensitive), MS (medium sensitive) or LS (low sensitive) were used for defective growth, accordingly to phenotype's severity. BY4742 ρ^0 and wild type strains were included as control. In the secondary screening 4µl of 10-fold dilutions ranging from 10e7 to 10e3 cells/ml were spotted in an ordered fashion.

In order to consider reliable the data obtained in primary screening, a secondary screening was performed as described in section 4.2.2. This allowed to confirm or refute primary results and to choose the cut-off value for phenotypes observed. Phenotype could indeed be observed in 4/4, 3/4, 2/4 or 1/4 replicates. The concordance rate is defined as percentage of phenotypes observed in primary screening later confirmed. Concordance was calculated considering phenotypes registered 3 times and 4 times or 2, 3 and 4 times out of 4 independent replicates. Already applying a cut-off to 2 out of 4 the concordance rate was 79% at 30˚C and 82% at 37˚C. These values were considered optimal. Also the false-negative rate analysis was also calculated on a subset of deletants with positive growth in primary screening. Strains are considered false-negatives when showing no defects in primary screening but being sensitive in the subsequent analyses. In the present screening false-negative rate was also good with 14% and 24% at 30 and 37˚C respectively.

A final list of strains that showed a specific defect in primary screening for ethanol utilization at both temperatures was obtained from comparison between YPD and YPE conditions. Excluding 42 thermo-sensitive strains (deficient at YPD37˚C) a total of 488 strains resulted defective in the tested conditions (Appendix 1.1). Phenotypes could be temperature specific (37˚C or 30˚C) or not, as shown in figure 1.9. In support of the chosen working hypothesis a specific defective growth at high temperature was identified in 133 strains (27%). Among 348 strains that displayed phenotype at both temperatures 19 showed a severe worsening at 37˚C compared to 30˚C and 67 a slight worsening. In these mutants could be reasoned that temperature gives an important contribution to the deficiency. Remaining 262 strains displayed the same phenotype regardless temperature.

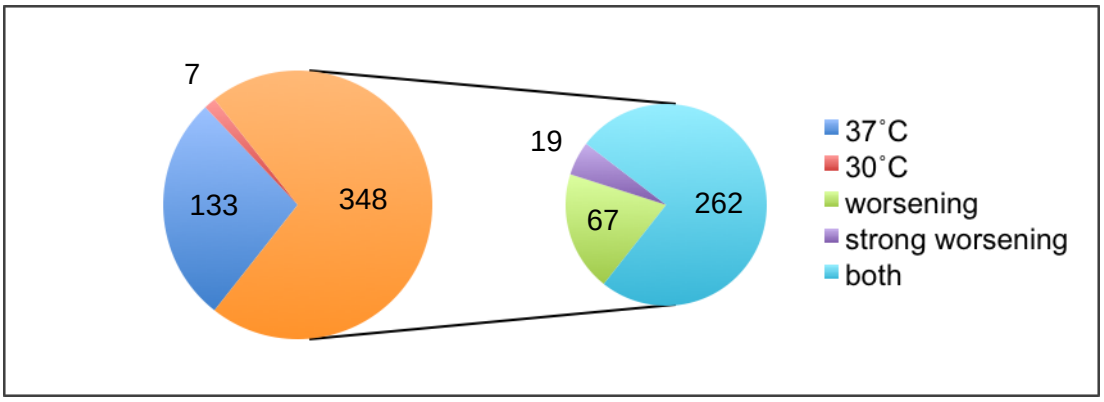

FIG 1.9: Chart-pie showing results of the screening. A total of 488 strains represented in the left pie were defective in the tested conditions. Among those 348 were defective at both temperature and are organized in the right pie.

An index for the quality of the screening is the analysis of functional categories represented in the dataset. GO consortium created a controlled hierarchical vocabulary of terms that allow description of biological functions, processes and localizations to characterize genes and coded proteins (Ashburner *et al.* 2000). Different tools to analyze datasets are available through the Saccharomyces Genome Database, as GO Term Finder. This tool analyzes an input dataset returning a list of GO terms that are significantly enriched. The final list of 488 defective strains was analyzed with GO Term Finder tool for cellular component and biological process terms. As expected, majority of the enriched terms are directly connected with mitochondria (Table 1.1). We can therefore identify proteins essential for each process of mitochondrial biogenesis like mitochondrial organization, maintenance and expression of mitochondrial genome, mitochondrial respiratory chain assembly and ATP synthesis. The same biological

processes are reflected in the subcellular enriched localizations: i.e. mitochondrial ribosomes, nucleoid and respiratory complexes.

TABLE 1.1: GO Term Finder restricted results applied to the 488 genes list. Complete results are available in Appendix 4.

GO TERM	BIOLOGICAL PROCESS	P-value	Genes
GO:0007005	mitochondrion organization	6.45E-75	146
GO:0032543	mitochondrial translation	1.84E-56	83
GO:0097034	mitochondrial respiratory chain complex IV biogenesis	1.71E-16	18
GO:0045333	cellular respiration	7.58E-15	38
GO:0033108	mitochondrial respiratory chain complex assembly	8.80E-15	19
GO:0000959	mitochondrial RNA metabolic process	2.27E-13	17
GO:0000002	mitochondrial genome maintenance	1.10E-11	19
GO:0033617	mitochondrial respiratory chain complex IV assembly	3.82E-10	11
GO:0015980	energy derivation by oxidation of organic compounds	6.04E-10	39
GO:0042773	ATP synthesis coupled electron transport	7.98E-10	15
GO:0042775	mitochondrial ATP synthesis coupled electron transport	7.98E-10	15
GO:0006119	oxidative phosphorylation	1.53E-09	15
GO:0070127	tRNA aminoacylation for mitochondrial protein translation	3.65E-09	10
GO:0008535	respiratory chain complex IV assembly	3.92E-09	11
GO:0022904	respiratory electron transport chain	5.05E-09	15
GO:0009060	aerobic respiration	5.81E-09	26
GO:0017004	cytochrome complex assembly	9.11E-08	8
GO:0097033	mitochondrial respiratory chain complex III biogenesis	2.72E-06	7
GO:0006122	mitochondrial electron transport, ubiquinol to cytochrome c	6.95E-06	7

GO TERM	CELLULAR COMPONENT	p-value	genes
GO:0044429	mitochondrial part	4.21E-78	191
GO:0005739	mitochondrion	2.78E-58	242
GO:0005759	mitochondrial matrix	2.64E-57	102
GO:0005761	mitochondrial ribosome	3.35E-44	58
GO:0005743	mitochondrial inner membrane	4.43E-32	80
GO:0005740	mitochondrial envelope	1.61E-28	102
GO:0005762	mitochondrial large ribosomal subunit	4.27E-26	32
GO:0031966	mitochondrial membrane	1.73E-24	92
GO:0005763	mitochondrial small ribosomal subunit	1.75E-17	23
GO:0044455	mitochondrial membrane part	4.84E-16	46
GO:0005746	mitochondrial respiratory chain	1.63E-11	16
GO:0070469	respiratory chain	4.10E-11	17
GO:0016469	proton-transporting two-sector ATPase complex	1.10E-06	13
GO:0005758	mitochondrial intermembrane space	1.28E-06	15
GO:0005750	mitochondrial respiratory chain complex III	2.19E-06	7
GO:0042645	mitochondrial nucleoid	6.26E-05	9

Enrichment of these GO terms in the dataset is index of high quality and reliability.

A comparison of quality among different genome-wide screenings was also performed. Sensibility and specificity of results were calculated for our dataset as described elsewhere (Elstner *et al.* 2009). The same parameters were also calculated for three comparable genome-wide screenings (Dimmer 2002; Luban *et al.* 2005; Merz *et al.* 2009). A list of 336 mitochondrial proteins was used as reference set for the calculations. This was obtained subtracting mitochondrial encoded proteins and genes coding for essential proteins from MitoP2 database (Elstner *et al.* 2008). Sensibility is defined as portion of a reference set covered by an input list. The present screening, along with the one performed by Dimmer KS *et al*., showed the highest sensibility (40%), as reported in Table 1.2. Specificity, defined as the portion percentage of a dataset being part of the reference, scored instead the lowest value: 28% against a mean of 36%. This was quite expected as reference set is composed only of mitochondrial proteins playing presumably essential roles. The working hypothesis of 37˚C of course shifts to a certain extent the dataset to mitochondrial related functions, essential under stress condition. Those functions could be played also in the cytoplasm. If dataset is enriched in such functions a lower specificity in covering a mitochondrial proteome is justifiable. Nevertheless to have a complete quality comparison specificity was calculated also with the portion of our dataset comprising deletions with phenotype already at 30°C. Notably our dataset scored again the highest value along with Dimmer *et al.* one.

Screening	identified	SENSIBILITY	identified	SPECIFICITY
our screening (tot.)	135 out of 336	**40%**	135 out of 488	**28%**
Merz et al.	111 out of 336	33%	111 out of 319	35%
Luban et al.	121 out of 336	36%	121 out of 357	34%
Dimmer et al.	134 out of 336	40%	134 out of 341	39%
our screening (30°C)	109 out of 336	**32%**	109 out of 276	**39%**

TABLE 1.2: Specificity and sensibility values for comparable genome-wide screenings. Parameters were calculated as described in Elstner et al. 2009 using a restricted MitoP2 database as reference set (see text for details).

The parameters used for this ranking, showed again the high quality of the screening performed. The list of 488 deletions was thus considered reliable and used for subsequent analysis in order to define the number of genes connected for the first time to mitochondrial biogenesis.

1.2.2 Data Filtering Allows Selection of 177 Genes

Aim of the performed screening was to identify nuclear genes with a role in mitochondrial biogenesis under stress condition. To this purpose from the original dataset obtained (488 genes) both nuclear genes with a mitochondrial role previously not shown and genes whose function is still poorly understood/unknown were considered suitable candidates. To select candidates both data mining and experimental confirmations were implemented, allowing selection of 177 genes. A flowchart of the process is given in figure 1.10.

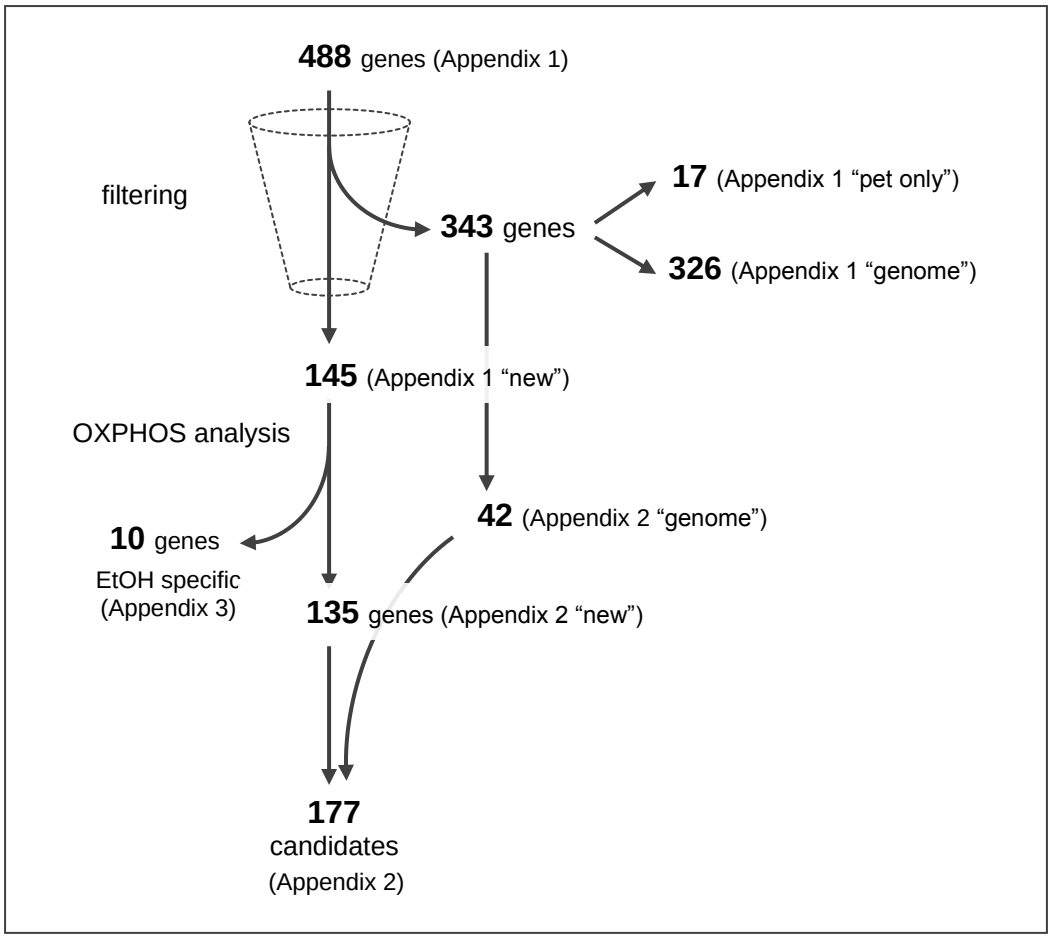

FIG 1.10: Flowchart of the selection process.

The final list of 488 deletions was compared to the available data in the SGD and to four different genome-wide screenings aimed to the study of mitochondrial biogenesis (Dimmer 2002; Luban *et al.* 2005; Hess *et al.* 2009; Merz *et al.* 2009). As mentioned previously the screening performed by Hess DC *et al.* was not relied on phenotypic test firstly but rather on a bioinformatical prediction later confirmed by experimental tests. For the different approach used by Hess DC those results were not included in quality analysis but used in the data filtering.

This tight filter excluded 343 identified (70%) and only genes never related to mitochondrial function in single gene or high-throughput analysis were retained representing the 30% of the entire dataset. This is index of high concordance among present screening and literature. A total of 326 out of 343 were already related to mitochondrial biogenesis in at least one other genome-wide screening (reported in Appendix 1 with the signature “genome”). In details: 20 were identified four times, 126 three times, and the remaining 180 only in one or two other screenings. As postulated in Merz *et al.* 2009 the number of times that a nuclear gene was identified could be related to the penetrancy (i.e. severity) of associated *pet* phenotype. On the other hand it could be reasoned that lack of essential functions, played by mitochondrial proteins, underlies highly penetrant phenotypes. In accordance with this the proportion of genes coding for mitochondrial proteins increases constantly in those sets, ranging from 33% for proteins identified in only one other screening, to 90% in ones identified four times. A total of 37 out of 326 genes, yet identified at 30˚C, displayed *pet* phenotype only at 37°C in our screening. Interestingly 27 of those were identified only one other time. In some cases the discrepancy could be due to the different genetic contest used. Indeed only Merz S. and colleagues analyzed mutants in *BY4742* contest while Dimmer K.S. and Luban C. worked with *BY4741* and *BY4743*. Different genetics contest could cause a sort of phenotypic plasticity. The remaining 17 genes out of 343 had already clear mitochondrial roles described in the SGD entry and were thus excluded (reported in Appendix 1 with “pet only” signature). Interestingly enough those genes were never identified with high-throughput techniques so the applied strategy here described was successful. Eventually a list of 145 genes was obtained (reported in Appendix 2 with “new” signature). Among those 31 reported a *“decreased rate of respiratory growth”* phenotype in Saccharomyces Genome Database and were retained.

An OXPHOS negative phenotype is usually related to mutants unable to perform oxidative growth regardless the carbon source provided. The screening performed used in first instance ethanol as sole carbon source, in combination or not with a temperature

stress. The observed phenotype could be due to a general OXPHOS impairment or defects in ethanol utilization or tolerance. Concerning this last possibility it has to be noted that ethanol is a well-known stressing agent. A concentration of 2%, chosen for the analysis, does not represent a stressing condition at 37˚C for *S. cerevisiae* wild type strain. Nevertheless it cannot be excluded that such condition might be toxic in mutants for proteins with a protective role. To rule out these possibilities the 145 strains were individually verified at least two times by spotting serial dilutions onto rich medium plates with lactate, acetate or glycerol as carbon sources. A total of 135 strains resulted defective in at least two different respiratory carbon sources suggesting a general OXPHOS impairment. Conversely 10 strains showed a growth defect only on ethanol-containing medium (Appendix 3). Based on data from *Saccharomyces Genome Database* we suggest for the large part of these genes an involvement at high temperature in ethanol tolerance. Although only one gene (*CIK1*) has a demonstrated direct role in resistance to ethanol some others are involved in cell wall and plasma membrane organization (*SSD1, ACK1, SER1*), a process known to be involved in ethanol tolerance (Teixeira *et al.* 2009). Additionally 4 genes (*YGR127W, UTR1, MAL31, YPL066W*) encode for proteins with roles in response to external stimuli as thermal stress, process that exhibits an extensive similarity and functional overlap with ethanol stress response (Piper 1995).

The 135 deletants corresponding to the identified OXPHOS genes were considered for further analyses and are represented in figure 1.11. A total of 83 genes (61%) displayed a specific phenotype only at 37˚C. Among 50 genes with a phenotype at both temperatures, 25 displayed a worsening at higher temperature. The majority of deletions in the identified genes caused a defect only at high temperature thus underlining the efficiency of the present screening.

FIG 1.11: Phenotypes distribution of 135 genes related to mitochondrial biogenesis for the first time.

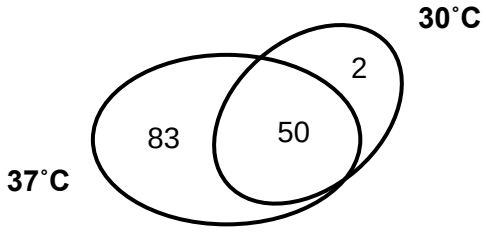

Nevertheless, in order to increase the knowledge about mitochondrial biogenesis or related processes, 42 additional deletants were considered for a total of 177 genes (Appendix 1.3). These additional candidates were selected from the filtered genes

because functional roles, at the moment of the screening, were totally unknown or still poorly understood. The OXPHOS nature was in this case guaranteed by the independent discovery in at least one other screening (in all cases performed in a carbon source different from ethanol). This dataset of 177 genes can be organized again according to the phenotypes displayed and represented in a Venn diagram (figure 1.12). A total of 88 genes displayed a specific phenotype at 37˚C and 86 at both temperatures. Three deletants showed a growth defect only at 30˚C. Among the 86 deletants with phenotype in both conditions 31 scored a worsening at high temperature that was severe in five cases. It can be reasoned that for about the 67% of the selected deletions the temperature played a key role in phenotype generation.

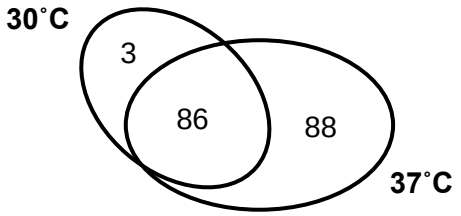

FIG 1.12: Phenotypes distribution of 177 new candidates.

How is composed this set of candidates? Among the 177 candidates, 24 genes (13%) code for mitochondrial proteins and 4 additional for proteins with probable mitochondrial localization. Nevertheless 15 other proteins still have a subcellular localization yet to be defined. Thus most of identified genes code for proteins localized in a compartment different from mitochondria.

Gene Ontology analysis for *"biological process unknown"* term revealed the presence of 34 gene products with totally uncharacterized function. Among those 15 have a mitochondrial location and could therefore play new yet uncharacterized mitochondrial roles.

Moreover a total of 75 proteins (42%) have a homolog in *Homo sapiens.* This allows potential discovery of new genes involved in mitochondrial biogenesis in higher eukaryotes and *Homo sapiens* that could also be related to the onset of human mitochondrial pathologies. Yeast represented a valuable tool as model organism in such disorders (Di Fonzo *et al.* 2009; Tuppen *et al.* 2010).

1.2.3 Functional Characterization of 177 Candidates

In order to characterize selected mutants and achieve insights into connection to mitochondrial biogenesis, classic tools were used.

The intactness of mitochondrial respiratory chain (MRC) was assessed registering the cytochrome spectra absorption profiles as described in section 4.2.3. This analysis evaluates the absorption of cytochrome c (550nm), cytochrome b (570nm) and cytochrome aa_3 (complex IV, 603nm); cytochrome content is an index of structural integrity of MRC.

Basing on the cytochrome spectra profile, the 177 candidates were organized in four different phenotypic classes: A, B, C and D. Each class reflected the status of MRC cytochromes compared to the wild type in the same conditions (wild type was present in each experiment). Strains were assigned to class A when strong defects were observed in the cytochromes profiles. Class D was chosen when profiles were perfectly comparable to a wild type. Class C and B represent middle classes with major variability. Class C resembles strains with cytochrome defects mostly quantitative (i.e. all cytochromes are present in a lower content). Instead class B, besides evident quantitative defects, could also share qualitative impairments in specific cytochromes (mainly COX or cytochrome b). As shown in figure 1.13 and related table, 88% of the dataset was distributed among classes A, B and C. For these genes MRC impairment could be the reason underlying the observed respiratory growth deficiency. Supporting this hypothesis high accordance between classes and primary screening phenotypes exist. Considering 37˚C condition, the highest number of HS strains is indeed in class A and the lowest in class C. *Viceversa* LS strains are mostly represented in class C whilst only 8 were scored in class A.

An evaluation of real functionality was at the same time achieved recording oxygen consuming on whole cells, as described in section 4.2.4. Absolute values (expressed in nmol O_2/minute*weight) were converted in respiratory efficiencies as percentage of the wild type, included in each analysis. Median values of efficiency were then associated to each phenotypic class, as reported in figure 1.13.

a

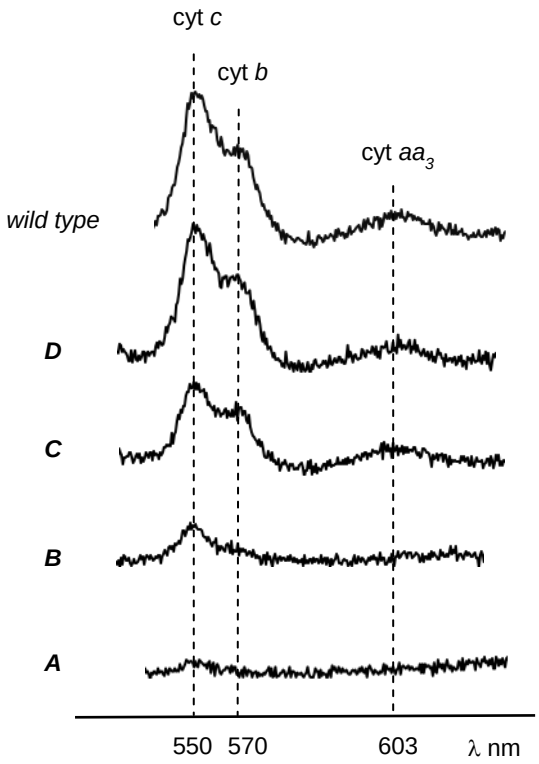

c

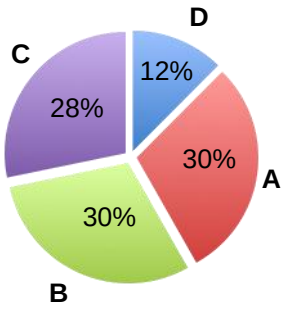

b

strain	class	N. of del.	resp. efficiency (% median)
bre2Δ	**D**	22	85%
arl3Δ	**C**	52	57%
pat1Δ	**B**	53	32%
htz1Δ	**A**	50	4%

FIG 1.13: A B C D classes **(a)** Cytochrome spectra profile of a wild-type strain and of four representative deletants, chosen to depict each class. Classes range from less (D) to most severe (A). **(b)** Number of deletants scored in each class with associated respiratory efficiency (median) expressed as percentage of wild-type. **(c)** Distribution of deletants among classes represented in pie-chart.

A good correlation between spectra and respiratory rates was present. Class A scored the lowest median value of 4%. Class B and Class C scored 32% and 57% respectively. As expected class D was the less affected with a median respiratory efficiency value of 85%. Concluding, an explanation for the observed OXPHOS negative phenotype can be postulated for 88% of the dataset and could be related to impairments in MRC.

For some class D mutants showing a LS or MS growth defect cannot be excluded the hypothesis that the mild respiratory impairment could be the cause of the observed phenotype. Nevertheless this is not possible for the 8 mutants showing an HS phenotype, which could harbor defects in other processes affecting mitochondrial function, rather then respiration. To this concern further investigations are required.

The unexpected behavior of *vam10Δ* mutant is still to elucidate. This strain showed a MS OXPHOS phenotype at 37˚C but higher cytochrome content and at the same time oxygen consumption almost three times higher that wild type (figure 1.14).

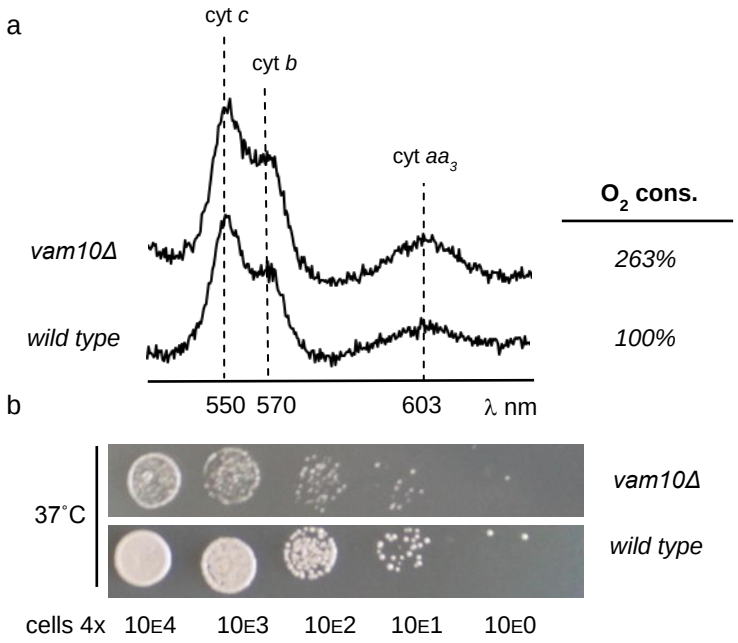

FIG 1.14: Phenotype of the *vam10Δ* strain. **(a)** Cytochromes profile and oxygen consumption. **(b)** Growth phenotype in complete ethanol media at 37˚C.

VAM10 is part of a cluster of genes involved in membrane trafficking, and its deletion causes vacuole fragmentation. Vacuoles and mitochondria are known to be functionally related and this also influence processes such as mitophagy and apoptosis, essential for proper mitochondrial function (Kanki *et al.* 2009; Li *et al.* 2009; Bhatia-Kissova *et al.* 2010; Johansson *et al.* 2010; Repnik *et al.* 2010; Sousa *et al.* 2011).

Many vacuole mutants have been identified in screenings for *pet* mutants and also in the present one. To our knowledge a vacuolar mutant is for the first time associated with increased cytochrome content and oxygen consumption. If these phenotypes are due to a reduced turnover of mitochondria remain to be demonstrated and similarly it is unclear how cells with an apparently functional respiratory apparatus can be defective in oxidative growth. One possible explanation, yet to be confirmed, is an accumulation of defective mitochondria with abnormal membrane potential, tied-up in futile respiratory cycles uncoupled to ATP production. If true this observation could be also related to two other phenotypes reported at SGD for *vam10Δ* mutant: *"nutrient utilization increased"* and *"decreased fitness"*.

1.2.4 Gene Ontology Analysis and Comments about Identified Functions

As mentioned previously GO analyses can be used to analyze datasets looking for functional classes significantly enriched or to have an overview on all the processes represented. Analysis of present dataset could allow identification of new proteins or new pathways possibly involved in mitochondrial biogenesis or in mitochondrial stress response.

Slim Mapper tool is used to map each gene of a list to a GO term that can represent either a biological process, a subcellular localization or a molecular function. The list of 177 candidates was analyzed and the terms associated are shown in Figure 1.15.

FIG 1.15: Go Slim Mapper tool applied to 177 candidates. Output is represented in a bar chart with functional categories and number of genes *per* GO term. Total results shown in Appendix 5.

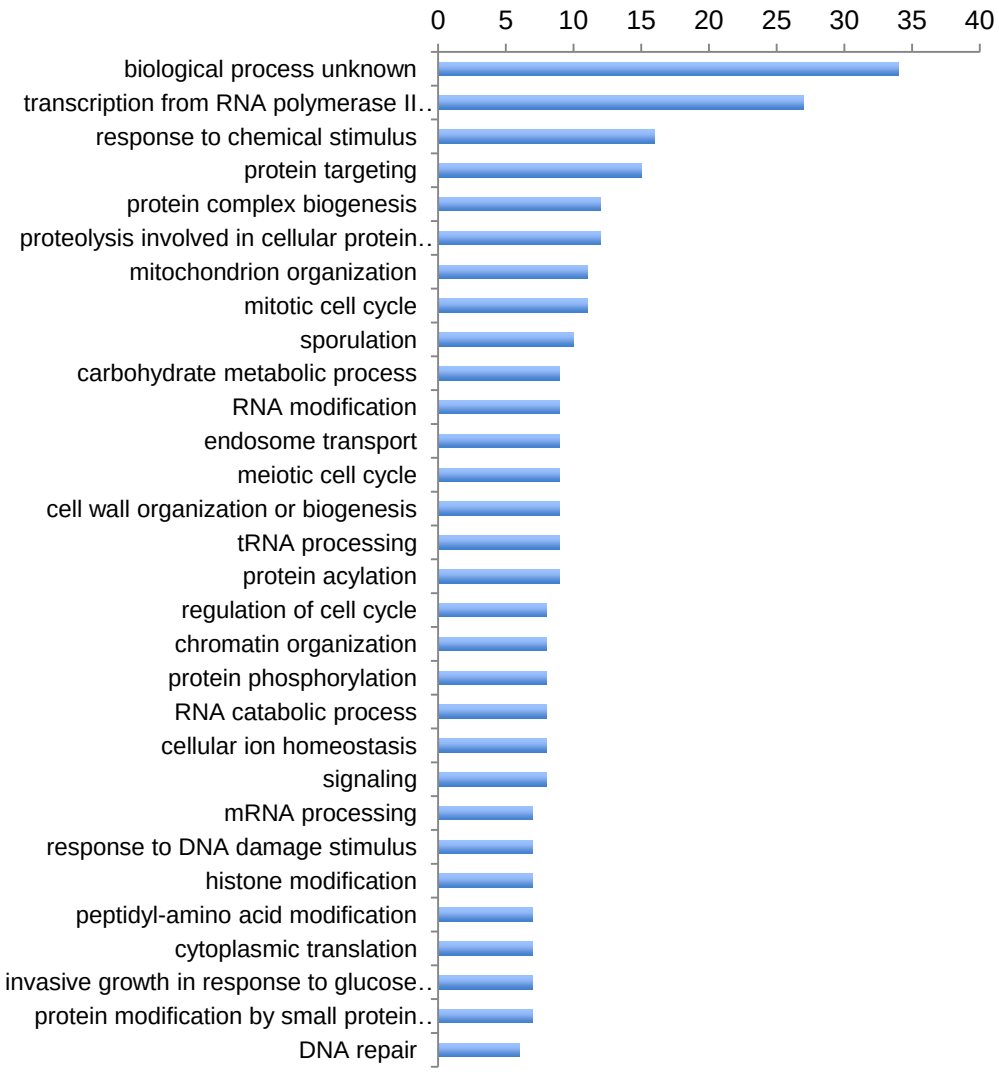

Some observations can already be made from this first general list. Genes were mapped to many different functional categories, ranging from *"transcription from RNA polymerase II promoter"* to *"cell cycle regulation"* and *"endosome transport"*. Therefore majority of these genes doesn't code for mitochondrial proteins leading to the observation that mitochondrial stress response could heavily rely on integration of mitochondria in other cellular processes. Interestingly a number of genes were mapped to *"biological process unknown"* that as pointed out previously represents a challenging research focus as they could represent new mitochondrial functions.

An additional interesting aspect is that at least 24 of genes in the 177 dataset could be mapped to mitochondria cellular component and moreover all these proteins did not have a characterized function at the moment of the screening. For some of those, as Mzm1p, the role in mitochondrial biogenesis was uncovered during last steps of data analysis(Atkinson *et al.* 2011).

In Chapter 3 of this dissertation is described a functional characterization of *YIR024C* gene product, considered interesting for different aspects later mentioned.

Using GO Term Finder an input list is analyzed in a way similar to Slim Mapper but results highlight only classes that are significantly enriched in comparison to the normal genome frequency. Term Finder analysis of 177 candidates list was carried out using Holm-Bonferroni multiple test hypothesis correction and p-value <0.05, algorithm implemented among YeastMine online resources (results are shown in table 1.3). As can be seen some biological processes and cellular components are significantly enriched in the input dataset and must represent important functions related to mitochondrial biogenesis.

The most significant enriched terms are the biological processes *"tRNA wobble base modification"*, *"tRNA wobble uridine modification"* and the cellular component *"elongator holoenzyme complex"* that represent one of the catalytic cores of this process. Strikingly the same terms are identified also if Term Finder algorithm is applied to the list of 88 genes with specific phenotype at 37˚C and moreover also *"protein urmylation"* term, relative to an ubiquitin-related protein modification with a role in tRNA modification, became significantly enriched (see table 1.4). These results underline an important role importance of this pathway in mitochondrial biogenesis under stress conditions and this interesting process was object of additional analyses, described in the Chapter 2 of this dissertation.

TABLE 1.3: Results of Go Term Finder tool applied to total list of 177 candidates.

GO TERM	BIOLOGICAL PROCESS	p-value	genes
GO:0002097	tRNA wobble base modification	1.47E-08	9
GO:0002098	tRNA wobble uridine modification	1.47E-08	9
GO:0006357	regulation of transcription from RNA polymerase II promoter	1.07E-06	26
GO:0043162	ubiquitin-dependent protein catabolic process via the MVB pathway	1.24E-06	7
GO:0006473	protein acetylation	2.59E-06	10
GO:0040007	growth	5.91E-06	15
GO:0043543	protein acylation	1.02E-05	10

GO TERM	CELLULAR COMPONENT	p-value	genes
GO:0033588	Elongator holoenzyme complex	9.79E-08	5
GO:0044440	endosomal part	5.34E-06	12
GO:0005768	endosome	2.88E-05	14
GO:0031248	protein acetyltransferase complex	3.89E-05	4
GO:0031414	N-terminal protein acetyltransferase complex	3.89E-05	4

TABLE 1.4: Term Finder tool was used to analyze a list of 88 deletions with phenotype at 37˚C.

GO TERM	BIOLOGICAL PROCESS	p-value	genes
GO:0002097	tRNA wobble base modification	5.02E-11	9
GO:0002098	tRNA wobble uridine modification	5.02E-11	9
GO:0006400	tRNA modification	5.48E-07	9
GO:0032447	protein urmylation	1.45E-06	4
GO:0045324	late endosome to vacuole transport	1.12E-05	6
GO:0015031	protein transport	1.17E-05	21

GO TERM	CELLULAR COMPONENT	p-value	genes
GO:0033588	Elongator holoenzyme complex	3.00E-09	5
GO:0034518	RNA cap binding complex	2.69E-05	3
GO:0044440	endosomal part	2.95E-05	8

Nevertheless other terms significantly represented in the 177 genes dataset were noteworthy; a brief description and comment will be made on the following: N-terminal acetylation of cytoplasmic proteins, histones acetylation, gene expression regulation, and cellular response to alkaline pH. A total of 45 genes are described in the following dissertations and mitochondrial phenotypes observed are reported in table 1.5.

N-terminal acetylation: acetylation of protein N-terminus is one of the most common post-translational modifications, occurring in the vast majority of eukaryotic proteins. Corresponding GO term was identified with high frequency in GO Slim Mapper tool and the corresponding enzymatic process was statistically enriched in the 177 dataset (*"protein acylation", "protein acetylation",* "*N-terminal protein acetyltransferase complex*"*)*. Three principal N-terminal acetyltransferase complexes are known in yeast: NatA, NatB and NatC (Polevoda *et al.* 2003; Polevoda *et al.* 2003). Those complexes physically interact with ribosomes to modify proteins during translation (Gautschi *et al.* 2003; Polevoda *et al.* 2008). These complexes are formed by a catalytic subunit and ancillatory subunits. All the three catalytic subunits of NatA, NatB and NatC (respectively Ard1p, Nat3p and Mak3p) were identified. Additionally for NatB also the other component (Mdm20p) was identified thus completing the complex, and for NatC one of the two ancillary subunits (Mak31p) was identified too. Notably only Nat3p/Mdm20p complex was reported to have some mitochondrial phenotypes *via* acetylation of Tpm1p (also identified in the present screening), component of the actine cytoskeleton (Singer *et al.* 2003). The data obtained in the present screening show a role for all three complexes in mitochondrial biogenesis under thermal stress.

Two considerations are worth mentioning. First, Ard1p dysregulation is involved in tumorigenesis and neurodegenerative disorders in humans and could be a novel target for cancer drugs (Arnesen *et al.* 2008; Kuo *et al.* 2010). Second, as mentioned previously Nat complexes interact physically with ribosomes to modify proteins during translation process and we also identified several genes whose product is involved in 40S and 60S ribosomes formation or assembly (*MTG2, RPL13B, RPL14A, RPL23B, RPL39, RPL43A, RPS27B, REI1, YVH1*). Thus it could be postulated that these subunits could modulate translation and concomitant post-translational modification under stress conditions. However only *RPL43A* deletion showed a specific phenotype at 37˚C while *RPL14A* and *RPL23B* deletions showed a pejorative phenotype with increased temperature.

Histones Acetylation: Histone tails modification is a well-known process essential for modulation of gene expression. GO terms representative of this class are the same of N-terminal acetylation as the chemical addition is basically the same. Principal kinds of regulatory modifications are acetylation, de-acetylation and methylation in the H3 and H4 histone subunits. The most common description of this phenomenon is that acetylation is a positive regulation event while methylation is negative (Lewin 2004). However many

modifiers are nowadays known to introduce modifications that can also be combined to achieve a real fine-tuning of gene expression, event described by the “histone code” theory.

SAGA complex is a big HAT complex (histone tail acetylation complex) that works as co-activator of gene expression acetylating lysine residues on histone H3 tail, but retains also repressing functions (Baker *et al.* 2007). Three subunits of SAGA complex were included in 177 genes list: Sgf29p, Spt8p and Spt7p. Looking back in the total list of 488 identified also Ngg1p and Gcn5p can be found, also if they have not been considered as yet identified in other screenings. *GCN5* codes for a catalytic subunit of the SAGA complex and mediates mitochondrial retrograde response (Grant *et al.* 1997; Kim S. *et al.* 2004). The scored phenotype of *gcn5Δ* strain was MS on ethanol at 37˚C. It can be postulated that this activity might be involved in mitochondrial stress response modulated by other subunits of the SAGA complex that could act as modulators of target specificity. Two other proteins with an HAT role were also identified and included in the 177 list: Eaf7p and Rtt109p.

Although not involved in acetylation and thus not included in this functional class, also identification of Bre2p is really noteworthy. Deletion in *BRE2* caused a specific phenotype at 37˚C and was never related to mitochondrial biogenesis. This protein is part of the highly conserved COMPASS complex involved in tri-methylation of Lys4 on histone H3 and contributes to generate a domain essential for a proper catalytic activity (South *et al.* 2010; Takahashi *et al.* 2011). This kind of modification conversely to other methylations induces gene expression from a subset of genes and is involved in a number of cellular processes (Dehe *et al.* 2006; Shilatifard 2008). Strikingly this modification seems to occur and regulate H3Lys4 acetylation on active promoters, which is introduced by the aforementioned identified Gcn5p and Rtt109p modifiers (Guillemette *et al.* 2011). Very suggestive would be the hypothesis of a combined regulation of genes involved in mitochondrial stress response by this kind of modifications. Indeed Bre2p is an ancillary subunit that could modulate activity of COMPASS complex at 37˚C in order to positively regulate histone modifications by Gcn5p and Rtt109p and in turn to activate genes essential for mitochondrial stress response.

TABLE 1.5: 45 genes representing interesting functional categories identified in the present screening. Mitochondrial phenotypes observed are reported. YPE30˚C and YPE37˚C columns refer to the phenotype in primary screening.

GENE	YPE30°C	YPE37°C	List	OXPHOS	CLASS	R. EFF%	Process
ARD1	0	LS	177	yes	A	4	NatA complex
MDM20	0	HS	488				NatB complex
NAT3	LS	LS	177	yes	A	11	NatB complex
TPM1	0	MS	488				NatB target
MAK31	LS	LS	177	yes	C	38	NatC complex
MAK3	LS	MS	177	yes	B	24	NatC complex
SPT7	MS	MS	177	yes	C	57	SAGA complex
SGF29	HS	HS	177	yes	A	2	SAGA complex
GCN5	0	MS	488				SAGA complex
SPT8	LS	LS	177	yes	A	27	SAGA complex
RTT109	LS	MS	177	yes	B	31	Rtt109 complex
EAF7	0	HS	177	yes	B	8	Nua4 complex
BRE2	0	MS	177	yes	D	65	COMPASS
CCR4	LS	LS	177	yes	C	79	Trascription
GCR2	LS	MS	177	yes	A	41	Trascript. Factor
SWI6	LS	MS	177	yes	B	38	Trascript. Factor
SMI1	0	HS	177	yes	C	59	Trascript. Factor
MAF1	0	HS	177	yes	B	46	Trascript. Factor
UME6	MS	HS	177	yes	B	21	Trascript. Factor
MSS11	0	HS	177	yes	B	56	Trascript. Factor
RIM101	0	HS	177	yes	B	19	Trascript. Factor
RIM8	0	MS	177	yes	C	51	Rim101 pathway
RIM9	MS	HS	177	yes	B	27	Rim101 pathway
RIM13	0	LS	177	yes	C	68	Rim101 pathway
DFG16	0	MS	177	yes	B	41	Rim101 pathway
RIM20	0	HS	177	yes	A	14	Rim101 pathway
STP22	0	HS	177	yes	B	67	ESCRT-complex I
SRN2	LS	HS	177	yes	D	87	ESCRT-complex I
VPS28	0	HS	177	yes	B	41	ESCRT-complex I
VPS25	LS	HS	488				ESCRT-complex II
VPS36	LS	HS	177	yes	C	46	ESCRT-complex II
SNF8	0	HS	177	yes	C	49	ESCRT-complex II
DID4	MS	HS	177	yes	B	74	ESCRT-complex III
SNF7	LS	HS	488				ESCRT-complex III
VPS20	HS	HS	488				ESCRT-complex III
DOA4	0	HS	488				MVB pathway
BRO1	0	HS	177	yes	B	23	MVB pathway
SAC6	0	HS	488				Rim101p regulated
PEP7	MS	HS	488				Rim101p regulated
DIT1	0	MS	177	yes	C	70	Rim101p regulated
CCM1	HS	HS	488				Rim101p regulated
COX7	HS	HS	488				Rim101p regulated
MDH2	0	LS	177	yes	D	83	Rim101p regulated
ELP3	0	MS	177	yes	C	50	Rim101p regulated
POS5	MS	HS	488				Rim101p regulated

Gene expression regulation: among the non-mitochondrial proteins identified one expected functional class was of course the transcription regulation by transcriptional factors. These proteins can indeed regulate several genes at the same time representing an essential strategy to adapt cellular responses to environmental stimuli. In this case regulation of gene expression could be used to integrate correctly mitochondria and mitochondrial stress response in the cellular network. Among the 177 candidates different genes coding for transcriptional factors were identified: *UME6, MAF1, MSS11, GCR2, SMI1, RIM101* and the cofactor coded by *SWI6*.

For some of those transcriptional factors (Maf1p, Smi1p, Mss11p, Rim101p) a role in mitochondrial biogenesis under heat stress can be postulated. Indeed phenotypes for the corresponding deletion strains were identified specifically at 37˚C. The role of Rim101p transcriptional factor, involved in environmental pH sensing, will be later described.

Maf1p was proposed to negatively regulate tRNAs transcription in response to nutrient availability and stress. Under non favorable conditions it become dephosporylated and is translocated to the nucleus down regulating RNA Pol III (Ciesla *et al.* 2008). Remarkably one specific defect observed in *maf1* mutant strains is a dysregulation of Mod5p protein, enzyme involved in the biosynthesis of isopentenyladenosine in cytoplasmic and mitochondrial tRNAs (Murawski *et al.* 1994). However *MOD5* deletion was not identified in the present screening.

Smi1p is a transcriptional factor involved in cell cycle regulation and cell wall integrity (Martin *et al.* 1999; Martin-Yken *et al.* 2002; Martin-Yken *et al.* 2003; Basmaji *et al.* 2006). Interestingly cell wall integrity was recently related to mitochondria in *C. albicans.* Indeed *ccr4* mutants (an mRNA de-adenylase) showed defects in cell wall integrity, mitochondrial function and phospholipids trafficking (Dagley *et al.* 2011). In the same work authors identified several mitochondrial known mutants (as components of outer membrane complex Sam) as defective in cell wall integrity and phospholipids trafficking between ER and mitochondria. Notably in the present screening also *CCR4* (ortholog in *S. cerevisiae*) was identified as new gene involved in mitochondrial biogenesis. Interestingly Caf4p, a protein involved in mitochondrial dynamics (i.e. fusion and fission) recruiting Dnm1p to mitochondria, was shown to be physically associated to the CCR4 complex in *S. cerevisiae* interacting with several components (Liu H. Y. *et al.* 2001; Griffin *et al.* 2005).

Mss11p is implicated in invasive growth, pseudohyphal differentiation and starch utilization (Gagiano *et al.* 1999; Gagiano *et al.* 2003).

Deletion in *SWI6, UME6* and *GCR2* caused a phenotype at both temperatures tested. In these cases a more general role in mitochondrial biogenesis can be postulated. *SWI6* codes for a transcriptional cofactor that forms a complex with Swi4p involved in cell-cycle regulation and also involved in cell wall integrity sensing (Dirick *et al.* 1992; Leem *et al.* 1998; Kim K. Y. *et al.* 2010). Interestingly a Swi6p role as oxidative-stress sensor was recently characterized: cysteine 404 residue was found to regulate the activity of Swi6/Swi4 complex causing a delay in the cell cycle upon induction of oxidative stresses (Fong *et al.* 2008; Chiu *et al.* 2011). Ume6p is involved in coupling metabolic sensing with mitosis, repressing or up-regulating early mitosis genes during the late step of the process (SGD). Gcr2p instead interact with Gcr1p regulating glycolytic genes (Uemura *et al.* 1992).

Alkaline pH response: Although a unique *"Alkaline pH response"* term doesn't exist and thus this pathway wasn't statistically enriched, its implication in mitochondrial biogenesis and mitochondrial stress response has to be pointed out. Indeed a high coverage of this pathway was achieved in the present screening and probably lack of statistically significance could be due to the high dispersion among different GO terms. Nevertheless in Term Finder output the categories "*ubiquitin-dependent protein catabolic process via the multivesicular body sorting pathway"*, *"endosomal part"* and *"late endosome to vacuole transport"* were statistically enriched. As mentioned above these classes take part in alkaline pH response.

Yeast grows far better in acidic or neutral condition whilst also a slight alkaline pH represent a stress that the cell has to manage. This response is essential in many yeast species moreover on some commensal/pathogens like *Candida albicans* that colonizes mucoses with a pH range from 2 to 10 (Davis 2003). At least three important pathways are implicated in the alkaline pH response: Rim101 pathway, the calcium activated calcineurin pathway, Wnt1/Slt2/Pkc1 MAP kinases and also the recently associated PKA kinase pathway (Arino 2010; Casado *et al.* 2011).

Rim101 pathway is a complex signal transducing chain that ends with the proteolytic activation of Rim101p. Free of its C-terminus it translocates to the nucleus and works as zinc finger transcription factor, acting both as repressor and activator (Su *et al.* 1993; Lamb *et al.* 2003). The final proteolytic event is catalyzed by the caspase Rim13p. Rim13p cleaves Rim101p when alkaline pH is sensed at level of plasma membrane. The sensing is performed by at least three proteins integral to the plasma membrane: Rim9p, Rim21p and Dfg16p. Finally Rim8p and Rim20p are also necessary for a correct

Rim101p processing. That's more: the Multi Vescicular Body pathway was recently connected to the alkaline pH sensing. Indeed all the three ESCRT complexes (I, II and III) and Bro1p were shown to be essential for a correct Rim101p activation (Boysen 2005; Hayashi *et al.* 2005; Boysen *et al.* 2010). A molecular model for the whole process has only been postulated: Rim9p and Rim21p sense the pH in association with Dfg16p, or help its biogenesis. Bro1p is involved in the MVB pathway and is recruited to the endosomes *via* ESCRT complexes proteins where its proposed role is to be a scaffold for the subsequent steps of MVB pathway. Interestingly Bro1p is very similar to Rim20p: they share the same endosome localization and probably the same scaffold role. Based on experimental evidences Rim20p could replace Bro1p when the alkaline pH is sensed at plasma membrane. The mechanism proposed is therefore a recruiting of Rim8p to the membrane *via* Dfg16p that is internalized in membrane vesicles, step that requires an intact endosome-trafficking system (i.e. ESCRT complexes). The presence of Dfg16p would allow dissociation of Bro1p and recruiting of Rim20p that could act as scaffold for Rim13p and Rim101p that is eventually processed.

The RIM101 pathway was almost completely covered in the performed genomic wide screening and included in the 177 candidates list. Namely *RIM8, RIM9, RIM13, RIM20, RIM101, DFG16* and *BRO1* were identified, with the only exception of *RIM21*. Additionally ESCRT-complex I (*MVB12, SRN2, STP22, VPS28*), ESCRT-complex II (*SNF8, VPS25, VPS36*) and ESCRT-complex III (*DID4, SNF7, VPS20, VPS24*) were totally covered with the only exception of *MVB12* and *VPS24*. Additionally *DOA4* was also identified, coding for a member of MVB pathway implicated in Bro1p dependent de-ubiquitination of cargoes destined for endosome import (Luhtala *et al.* 2004).

Several observations however pointed out that Rim101p has a broader role than simply promote alkaline pH inducible responses regulating also a number of cellular processes as meiosis, ions tolerance, cell differentiation, adaptive response to weakly acids (Su *et al.* 1993; Lamb *et al.* 2003; Mira *et al.* 2009). Basing on the results of the present screening a new role in regulation of mitochondrial biogenesis in thermal stress conditions is strongly suggested. The OXPHOS high sensitive phenotype of *rim101Δ* mutant is indeed displayed exclusively at 37˚C while growth is totally comparable to a wild type at 30˚C. This was observed also in almost every identified gene involved in the Rim101 signaling cascade.

However lacking an experimental confirmation, it cannot be excluded that conditions used in the screening could have caused an alkalization of the environment and effects on mitochondrial biogenesis have been only a secondary effect. Indeed relationships

between alkaline conditions and mitochondria are known. For instance in yeast *Yarrowia lypolitica* respiratory metabolism is very high at alkaline pH (Zvyagilskaya *et al.* 2004). In *S. cerevisiae* iron and copper uptake, whose function in mitochondrial biogenesis is well established, were identified as limiting factors in growth under alkaline stress (Serrano *et al.* 2004). In murine cell lines alkaline pH can induce oxidative stress stabilizing oxygen reactive species (ROS) produced by either complex III or I (Selivanov *et al.* 2008). Furthermore an alkaline dependent ROS production with consequent mtDNA fragmentation leading to alkaline-induced cell death was observed in murine lines, phenotypes rescued by overexpression of MnSOD (Majima *et al.* 1998). However, the present screening failed in identifying any of the other three pathways previously mentioned and generally induced by alkaline pH (only exception is one single protein, Slt2p). This suggests that Rim101p could act in mitochondrial biogenesis regardless its role in alkaline pH sensing, i.e. alkaline pH and other stimuli faced with Rim101p might require the same adaptations that a proper mitochondrial stress response does.

A list of documented Rim101p targets was obtained from YEASTRACT database (http://www.yeastract.com) and analyzed. Supporting the aforementioned hypothesis the list contained several genes already known to be involved in mitochondrial biogenesis (SGD): namely *CAF4, CCM1, COX7, NFU1, POS5, SHE9, UTH1* and *YFR045W*. *CCM1, COX7* and *POS5* were identified in the present screening and included in the 488 genes. Noteworthy the present screening identified six other genes regulated by Rim101p: *PRM7, SAC6, PEP7, DIT1, MDH2, ELP3.* Possibly mis-regulation of one or more of these genes could be the direct or indirect cause of mitochondrial biogenesis defect observed in mutants of Rim101 pathway. Strikingly Elp3p, catalytic core of the Elongator complex yet involved in cytoplasmic tRNA modification, is among Rim101 targets. A demonstration for the role of this complex in mitochondrial biogenesis under stress condition will be given in the next chapter of this dissertation.

1.3 References

Alkhaja AK, Jans DC, Nikolov M, Vukotic M, Lytovchenko O, Ludewig F, . . . Deckers M (2012). "MINOS1 is a conserved component of mitofilin complexes and required for mitochondrial function and cristae organization." Mol Biol Cell **23**(2): 247-257.

Arino J (2010). "Integrative responses to high pH stress in S. cerevisiae." OMICS **14**(5): 517-523.

Arnesen T, Thompson PR, Varhaug JE and Lillehaug JR (2008). "The protein acetyltransferase ARD1: a novel cancer drug target?" Curr Cancer Drug Targets **8**(7): 545-553.

Ashburner M, Ball CA, Blake JA, Botstein D, Butler H, Cherry JM, . . . Sherlock G (2000). "Gene ontology: tool for the unification of biology. The Gene Ontology Consortium." Nat Genet **25**(1): 25-29.

Atkinson A, Smith P, Fox JL, Cui TZ, Khalimonchuk O and Winge DR (2011). "The LYR protein Mzm1 functions in the insertion of the Rieske Fe/S protein in yeast mitochondria." Mol Cell Biol **31**(19): 3988-3996.

Auesukaree C, Damnernsawad A, Kruatrachue M, Pokethitiyook P, Boonchird C, Kaneko Y and Harashima S (2009). "Genome-wide identification of genes involved in tolerance to various environmental stresses in Saccharomyces cerevisiae." J Appl Genet **50**(3): 301-310.

Baker SP and Grant PA (2007). "The SAGA continues: expanding the cellular role of a transcriptional co-activator complex." Oncogene **26**(37): 5329-5340.

Basmaji F, Martin-Yken H, Durand F, Dagkessamanskaia A, Pichereaux C, Rossignol M and Francois J (2006). "The 'interactome' of the Knr4/Smi1, a protein implicated in coordinating cell wall synthesis with bud emergence in Saccharomyces cerevisiae." Mol Genet Genomics **275**(3): 217-230.

Bereiter-Hahn J (1990). "Behavior of mitochondria in the living cell." Int Rev Cytol **122**: 1-63.

Bhatia-Kissova I and Camougrand N (2010). "Mitophagy in yeast: actors and physiological roles." FEMS Yeast Res **10**(8): 1023-1034.

Boysen JH (2005). "Control of Bro1-Domain Protein Rim20 Localization by External pH, ESCRT Machinery, and the Saccharomyces cerevisiae Rim101 Pathway." Molecular Biology of the Cell **17**(3): 1344-1353.

Boysen JH, Subramanian S and Mitchell AP (2010). "Intervention of Bro1 in pH-Responsive Rim20 Localization in Saccharomyces cerevisiae." Eukaryotic Cell **9**(4): 532-538.

Bulder CJ (1964). "Lethality of the Petite Mutation in Petite Negative Yeasts." Antonie Van Leeuwenhoek **30**: 442-454.

Casado C, González A, Platara M, Ruiz A and Ariño J (2011). "The role of the protein kinase-A pathway in the response to alkaline pH stress in yeast." Biochemical Journal.

Chacinska A, Koehler CM, Milenkovic D, Lithgow T and Pfanner N (2009). "Importing Mitochondrial Proteins: Machineries and Mechanisms." Cell **138**(4): 628-644.

Chen XJ, Wang X, Kaufman BA and Butow RA (2005). "Aconitase couples metabolic regulation to mitochondrial DNA maintenance." Science **307**(5710): 714-717.

Chiu J, Tactacan CM, Tan SX, Lin RC, Wouters MA and Dawes IW (2011). "Cell cycle sensing of oxidative stress in Saccharomyces cerevisiae by oxidation of a specific cysteine residue in the transcription factor Swi6p." J Biol Chem **286**(7): 5204-5214.

Ciesla M and Boguta M (2008). "Regulation of RNA polymerase III transcription by Maf1 protein." Acta Biochim Pol **55**(2): 215-225.

Contamine V and Picard M (2000). "Maintenance and integrity of the mitochondrial genome: a plethora of nuclear genes in the budding yeast." Microbiol Mol Biol Rev **64**(2): 281-315.

Dagley MJ, Gentle IE, Beilharz TH, Pettolino FA, Djordjevic JT, Lo TL, . . . Traven A (2011). "Cell wall integrity is linked to mitochondria and phospholipid homeostasis in Candida albicans through the activity of the post-transcriptional regulator Ccr4-Pop2." Mol Microbiol **79**(4): 968-989.

Dallabona C, Marsano RM, Arzuffi P, Ghezzi D, Mancini P, Zeviani M, . . . Donnini C (2010). "Sym1, the yeast ortholog of the MPV17 human disease protein, is a stress-induced bioenergetic and morphogenetic mitochondrial modulator." Human Molecular Genetics **19**(6): 1098-1107.

Davis D (2003). "Adaptation to environmental pH in Candida albicans and its relation to pathogenesis." Current Genetics **44**(1): 1-7.

Dehe PM and Geli V (2006). "The multiple faces of Set1." Biochem Cell Biol **84**(4): 536-548.

Deponte M and Hell K (2009). "Disulphide bond formation in the intermembrane space of mitochondria." J Biochem **146**(5): 599-608.

Di Fonzo A, Ronchi D, Lodi T, Fassone E, Tigano M, Lamperti C, . . . Comi GP (2009). "The mitochondrial disulfide relay system protein GFER is mutated in autosomal-recessive myopathy with cataract and combined respiratory-chain deficiency." Am J Hum Genet **84**(5): 594-604.

Diaz F and Moraes CT (2008). "Mitochondrial biogenesis and turnover." Cell Calcium **44**(1): 24-35.

DiMauro S and Schon EA (2003). "Mitochondrial respiratory-chain diseases." N Engl J Med **348**(26): 2656-2668.

Dimmer KS (2002). "Genetic Basis of Mitochondrial Function and Morphology in Saccharomyces cerevisiae." Molecular Biology of the Cell **13**(3): 847-853.

Dirick L, Moll T, Auer H and Nasmyth K (1992). "A central role for SWI6 in modulating cell cycle Start-specific transcription in yeast." Nature **357**(6378): 508-513.
Duffy LM, Chapman AL, Shaw PJ and Grierson AJ (2011). "Review: The role of mitochondria in the pathogenesis of amyotrophic lateral sclerosis." Neuropathol Appl Neurobiol **37**(4): 336-352.
Duvezin-Caubet S, Jagasia R, Wagener J, Hofmann S, Trifunovic A, Hansson A, . . . Reichert AS (2006). "Proteolytic processing of OPA1 links mitochondrial dysfunction to alterations in mitochondrial morphology." J Biol Chem **281**(49): 37972-37979.
Elstner M, Andreoli C, Ahting U, Tetko I, Klopstock T, Meitinger T and Prokisch H (2008). "MitoP2: an integrative tool for the analysis of the mitochondrial proteome." Mol Biotechnol **40**(3): 306-315.
Elstner M, Andreoli C, Klopstock T, Meitinger T and Prokisch H (2009). "The mitochondrial proteome database: MitoP2." Methods Enzymol **457**: 3-20.
Fong CS, Temple MD, Alic N, Chiu J, Durchdewald M, Thorpe GW, . . . Dawes IW (2008). "Oxidant-induced cell-cycle delay in Saccharomyces cerevisiae: the involvement of the SWI6 transcription factor." FEMS Yeast Res **8**(3): 386-399.
Foury F, Roganti T, Lecrenier N and Purnelle B (1998). "The complete sequence of the mitochondrial genome of Saccharomyces cerevisiae." FEBS Lett **440**(3): 325-331.
Gagiano M, Bester M, van Dyk D, Franken J, Bauer FF and Pretorius IS (2003). "Mss11p is a transcription factor regulating pseudohyphal differentiation, invasive growth and starch metabolism in Saccharomyces cerevisiae in response to nutrient availability." Mol Microbiol **47**(1): 119-134.
Gagiano M, van Dyk D, Bauer FF, Lambrechts MG and Pretorius IS (1999). "Msn1p/Mss10p, Mss11p and Muc1p/Flo11p are part of a signal transduction pathway downstream of Mep2p regulating invasive growth and pseudohyphal differentiation in Saccharomyces cerevisiae." Mol Microbiol **31**(1): 103-116.
Gautschi M, Just S, Mun A, Ross S, Rucknagel P, Dubaquie Y, . . . Rospert S (2003). "The yeast N(alpha)-acetyltransferase NatA is quantitatively anchored to the ribosome and interacts with nascent polypeptides." Mol Cell Biol **23**(20): 7403-7414.
Giaever G, Chu AM, Ni L, Connelly C, Riles L, Veronneau S, . . . Johnston M (2002). "Functional profiling of the Saccharomyces cerevisiae genome." Nature **418**(6896): 387-391.
Grandin N and Charbonneau M (1999). "Dbf2 is implicated in a Cbt1-dependent pathway following a shift from glucose to galactose or non-fermentable carbon sources in Saccharomyces cerevisiae." Molecular and General Genetics **261**(2): 402-407.
Grant PA, Duggan L, Cote J, Roberts SM, Brownell JE, Candau R, . . . Workman JL (1997). "Yeast Gcn5 functions in two multisubunit complexes to acetylate nucleosomal histones: characterization of an Ada complex and the SAGA (Spt/Ada) complex." Genes Dev **11**(13): 1640-1650.
Griffin EE, Graumann J and Chan DC (2005). "The WD40 protein Caf4p is a component of the mitochondrial fission machinery and recruits Dnm1p to mitochondria." J Cell Biol **170**(2): 237-248.
Guillemette B, Drogaris P, Lin HH, Armstrong H, Hiragami-Hamada K, Imhof A, . . . Festenstein RJ (2011). "H3 lysine 4 is acetylated at active gene promoters and is regulated by H3 lysine 4 methylation." PLoS Genet **7**(3): e1001354.
Harner M, Korner C, Walther D, Mokranjac D, Kaesmacher J, Welsch U, . . . Neupert W (2011). "The mitochondrial contact site complex, a determinant of mitochondrial architecture." EMBO J **30**(21): 4356-4370.
Hayashi M, Fukuzawa T, Sorimachi H and Maeda T (2005). "Constitutive activation of the pH-responsive Rim101 pathway in yeast mutants defective in late steps of the MVB/ESCRT pathway." Mol Cell Biol **25**(21): 9478-9490.
Herlan M, Bornhovd C, Hell K, Neupert W and Reichert AS (2004). "Alternative topogenesis of Mgm1 and mitochondrial morphology depend on ATP and a functional import motor." J Cell Biol **165**(2): 167-173.
Herrmann JM (2011). "MINOS is plus: a Mitofilin complex for mitochondrial membrane contacts." Dev Cell **21**(4): 599-600.
Hess DC, Myers CL, Huttenhower C, Hibbs MA, Hayes AP, Paw J, . . . Caudy AA (2009). "Computationally driven, quantitative experiments discover genes required for mitochondrial biogenesis." PLoS Genet **5**(3): e1000407.
Hibbs MA, Hess DC, Myers CL, Huttenhower C, Li K and Troyanskaya OG (2007). "Exploring the functional landscape of gene expression: directed search of large microarray compendia." Bioinformatics **23**(20): 2692-2699.
Hibbs MA, Myers CL, Huttenhower C, Hess DC, Li K, Caudy AA and Troyanskaya OG (2009). "Directing experimental biology: a case study in mitochondrial biogenesis." PLoS Comput Biol **5**(3): e1000322.
Hoppins S, Collins SR, Cassidy-Stone A, Hummel E, DeVay RM, Lackner LL, . . . Nunnari J (2011). "A mitochondrial-focused genetic interaction map reveals a scaffold-like complex required for inner membrane organization in mitochondria." The Journal of Cell Biology **195**(2): 323-340.

Huttenhower C, Hibbs M, Myers C and Troyanskaya OG (2006). "A scalable method for integration and functional analysis of multiple microarray datasets." Bioinformatics **22**(23): 2890-2897.
Ishihara N, Fujita Y, Oka T and Mihara K (2006). "Regulation of mitochondrial morphology through proteolytic cleavage of OPA1." EMBO J **25**(13): 2966-2977.
Jazayeri A and Jackson SP (2002). "Screening the yeast genome for new DNA-repair genes." Genome Biol **3**(4): REVIEWS1009.
Johansson AC, Appelqvist H, Nilsson C, Kagedal K, Roberg K and Ollinger K (2010). "Regulation of apoptosis-associated lysosomal membrane permeabilization." Apoptosis **15**(5): 527-540.
Kamp DW, Shacter E and Weitzman SA (2011). "Chronic inflammation and cancer: the role of the mitochondria." Oncology (Williston Park) **25**(5): 400-410, 413.
Kanki T, Wang K, Cao Y, Baba M and Klionsky DJ (2009). "Atg32 is a mitochondrial protein that confers selectivity during mitophagy." Dev Cell **17**(1): 98-109.
Kim KY, Truman AW, Caesar S, Schlenstedt G and Levin DE (2010). "Yeast Mpk1 cell wall integrity mitogen-activated protein kinase regulates nucleocytoplasmic shuttling of the Swi6 transcriptional regulator." Mol Biol Cell **21**(9): 1609-1619.
Kim S, Ohkuni K, Couplan E and Jazwinski SM (2004). "The histone acetyltransferase GCN5 modulates the retrograde response and genome stability determining yeast longevity." Biogerontology **5**(5): 305-316.
Kucej M, Kucejova B, Subramanian R, Chen XJ and Butow RA (2008). "Mitochondrial nucleoids undergo remodeling in response to metabolic cues." J Cell Sci **121**(Pt 11): 1861-1868.
Kuo HP and Hung MC (2010). "Arrest-defective-1 protein (ARD1): tumor suppressor or oncoprotein?" Am J Transl Res **2**(1): 56-64.
Kurihara Y, Kanki T, Aoki Y, Hirota Y, Saigusa T, Uchiumi T and Kang D (2011). "Mitophagy plays an essential role in reducing mitochondrial production of reactive oxygen species and mutation of mitochondrial DNA by maintaining mitochondrial quantity and quality in yeast." J Biol Chem.
Lamb TM and Mitchell AP (2003). "The Transcription Factor Rim101p Governs Ion Tolerance and Cell Differentiation by Direct Repression of the Regulatory Genes NRG1 and SMP1 in Saccharomyces cerevisiae." Molecular and Cellular Biology **23**(2): 677-686.
Leem SH, Chung CN, Sunwoo Y and Araki H (1998). "Meiotic role of SWI6 in Saccharomyces cerevisiae." Nucleic Acids Res **26**(13): 3154-3158.
Lewin B (2004). Genes 8, Pearson Prentice Hall.
Li SC and Kane PM (2009). "The yeast lysosome-like vacuole: endpoint and crossroads." Biochim Biophys Acta **1793**(4): 650-663.
Lipinski KA, Kaniak-Golik A and Golik P (2010). "Maintenance and expression of the S. cerevisiae mitochondrial genome--from genetics to evolution and systems biology." Biochim Biophys Acta **1797**(6-7): 1086-1098.
Liu HY, Chiang YC, Pan J, Chen J, Salvadore C, Audino DC, . . . Denis CL (2001). "Characterization of CAF4 and CAF16 reveals a functional connection between the CCR4-NOT complex and a subset of SRB proteins of the RNA polymerase II holoenzyme." J Biol Chem **276**(10): 7541-7548.
Liu Z and Butow RA (2006). "Mitochondrial retrograde signaling." Annu Rev Genet **40**: 159-185.
Luban C, Beutel M, Stahl U and Schmidt U (2005). "Systematic screening of nuclear encoded proteins involved in the splicing metabolism of group II introns in yeast mitochondria." Gene **354**: 72-79.
Luhtala N and Odorizzi G (2004). "Bro1 coordinates deubiquitination in the multivesicular body pathway by recruiting Doa4 to endosomes." J Cell Biol **166**(5): 717-729.
Majima HJ, Oberley TD, Furukawa K, Mattson MP, Yen HC, Szweda LI and St Clair DK (1998). "Prevention of mitochondrial injury by manganese superoxide dismutase reveals a primary mechanism for alkaline-induced cell death." J Biol Chem **273**(14): 8217-8224.
Margulis L (1975). "Symbiotic theory of the origin of eukaryotic organelles; criteria for proof." Symp Soc Exp Biol(29): 21-38.
Margulis L and Bermudes D (1985). "Symbiosis as a mechanism of evolution: status of cell symbiosis theory." Symbiosis **1**: 101-124.
Martin H, Dagkessamanskaia A, Satchanska G, Dallies N and Francois J (1999). "KNR4, a suppressor of Saccharomyces cerevisiae cwh mutants, is involved in the transcriptional control of chitin synthase genes." Microbiology **145 (Pt 1)**: 249-258.
Martin-Yken H, Dagkessamanskaia A, Basmaji F, Lagorce A and Francois J (2003). "The interaction of Slt2 MAP kinase with Knr4 is necessary for signalling through the cell wall integrity pathway in Saccharomyces cerevisiae." Mol Microbiol **49**(1): 23-35.
Martin-Yken H, Dagkessamanskaia A, Talibi D and Francois J (2002). "KNR4 is a member of the PKC1 signalling pathway and genetically interacts with BCK2, a gene involved in cell cycle progression in Saccharomyces cerevisiae." Curr Genet **41**(5): 323-332.
McBride HM, Neuspiel M and Wasiak S (2006). "Mitochondria: more than just a powerhouse." Curr Biol **16**(14): R551-560.

Medina-Silva R, Barros MP, Galhardo RS, Netto LES, Colepicolo P and Menck CFM (2006). "Heat stress promotes mitochondrial instability and oxidative responses in yeast deficient in thiazole biosynthesis." Research in Microbiology **157**(3): 275-281.
Merz S and Westermann B (2009). "Genome-wide deletion mutant analysis reveals genes required for respiratory growth, mitochondrial genome maintenance and mitochondrial protein synthesis in Saccharomyces cerevisiae." Genome Biology **10**(9): R95.
Mieszczak M, Kozlowski M and Zagorski W (1988). "Protein composition of Saccharomyces cerevisiae mitochondrial ribosomes." Acta Biochim Pol **35**(2): 105-118.
Mira NP, Lourenco AB, Fernandes AR, Becker JD and Sa-Correia I (2009). "The RIM101 pathway has a role in Saccharomyces cerevisiae adaptive response and resistance to propionic acid and other weak acids." FEMS Yeast Res **9**(2): 202-216.
Muller HJ (1964). "The Relation of Recombination to Mutational Advance." Mutat Res **106**: 2-9.
Muller M and Reichert AS (2011). "Mitophagy, mitochondrial dynamics and the general stress response in yeast." Biochem Soc Trans **39**(5): 1514-1519.
Murawski M, Szczesniak B, Zoladek T, Hopper AK, Martin NC and Boguta M (1994). "maf1 mutation alters the subcellular localization of the Mod5 protein in yeast." Acta Biochim Pol **41**(4): 441-448.
Myers CL, Robson D, Wible A, Hibbs MA, Chiriac C, Theesfeld CL, . . . Troyanskaya OG (2005). "Discovery of biological networks from diverse functional genomic data." Genome Biol **6**(13): R114.
Myers CL and Troyanskaya OG (2007). "Context-sensitive data integration and prediction of biological networks." Bioinformatics **23**(17): 2322-2330.
Narendra DP, Jin SM, Tanaka A, Suen DF, Gautier CA, Shen J, . . . Youle RJ (2010). "PINK1 is selectively stabilized on impaired mitochondria to activate Parkin." PLoS Biol **8**(1): e1000298.
Okamoto K, Kondo-Okamoto N and Ohsumi Y (2009). "Mitochondria-anchored receptor Atg32 mediates degradation of mitochondria via selective autophagy." Dev Cell **17**(1): 87-97.
Pagliarini DJ, Calvo SE, Chang B, Sheth SA, Vafai SB, Ong SE, . . . Mootha VK (2008). "A mitochondrial protein compendium elucidates complex I disease biology." Cell **134**(1): 112-123.
Panavas T, Serviene E, Brasher J and Nagy PD (2005). "Yeast genome-wide screen reveals dissimilar sets of host genes affecting replication of RNA viruses." Proc Natl Acad Sci U S A **102**(20): 7326-7331.
Perocchi F, Jensen LJ, Gagneur J, Ahting U, von Mering C, Bork P, . . . Steinmetz LM (2006). "Assessing systems properties of yeast mitochondria through an interaction map of the organelle." PLoS Genet **2**(10): e170.
Phillips JD and Trumpower BL (1993). "Qcr9, the Nuclear Gene Encoding a Small Subunit of the Mitochondrial Cytochrome-Bc1 Complex, Maps to the Right Arm of Chromosome-Vii in Saccharomyces-Cerevisiae." Yeast **9**(1): 95-97.
Piper PW (1995). "The heat shock and ethanol stress responses of yeast exhibit extensive similarity and functional overlap." FEMS Microbiol Lett **134**(2-3): 121-127.
Polevoda B, Brown S, Cardillo TS, Rigby S and Sherman F (2008). "Yeast N(alpha)-terminal acetyltransferases are associated with ribosomes." J Cell Biochem **103**(2): 492-508.
Polevoda B, Pandera Y, Brown SP, Wei J and Sherman F (2006). "Phenotypes of yeast mutants lacking the mitochondrial protein Pet20p." Yeast **23**(2): 127-139.
Polevoda B and Sherman F (2003). "Composition and function of the eukaryotic N-terminal acetyltransferase subunits." Biochem Biophys Res Commun **308**(1): 1-11.
Polevoda B and Sherman F (2003). "N-terminal acetyltransferases and sequence requirements for N-terminal acetylation of eukaryotic proteins." J Mol Biol **325**(4): 595-622.
Repnik U and Turk B (2010). "Lysosomal-mitochondrial cross-talk during cell death." Mitochondrion **10**(6): 662-669.
Ruotolo R, Marchini G and Ottonello S (2008). "Membrane transporters and protein traffic networks differentially affecting metal tolerance: a genomic phenotyping study in yeast." Genome Biol **9**(4): R67.
Schafer A and Reichert AS (2009). "Emerging roles of mitochondrial membrane dynamics in health and disease." Biol Chem **390**(8): 707-715.
Scherens B and Goffeau A (2004). "The uses of genome-wide yeast mutant collections." Genome Biol **5**(7): 229.
Selivanov VA, Zeak JA, Roca J, Cascante M, Trucco M and Votyakova TV (2008). "The Role of External and Matrix pH in Mitochondrial Reactive Oxygen Species Generation." Journal of Biological Chemistry **283**(43): 29292-29300.
Serrano R, Bernal D, Simon E and Arino J (2004). "Copper and iron are the limiting factors for growth of the yeast Saccharomyces cerevisiae in an alkaline environment." J Biol Chem **279**(19): 19698-19704.
Shi F, Kawai S, Mori S, Kono E and Murata K (2005). "Identification of ATP-NADH kinase isozymes and their contribution to supply of NADP(H) in Saccharomyces cerevisiae." Febs Journal **272**(13): 3337-3349.
Shilatifard A (2008). "Molecular implementation and physiological roles for histone H3 lysine 4 (H3K4) methylation." Curr Opin Cell Biol **20**(3): 341-348.

Sickmann A, Reinders J, Wagner Y, Joppich C, Zahedi R, Meyer HE, . . . Meisinger C (2003). "The proteome of Saccharomyces cerevisiae mitochondria." Proc Natl Acad Sci U S A **100**(23): 13207-13212.
Singer JM and Shaw JM (2003). "Mdm20 protein functions with Nat3 protein to acetylate Tpm1 protein and regulate tropomyosin-actin interactions in budding yeast." Proc Natl Acad Sci U S A **100**(13): 7644-7649.
Soto IC, Fontanesi F, Liu J and Barrientos A (2011). "Biogenesis and assembly of eukaryotic cytochrome c oxidase catalytic core." Biochimica et Biophysica Acta (BBA) - Bioenergetics.
Soto IC, Fontanesi F, Valledor M, Horn D, Singh R and Barrientos A (2009). "Synthesis of cytochrome c oxidase subunit 1 is translationally downregulated in the absence of functional F1F0-ATP synthase." Biochimica et Biophysica Acta (BBA) - Molecular Cell Research **1793**(11): 1776-1786.
Sousa MJ, Azevedo F, Pedras A, Marques C, Coutinho OP, Preto A, . . . Corte-Real M (2011). "Vacuole-mitochondrial cross-talk during apoptosis in yeast: a model for understanding lysosome-mitochondria-mediated apoptosis in mammals." Biochem Soc Trans **39**(5): 1533-1537.
South PF, Fingerman IM, Mersman DP, Du HN and Briggs SD (2010). "A conserved interaction between the SDI domain of Bre2 and the Dpy-30 domain of Sdc1 is required for histone methylation and gene expression." J Biol Chem **285**(1): 595-607.
Spinazzola A, Viscomi C, Fernandez-Vizarra E, Carrara F, D'Adamo P, Calvo S, . . . Zeviani M (2006). "MPV17 encodes an inner mitochondrial membrane protein and is mutated in infantile hepatic mitochondrial DNA depletion." Nature Genetics **38**(5): 570-575.
Steinmetz LM, Scharfe C, Deutschbauer AM, Mokranjac D, Herman ZS, Jones T, . . . Davis RW (2002). "Systematic screen for human disease genes in yeast." Nature Genetics.
Su SS and Mitchell AP (1993). "Molecular characterization of the yeast meiotic regulatory gene RIM1." Nucleic Acids Res **21**(16): 3789-3797.
Takahashi YH, Westfield GH, Oleskie AN, Trievel RC, Shilatifard A and Skiniotis G (2011). "Structural analysis of the core COMPASS family of histone H3K4 methylases from yeast to human." Proc Natl Acad Sci U S A **108**(51): 20526-20531.
Tatsuta T and Langer T (2008). "Quality control of mitochondria: protection against neurodegeneration and ageing." EMBO J **27**(2): 306-314.
Teixeira MC, Raposo LR, Mira NP, Lourenco AB and Sa-Correia I (2009). "Genome-wide identification of Saccharomyces cerevisiae genes required for maximal tolerance to ethanol." Appl Environ Microbiol **75**(18): 5761-5772.
Tuppen HA, Fehmi J, Czermin B, Goffrini P, Meloni F, Ferrero I, . . . Taylor RW (2010). "Long-term survival of neonatal mitochondrial complex III deficiency associated with a novel BCS1L gene mutation." Mol Genet Metab **100**(4): 345-348.
Tzagoloff A and Dieckmann CL (1990). "PET genes of Saccharomyces cerevisiae." Microbiol Rev **54**(3): 211-225.
Uemura H and Jigami Y (1992). "Role of GCR2 in transcriptional activation of yeast glycolytic genes." Mol Cell Biol **12**(9): 3834-3842.
Wallace DC (2001). "Mitochondrial defects in neurodegenerative disease." Ment Retard Dev Disabil Res Rev **7**(3): 158-166.
Westermann B (2010). "Mitochondrial fusion and fission in cell life and death." Nat Rev Mol Cell Biol **11**(12): 872-884.
Winzeler EA, Shoemaker DD, Astromoff A, Liang H, Anderson K, Andre B, . . . Davis RW (1999). "Functional characterization of the S. cerevisiae genome by gene deletion and parallel analysis." Science **285**(5429): 901-906.
Woodson JD and Chory J (2008). "Coordination of gene expression between organellar and nuclear genomes." Nat Rev Genet **9**(5): 383-395.
Yang MJ and Trumpower BL (1994). "Deletion of Qcr6, the Gene Encoding Subunit 6 of the Mitochondrial Cytochrome Bc1 Complex, Blocks Maturation of Cytochrome-C1, and Causes Temperature-Sensitive Petite Growth in Saccharomyces-Cerevisiae." Journal of Biological Chemistry **269**(2): 1270-1275.
Yoshikawa K, Tanaka T, Furusawa C, Nagahisa K, Hirasawa T and Shimizu H (2009). "Comprehensive phenotypic analysis for identification of genes affecting growth under ethanol stress inSaccharomyces cerevisiae." FEMS Yeast Research **9**(1): 32-44.
Zvyagilskaya RA, Parkhomenko OA, Gordeeva AV, Deryabina YI and Persson BL (2004). "Bioenergetics of Yarrowia lipolytica cells grown at alkaline conditions." Biosci Rep **24**(2): 117-126.

Chapter 2:

Cytoplasmic tRNAs Modification and Mitochondrial Stress Response

2.1 Introduction

2.1.1 Cytoplasmic Transfer RNAs (tRNAs)

2.1.2 tRNAs Chemical Modification

2.1.3 Modifications in the Anticodon Loop Bases

2.1.4 Biogenesis of Cytosolic tRNAs Wobble Modifications

2.1.5 tRNA Import into Mitochondria

2.2 Results and Discussion

2.2.1 Cytoplasmic tRNAs Chemical Modification is Essential for Mitochondrial Function at 37˚C

2.2.2 Phenotypical Analysis of ncs6Δ, trm9Δ and elp3Δ Null Mutants

2.2.3 Mitochondrial Protein Synthesis is Impaired in trm9Δ and elp3Δ Null Mutants under stress condition

2.3 References

2.1 Introduction

2.1.1 Cytoplasmic Transfer RNAs (tRNAs)

Transfer RNAs are the essential bricks of translation being adaptors between the messenger RNA language and protein one. Those adaptors are small molecules of 74-95 nucleotides that, despite sequence divergences, are folded in universal secondary and tertiary structures. The predominant 3D structure of a tRNA is commonly defined as an L shape, as shown in figure 2.1. A better understanding of the functional domains is given by a look in the typical cloverleaf representation of secondary structure, organized in stems, arms and loops. We can universally distinguish (fig 2.1 lower right panel):

- *Acceptor stem* (violet): it is formed from pairing of first and last bases and is substrate for the addition of a terminal 5'-CCA-3' triplet used to conjugate covalently the corresponding amino acid.
- *TΨC arm* (green): the name comes from the corresponding triplet with a modified base pseudouridine (Ψ)
- *D arm* (red): contains the modified base dihydrouridine
- *Variable loop* (orange): is located between the TΨC arm and anticodon one. Its length is variable (3-21 bases)
- *Anticodon arm* (blue): is the one containing the deciphering triplet (usually 34 35 36, in grey).

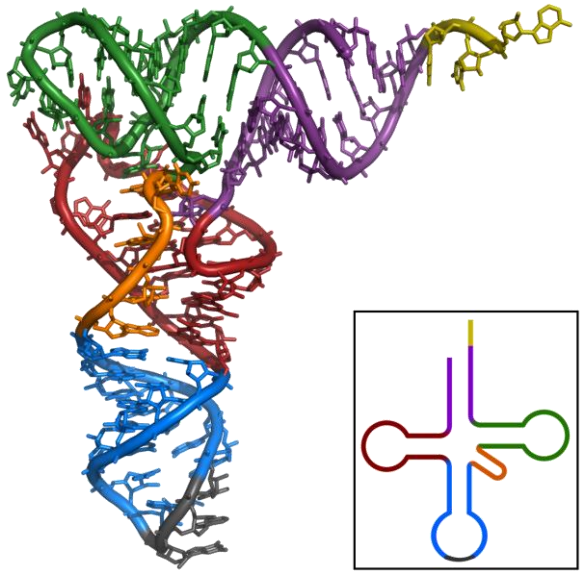

FIG 2.1: $tRNA^{Phe}$ 3D structure modeled from crystal diffraction analysis. Both tertiary and secondary structures are reported (Shi *et al.* 2000).

The double helices represented in the secondary structure are maintained in the 3D folding but their disposition creates two main double helices disposed with a 90° angle, giving rise to the L shape. One terminus contains the aminoacylated arm, in the other we find the anticodon loop with the decoding triplet (Lewin 2004).

Every tRNA, being loaded with a specific amino acid and harboring a precise anticodon, has the potential to translate the genetic code in an aminoacidic sequence. A faithful translation depends on the correct matching between tRNA and amino acids. Specific enzymes, called aminoacyl-tRNA synthetases (aaRS), catalyze the aminoacylation reaction (charging), which consists of two steps. The first step is the attack of ATP to the α-phosphate of the amino acid that is now activated in the form of aminoacyl-adenylate. In the second step the amino acid moiety is transferred to the 3'-terminal ribose (the adenine of the 5'-CCA-3' triplet) of a cognate tRNA, yielding an aminoacyl-tRNA and AMP (Arnez *et al.* 1997). Two classes of aaRS exist, differentiated by their folding and the site in which the amino acid moiety is transferred. Class I uses the 2'OH of terminal adenine and class II instead the 3'-OH. The only exception is PheRS that attaches the phenylalanine to the 2'OH of $tRNA^{Phe}$ (Arnez *et al.* 1997).

Protein synthesis is a fast process with an incorporation rate of 10-20 amino acids per second and an observed fidelity of 1 error in 10^3-10^4 polymerized amino acids (Andersson *et al.* 1982; Cochella *et al.* 2005). The fidelity of the reaction is based on two processes: first every tRNA must be recognized by the correct aaRS; second the aaRS must select the right amino acid for the cognate tRNA. Transfer RNAs are big and complicated molecules that harbor enough determinants to be correctly distinguished, but more difficult could be the discrimination of amino acids that sometimes are quite similar (i.e. threonine and the isosteric valine, or serine that shares the same γ-hydroxyl group). This is explained by the existence in the aaRS of two catalytic sites: the site of activation and the proofreading site. This led to the proposal of a "double-sieve" model of fidelity assurance. The first sieve is the activation site that can discriminate amino acids on the base of big differences in the side chain properties (dimension for instance). Although errors can be made at this step, the second site is smaller and more accurate and can discriminate also minor differences, leading to the high accuracy of the overall process (Cochella *et al.* 2005). A third layer of accuracy is given by the subsequently recognizing of the right aa-tRNA in the entry site of ribosomes (A site) where the major role is played by the pairing between codon and anticodon.

One common and important aspect of tRNA biology is that these small molecules are heavily modified. After transcription and maturation (i.e. 3’ and 5’ end processing and splicing) they are subject to chemical modification in several bases, with a great diversity of added groups and interested position. Effects of this editing range from structural properties to decoding capacities whether the affected bases are in the anticodon loop or in the remaining parts. Significance of chemical modification will be briefly discussed in the next sections.

2.1.2 tRNAs Chemical Modifications

A total of 107 different chemically modified nucleosides have been identified in RNA molecules, with the greatest variety in tRNAs: 92 in total with 81 specific (RNA modification database, http://rna-mdb.cas.albany.edu/RNAmods/). Effects of a modified base in a tRNA can be very different, depending on the base and moreover on the position involved. It is helpful to distinguish between modifications that affect codon-anticodon interaction and thus decoding capacities from those that act on the tRNA structure, shaping and fine-tuning it for peak performance (Motorin *et al.* 2010). The identity of such modifications can be a simple methylation in one of the esocyclic or endocyclic nitrogens, substitution of an oxygen with a thiol group, or addition in different steps of complicate chemical groups like 5-methylaminomethil (mnm^5), 2-methylthio-N^6-threonylcarbamoyl (ms^2t^6) and 5-methoxycarbonylmethyl-2-thio (mcm^5s^2).

In the group of structural modifications three major effects (extensively reviewed in 2010 by Yuri Motorin and Mark Helm) can be reported:

- *Nanoscale rearrangements:* these modifications can alter the normal pattern of hydrogen bonds formed in the double helices thus affecting the sugar, the Hoogsteen or the Watson-Crick edge of a base. In some cases the modification (or the lack of) can alter the thermodynamic equilibrium between different 3D structures leading to the significant appearance of alternative structures, often biologically inactive.
- *Subtle effects on the angstrom scale:* this kind of modification can favor one of the two alternative conformations of the sugar pucker: the 2'-endo or 3'-endo. The second one is implicated in the formation of alpha helices, like DNA, and thus a modification that shift the equilibrium toward the 3'-endo is favoring the formation of double helices. This is known for modification like methylation in the sugar 2'OH or thiolation of pyrimidine O2 atom.
- *Thermostability:* the key parameter for this property is the melting temperature (T_m). An increase of the T_m is usually indicative of a structural stabilization. From a biological point of view, a structural stabilization can be related to resistance against unspecific degradation by general bases or nucleases, whose mechanism involves a nucleophilic attack on the sugar 2'-OH. This terminal is more exposed in a not organized geometry (in-line); modifications favoring a helix conformation (see above) can thus improve the stability. In some extreme cases the thermostability is a physiological necessity, like in genus *Thermus*

thermopilus, a prokaryote that lives in near boiling water. Different strategies are implemented to resist in these conditions, like high GC content or imposing of particular chemical modifications in nucleic acids.

One general characteristic of these modifications is that usually the lack of only one doesn't have a strong phenotypic effect. This is in accordance with the concept of thermodynamic equilibrium that these modifications can alter, without an "all or nothing" effect. Nevertheless stronger defects are common when more than one modification lack, remarking the importance of a correct chemical editing for the structural fine tuning of these molecules.

2.1.3 Modifications in the Anticodon Loop Bases

Modifications in the anticodon loop bases have a different biological relevance. A pronounced hot spot can be found at positions 34 and 37 (Motorin *et al.* 2010). The significance of these modifications is relevant, directly affecting the decoding capacities of anticodon and being the fundament of modern genetic code evolution.

Francis Crick gave the first interpretation on how the genetic code works in 1966 (Crick 1966). It was clear that cells limited the number of tRNA in comparison to the number of possible codons of three letters. To read 61 possible codons (64 minus three stop codons) only 40 tRNA were evolved thus implicating that some anticodons had to recognize more than one codon (Agris *et al.* 2007). Crick explored this possibility with the proposal of the "Wobble Hypothesis". Briefly, the first two bases of the codon were read with a rigid canonical Watson-Crick base pairing, but in the third one the reading could be wobbling. The first base of the anticodon (named wobble position) could thus pair with different bases. The only modified base implemented by Crick was the Inosine in position 34, that was proposed to read U, C or A in the third position of the codon.

First published report of modified bases in a tRNA sequence was in 1968 (Goodman *et al.* 1968), and from that moment, in large parte, the science of Susumu Nishimura and colleagues was essential to improve the knowledge about chemical modifications in tRNA and their functional roles (Nishimura *et al.* 2006; Agris *et al.* 2007). The study of these modifications led to the expansion of original Crick hypothesis with the 1991 "Modified Wobble Hypothesis" that gave a first interpretation about chemical editing of anticodon bases. Nowadays the knowledge about chemical modification of anticodon loop bases is greatly improved and a lot of modifications have been studied and the roles cleared. Looking at the codon usage table is evident how some amino acids are encoded with six and four-fold degenerate codons while others are only one or two fold degenerate. This creates mixed and not mixed boxes, as shown in figure 2.2. The proposed and largely demonstrated role of chemical modifications in wobble base is to pre-structure the anticodon to allow recognizing of anticodon with wobbling rules, different for amino acids of mixed boxes and not. For instance cmo^5U_{34} modification is present only in tRNAs that read 4-fold degenerate codons and the modification would only stabilize the codon-anticodon pairing also with wobbling at third position, regardless the identity of the third codon base. The modification *per se* is not needed to recognize the cognate codon, but only to expand the decoding capacities. This is the case of $tRNA^{Val}_{UAC}$ that

harbors a cmo^5U_{34} modification and $tRNA^{Ala}_{UGC}$, $tRNA^{Ser}_{UGA}$ and $tRNA^{Pro}_{UGG}$, all coding for single amino acid codon boxes, able to pair the cognate codon although recognition was achieved with different affinities (Yarian 2002).

UUU	Phe	UCU	Ser	UAU	Tyr	UGU	Cys
UUC	Phe	UCC	Ser	UAC	Tyr	UGC	Cys
UUA	Leu	UCA	Ser	UAA	Stop	UGA	Stop
UUG	Leu	UCG	Ser	UAG	Stop	UGG	Trp
CUU	Leu	CCU	Pro	CAU	His	CGU	Arg
CUC	Leu	CCC	Pro	CAC	His	CGC	Arg
CUA	Leu	CCA	Pro	CAA	Gln	CGA	Arg
CUG	Leu	CCG	Pro	CAG	Gln	CGG	Arg
AUU	Ile	ACU	Thr	AAU	Asn	AGU	Ser
AUC	Ile	ACC	Thr	AAC	Asn	AGC	Ser
AUA	Ile	ACA	Thr	AAA	Lys	AGA	Arg
AUG	Met	ACG	Thr	AAG	Lys	AGG	Arg
GUU	Val	GCU	Ala	GAU	Asp	GGU	Gly
GUC	Val	GCC	Ala	GAC	Asp	GGC	Gly
GUA	Val	GCA	Ala	GAA	Glu	GGA	Gly
GUG	Val	GCG	Ala	GAG	Glu	GGG	Gly

FIG 2.2: Codon Usage table with color distinction for mixed boxes (grey). Image taken from Yarian C. et al 2002.

Different roles have been proven for ubiquitous $xm^5s^2U_{34}$ (tabella con modificazioni U34!) modifications of $tRNA^{Lys}_{UUU}$ $tRNA^{Glu}_{UUC}$ and $tRNA^{Gln}_{UUG}$ (Kruger *et al.* 1998; Yarian 2002). The modified bases in this case are necessary to enable U-A pairing with U-G wobbling, but U-U and U-C pairing would be excluded due to the more rigid conformation given by the 2-thiol group, regardless identity of 5'-terminus group.

Summarizing it seems that some U_{34} modifications expand the wobble rules and others restricts, at least in the prokaryotic systems largely used at that time (mostly *E. coli*). In eukaryotes anticodons ending with C_{34} are more common, observation that initially convinced about the absence of U-G wobbling. Using *S. cerevisiae* as model system, rules of eukaryotic wobbling were recently tested *in vivo*, studying the contribution of single modifications to the decoding process (Johansson *et al.* 2008). Given that thiolation and addition of 5' groups are independent processes, usage of mutants in both pathways was useful to dissect roles of ncm^5, mcm^5 and s^2 modifications. This analysis led to the conclusion that ncm^5 and mcm^5 groups promote reading of G ending codons, while concomitant mcm^5 and s^2 enhance decoding of both A and G ending codons (a table of yeast cytosolic tRNAs object of modification in wobble base is provided in the next section). This conclusion also challenges the notion of an absent U-G wobbling in eukaryotes.

In the anticodon loop one other base is almost ubiquitously modified, in combination with U_{34}, to enable wobbling: the purine 37. This base is the 3' adjacent to the anticodon and doesn't contact directly the codon bases but its importance is crucial,

especially when the first codon base is A. This extends the concept of codon recognition beyond that of the three bases pairing, leading to the final "Extended Anticodon Hypothesis". This modification is important in combination with ones in U_{34} to enable a codon-anticodon interaction stable enough to be accepted in the ribosome also with wobbling at third position (Agris *et al.* 2007). Indeed in Crick's original hypothesis a lot of emphasis was given to the geometry of the pairing in A site of ribosomes. The first two bases follow a Watson-Crick interaction, forming a canonical minihelix with the codon that can be distorted by the third base, if wobbling or mispaired. The geometry of the minihelix is assessed at A site by 16s rRNA, with a total of eight hydrogen bonds between three rRNA residues (namely A1492, A1493 and G530) and the minor groove of the minihelix. Fewer hydrogen bonds would be formed with a mismatched tRNA or an unmodified tRNA that "tries" a wobble pairing. This is completely true and unmodified in the recent hypothesis but complemented with the role of modified bases. Pur_{37} modifications, in combination with U_{34} ones, pre-structure the anticodon to a geometry that enables a stable pairing with the codon in the A site, also if the third base doesn't follow a canonical geometry.

These modifications are thus essential for wobbling with rules that change in a modification dependent manner.

Very interesting is the integration of chemical modifications roles in the evolution of genetic code and its tRNA adaptors. Crick proposed that the first "primitive code" was based on triplets but the number of amino acids was small and were all coded by unmodified tRNAs. A second phase was reached with an "intermediate code" were evolution pushed to use all the 64 codons trying to reduce the number of non-sense codons. The amino acids were still few and in this phase modifications such as cmo^5U_{34} could be critical to expand the decoding capacities enabling wobbling and decoding of four-fold degenerate codon boxes. This process could involve the simpler amino acids, and possibly earliest, with a simple side chain (i.e. Ala, Leu, Val, Ser and Thr) (Agris *et al.* 2007). The final step of evolution was the introduction of new amino acids that needed free decoding potential. In this case modifications like $xm^5s^2U_{34}$ could have played a pivotal role in order to split four-fold degenerate boxes in mixed ones.

The importance of tRNA chemical editing in the wobble base is otherwise demonstrated by different dysfunctions of mutants in the biogenesis of such modifications (Slaugenhaupt *et al.* 2002; Kirino *et al.* 2005; Simpson *et al.* 2008; Chen *et al.* 2009; Wang Xinjian *et al.* 2009; Wang Xinjian *et al.* 2010). Moreover, mutations in genes coding for human mitochondrial $tRNA^{Lys}_{UUU}$ and $tRNA^{Leu}_{UAA}$ are

cause of mitochondrial myoclonus epilepsy with ragged-red fibers (MERRF) and myopathy encephalopathy lactic acidosis and stroke-like episodes (MELAS) disorders (Goto *et al.* 1990; Kobayashi *et al.* 1990; Shoffner *et al.* 1990; Goto *et al.* 1991). These mitochondrial tRNAs were found to harbor two new kinds of taurine modified uridines: 5-taurinemethyluridine (τm^5U_{34}) and 5-taurinemethyl-2-thiouridine ($\tau m^5s^2U_{34}$) (Suzuki *et al.* 2002), known today to be a common modification in mammalian mitochondrial tRNAs. These particular modifications were lacking in the same mt-tRNAs from cell lines of MERRF and MELAS patients and the molecular pathogenesis of these disorders was subsequently explained. Presence of the modified group allow $tRNA^{Lys}_{UUU}$ and $tRNA^{Leu}_{UUR}$ to recognize efficiently their codons, respectively AAA AAG and UUA UUG, introducing the above mentioned wobbling rules. Lack of this modification impairs deciphering of both lysine codons with a whole translational defect, and leucine UUG codon with a consequent defect in UUG rich genes, leading to mitochondrial deficiencies (fig 2.3). A common symptom of MELAS patients is a complex I deficiency, nicely explained by a translational defect of ND6 gene, coding for a complex I subunit (Kirino *et al.* 2005; Suzuki *et al.* 2011). Notably almost every pathogenic mutation doesn't fall into anticodon bases, as shown in figure 2.3. This implies that other positions in the tRNA sequence influence the modification of wobble base. These mutations could influence the folding properties of the molecule impairing the modification by specific mitochondrial enzymes like Mtu1p.

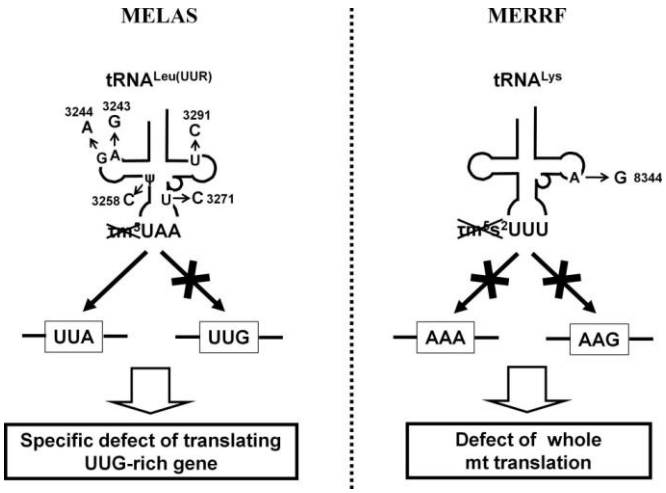

FIG 2.3: Schematic representation of pathogenic MELAS and MERRF mutations with consequence on mitochondrial translation. Image taken from Suzuki T. et al 2011.

Other examples underlining the importance of chemical modification in wobble bases come from the work in model organisms, like *S. cerevisiae*. For illustrative, yet incomplete purposes, can be cited the work on mitochondrial $tRNA^{Lys}$, $tRNA^{Glu}$ and

$tRNA^{Gln}$. These tRNAs harbor a 5-carboxymethylaminomethyl-2-thiouridine ($cmnm^5s^2U_{34}$) in position 34. Enzymes responsible for biosynthesis of this group are essentially three: Mto2p (alias Mtu1p, homolog of human Mtu1p), Mto1p and Mss1p. The first catalyzes the thiolation step while Mto1p and Mss1p are involved in the 5' modification. Indirect defects in mitochondrial RNA metabolism were already proven in *mto1* null mutant combined with a particular mutation in 15s rRNA (Wang Xinjian *et al.* 2009). Much stronger mitochondrial phenotypes were observed in *mto2* null mutant and in double mutant *mto1mss1*, probably due to the defects in mitochondrial translation caused by the absence of a correct U_{34} modification (Umeda *et al.* 2005). A complete dissection of this heavily related hub of genes was achieved with a complete analysis of double and triple mutants, confirming that combination of the loss in the two independent steps of U_{34} modification was causing a strong mitochondrial defect, based on the lack of a correct codon decoding during mitochondrial translation (Wang Xinjian *et al.* 2010).

As to be pointed out that very recently a defect in Mto1p in human cell lines was shown to have no effects on mitochondrial translation (Sasarman *et al.* 2011). Nevertheless all this results taken together demonstrate again the importance of a correct wobble base chemical modification: a highly conserved process in all the steps of evolution, that maybe implements the same general rules with genus specific exceptions.

2.1.4 Biogenesis of Cytosolic tRNAs Wobble Modifications

Cytsolic tRNAs undergo chemical modification in U_{34}. As in other fields of interest, work in the model system *S. cerevisiae* was essential to uncover enzymatic steps and the protein involved, a list yet to be completed. In yeast eleven cytosolic tRNAs are modified in 5' terminus of the nucleobase: a carbamoylmethyl group (ncm) or a methoxycarbonylmethyl (mcm) are added. Four have an additional substituent in the 2' in combination with the 5' modification. Three are thiol groups ($mcm^5s^2U_{34}$ in $tRNA^{Lys}$, $tRNA^{Glu}$ and $tRNA^{Gln}$) and one is an additional methyl ($ncm^5U_{34}m$ in $tRNA^{Leu}$). An exhaustive list is shown in figure 2.4, and structures are given in figure 2.5.

codon	anticodon	amino acid	codon	anticodon	amino acid	codon	anticodon	amino acid	codon	anticodon	amino acid
UUU	-	Phe	UCU	IGA	Ser	UAU	-	Tyr	UGU	-	Cys
UUC	GmAA		UCC	-		UAC	GΨA		UGC	GCA	
UUA	**ncm^{5}UmAA**	Leu	UCA	**ncm^{5}UGA**		UAA	-	n.a.	UGA	-	n.a.
UUG	m^{5}CAA		UCG	CGA		UAG	-		UGG	CmCA	Trp
CUU	-	Leu	CCU	AGG	Pro	CAU	-	His	CGU	ICG	Arg
CUC	GAG		CCC	-		CAC	GUG		CGC	-	
CUA	UAG		CCA	**ncm^{5}UGG**		CAA	**mcm^{5}s^{2}UUG**	Gln	CGA	-	
CUG	-		CCG	-		CAG	CUG		CGG	CCG	
AUU	IAU	Ile	ACU	IGU	Thr	AAU	-	Asn	AGU		Ser
AUC	-		ACC	-		AAC	GUU		AGC	GCU	
AUA	ΨAΨ		ACA	**ncm^{5}UGU**		AAA	**mcm^{5}s^{2}UUU**	Lys	AGA	**mcm^{5}UCU**	Arg
AUG	CAU	Met	ACG	CGU		AAG	CUU		AGG	CCU	
GUU	IAC	Val	GCU	IGC	Ala	GAU	-	Asp	GGU	-	Gly
GUC	-		GCC	-		GAC	GUC		GGC	GCC	
GUA	**ncm^{5}UAC**		GCA	**ncm^{5}UGC**		GAA	**mcm^{5}s^{2}UUC**	Glu	GGA	**mcm^{5}UCC**	
GUG	CAC		GCG	-		GAG	CUC		GGG	CCC	

FIG 2.4: Table showing cytosolic tRNAs subject of U_{34} modification. Eleven anticodons are interested. Seven tRNAs harbor a modification only in 5', three (namely $tRNA^{Lys}$, $tRNA^{Gln}$ and $tRNA^{Glu}$) also a thiolation in 2'. $tRNA^{Leu}$ has instead a methylation in 2'. Image taken from Johansson MJO *et al.* 2008.

Studies on the mechanisms involved in biosynthesis of such modifications are as old as the identification of modified nucleosides themselves, with first experimental evidences on intermediates of these reactions in 1970 (Tumaitis *et al.* 1970). Today is known that the 5' modification follows a sequential reaction and involves several gene products (at least 13), and most recent findings propose two alternative mechanisms. To this part the function of Elongator complex and Trm9/Trm112. Thiolation in 2' terminus requires at least other 8 genes and is a complex process partially residing on mitochondrial Fe/S clusters assembly, but independent from 5' modification enzymes. A brief overview on the mechanism will now be given.

Modification in 5': Elongator: One of the major contribution to the analysis of wobble base chemical modification pathways comes from the existence of a particular yeast toxin: γ-toxin or zymocin. Zymocin is a plasmid encoded toxin produced by killer

strains of *Kluyveromyces lactis*, made of three subunits (αβγ). A and β serves as docking factors and facilitator of γ subunit into target cells. Studies on the toxicity induced mechanism of γ subunit revealed its role of nuclease, with particular specificity in modified wobble base of tRNAs. Zymocin can digest tRNAs only if they harbor specific modifications in uridine 34 and thus all the null mutants in genes for biosynthesis of such modifications became resistant to the toxic effects. Gamma-toxin can be endogenously produced in *S. cerevisiae* strains with appropriate expression plasmids. This provides an excellent genetic strategy for the identification of genes involved in wobble bases chemical modification, excluding all the mutants resistant to exogenous toxin for different reasons (i.e. cell wall, permeability).

Elongator complex is an highly conserved multitasking enzyme (Svejstrup 2007; Versées *et al.* 2010). Its roles range from assisting RNApolII in the elongation phase and chromatin remodeling (H3 H4 histones acetylation, HAT) to exocytosis, all experimentally proven. Deficiencies in Elongator are commonly associated to the rare genetic disorder Familial Dysautonomia (Slaugenhaupt *et al.* 2002) while particular variants to motor neuron degeneration (SLA) (Simpson *et al.* 2008). The complex is formed of two discrete subcomplexes for a total of six subunits: Elp1-Elp2-Elp3 and Elp4-Elp5-Elp6 (Winkler 2001). The only essential gene is Elp5, even if Elp3p is probably considered the most important subunit and the center of catalytic activities. It harbors a potential acetyl-CoA binding site and a region of homology to the Radical SAM superfamily, an enzymatic class that use Fe/S clusters and methyl donor S-adenosylmethionine to perform radical reactions. Elp3p was recently proven to contain a functionally important Fe/S cluster whom proposed role is to structure the Elp3p domain and assist in a function unrelated to the HAT one (Paraskevopoulou *et al.* 2006; Greenwood *et al.* 2008).

FIG 2.5: Structure of modified uridines, R stands for ribose. Image taken from Huang B. *et al* 2005.

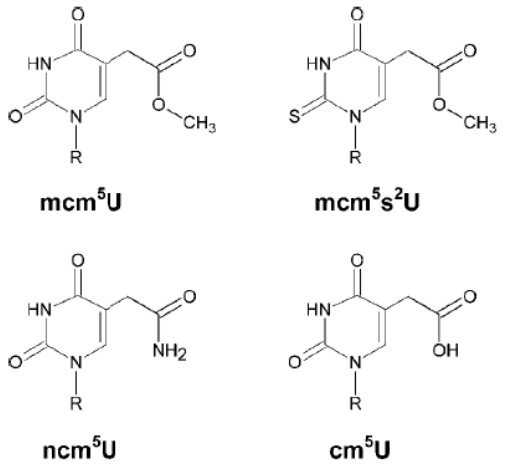

All *elp* null mutants were shown to be resistant to zymocin (Butler *et al.* 1991; Butler *et al.* 1994; Frohloff *et al.* 2001), suggesting a role in the resistance to this toxin. This was initially related to the well known functions of Elongator complex (Jablonowski *et al.* 2001). In 2005 a connection between Elongator complex (all Elp subunits) plus three other toxin resistance genes (*KTI11 KT12 KTI13*) and loss of modified uridines was found. Moreover the molecular mechanism of γ-toxin was explained: a nuclease that targets and cleaves specifically tRNAs modified in U_{34} with an ncm^5, mcm^5 and mcm^5s^2 (Huang *et al.* 2005; Lu 2005). The yet proposed role of Elongator in the early step of U_{34} modification was further demonstrated by HPLC on purified tRNAs showing a complete loss of ncm^5 and mcm^5 modifications, but not s^2 that was still observed in tRNAs with naturally occurring mcm^5s^2 modification. Moreover a physical interaction between Elp1p and Elp3p with $tRNA^{Glu}_{UUC}$ was shown, concomitantly with a functional importance of the potential acetyl-CoA binding site (Huang *et al.* 2005). As general comment should be noted how Elongator role is complex and pleiotropic and could be very difficult to dissect each function with relatives cause-effects relationships. Interestingly an almost total suppression of *elp*$^-$ phenotypes was recently achieved by overexpression of two tRNA (Esberg *et al.* 2006). This would push to a central role of Elongator complex in tRNA modification. The proposed molecular role of Elongator complex will be further discussed.

Modification in 5': Trm9/Trm112: Last theoretical step in the biosynthesis of mcm^5 and ncm^5 groups is the esterification of cm^5 to ncm^5 or mcm^5. Although the enzyme(s) responsible for the former has yet to be discovered, the biosynthesis of mcm^5 and the subsequent thiolation to mcm^5s^2 are more characterized processes.

YML014W gene codes for a methyltransferase, later named Trm9 (Kalhor *et al.* 2003). This enzyme is part of a big family of yeast transferases involved in the methylation of different tRNA positions. For instance Trm5 forms 1-methylguanosine (m1G37) at position 37 of tRNA (Bjork *et al.* 2001). Trm9p was clearly demonstrated to be essential in the biosynthesis of mcm^5 substituents using S-adenosylmethionine (SAM) as methyl donor. This was directly shown *via* HPLC analysis of defective products, identified as $tRNA^{Arg}_{UCU}$ and $tRNA^{Glu}_{UUC}$ lacking their mcm^5 modification. In total accordance to chemical data, a *trm9* null mutant shows resistance to zymocin (Lu 2005). Trm9p was found to interact with Trm112p, a 15Kda protein with a zinc finger domain (Gavin *et al.* 2002). Initial results on Trm9p were indicating that it could work by itself, as trace of mcm^5 could be detected complementing a *trm9* null mutant with *E. coli* Trm9p homolog (Kalhor *et al.* 2003). Conversely it was recently shown that the physical partner Trm112p was essential for methylase activity in yeast

(Studte *et al.* 2008; Mazauric *et al.* 2010). Trm112p seems to work as a sort of activator for a number of yeast methylases, with at least 6 physically proven interactor (Fig 2.6). All of them share a Rossman fold, typical of enzymes that use SAM as cofactor. Only Lys9p is not a methylase and is the only one lacking a complete Rossman fold (Mazauric *et al.* 2010). Trm11p is a tRNA methylase, catalyzing the formation of m^2G at position 10 (Purushothaman *et al.* 2005). Mtq2p is involved in the methylation of the class I terminator factor eRF1. The structure of Mtq2/Trm112 complex was recently determined and the proposed role for Trm112p is to improve binding of SAM and activate the Mtq2p catalytic site (Liger *et al.* 2011). Based on bioinformatics analysis and predictions, was postulated that the mechanism by which Trm112p works would be conserved also with other physical partners as the aforementioned Trm9p.
Noteworthy, as Elongator complex, also Trm9p is highly conserved in evolution.

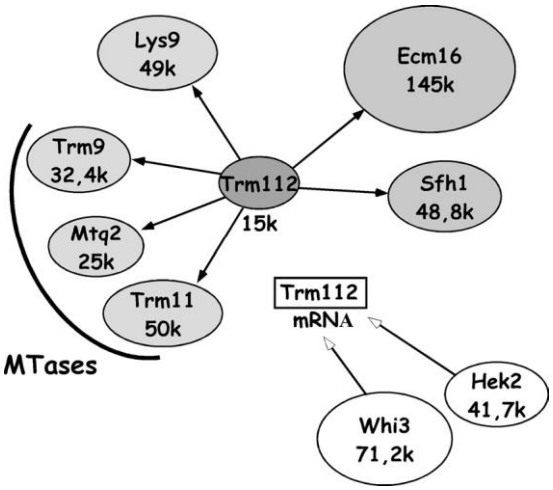

FIG 2.6: Physical partners shared by the "hub" protein Trm112p. Image taken from Mazauric MH *et al. 2010.*

Modification in 5': proposed mechanisms: All the biochemical and genetical results can be fitted in one linear mechanism, shown in Figure 2.7a. Elongator complex and potential regulators perform a first step of modification that might comprise an acetyl-CoA intermediate. This leads to a cm^5U_{34}. A yet unidentified enzyme may know use this intermediate to a final trans-esterification to ncm^5U_{34}. Conversely, the well-characterized Trm9/Trm112 complex uses the cm^5U_{34} for the final production of mcm^5U_{34} with a SAM based methylation. A line of evidence recently obtained strongly challenges this mechanism, leading to the proposal of an alternative path (Chen *et al.* 2011). The exhaustive HPLC analysis on tRNAs extracted from *trm9* and *trm112* null mutants wasn't successful in isolating the cm^5U_{34} intermediate, but rather shown an accumulation of $ncm^5(s^2)U_{34}$. This was fitted to a model in which Elongator

complex produces an ncm^5 modification immediately thiolated to $ncm^5s^2U_{34}$ or used by Trm9/Trm112 as substrate. In this case an unknown factor, or Trm9/Trm112 itself would convert ncm^5 to cm^5 and then catalyze the characterized reaction to mcm^5. This model is represented in figure 2.7b.

In order to expand the list of genes directly involved in wobble modification resistance to γ-toxin was a strategy widely used, as mentioned above. Of remarkable interest is the implementation of such phenotype in genome-wide screenings. From an analysis of 4826 homozygous diploid *S. cerevisiae* mutants, 63 were scored as resistant to γ-toxin, expanding the knowledge about this pathway and supporting other concomitants experimental findings (Huang *et al.* 2008).

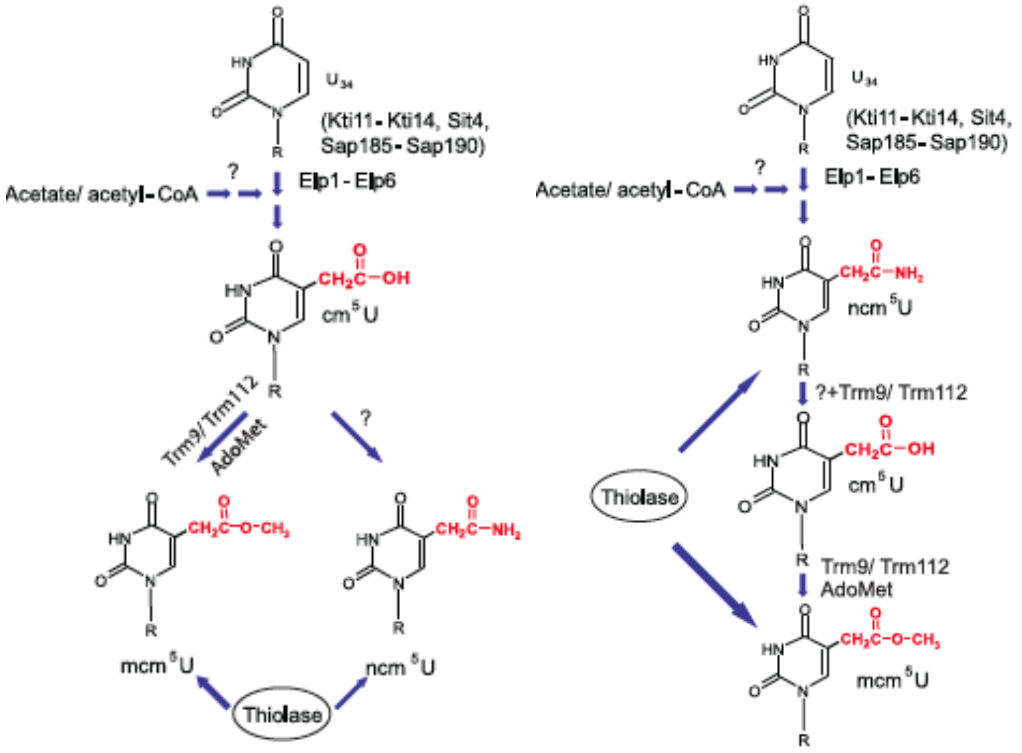

FIG 2.7: (left) original mechanism proposed on experimental evidences until identification in *trm9* null mutants of ncm^2U_{34} accumulation. **(right)** Alternative mechanism. Images taken from Chen C *et al* 2011.

Modification in 2': substitution of 2'-O with a thiol group

Largest contribution to the study of U_{34} thiolation has been given by Suzuki T. research group. Using an approach called "ribonucleome analysis" (a genome-wide reverse genetic technique combined with mass spectrometry) a total of 767 *S. cerevisiae* null mutants were analyzed, looking for defects U_{34} thiol derivatives (Noma *et al.* 2008). This led to the identification of four genes previously not known with specific defects in thiolation: *YHR111w (UBA4), YNL119w (NCS2), YGL211w (NCS6)* and *YOR251c* (named *TUM1*). These have to be added to the already identified *NFS1* (Nakai *et al.* 2007). Nfs1p is a cysteine desulfurase that receive a sulfur atom in the form of persulfide, used to catalyze other reactions. The sulfur is indeed transferred in the mitochondria to intermediate acceptors during Fe/S assembly, or shuttled to tRNA thiolation *via* other proteins. In *E. coli* a series of factors (TusA, TusB, TusC, TusD and TusE) transfer sequentially the persulfide to the final MnmA acceptor and eventually to the tRNA (Ikeuchi *et al.* 2006; Numata *et al.* 2006). *S. cerevisiae* uses a similar flow in the first steps, but a different chemistry for the last ones, involving a sulfur transfer with an ubiquitin-related process.

Besides the identification of the five genes involved, a hint into molecular mechanism has been given by *in vitro* analysis. Tum1p is protein containing a rhodanese-like domain in its C-terminus, with catalytic center in the Cys residue 259. This activates Nfs1p and receives a persulfide that is then shuttled in the same way to Uba4p on Cys397. Urm1p is an ubiquitin-related modifier, and its conjugation to a target (urmylation) depends on Uba4p, an E1-like activating enzyme (Furukawa *et al.* 2000). Urm1p forms a thioester link with Uba4p and in this activated form receive the sulfur atom on a C-terminal glycine, in thiocarboxylated form. Eventually the Ncs2/Ncs6 complex transfers the thiocarboxyl group to a tRNA (Nakai *et al.* 2008; Noma *et al.* 2008).

This process relies on at least five other genes, already known. These comprise three genes coding for proteins of the cytoplasmic Fe/S assembly machinery (CIA), namely Cfd1p Nbp35p and Cia1p. The role of these proteins could be only related; giving that at least one protein of the pathway (Elp3p) requires a Fe/S cluster for its activity, although not in the thiolation step. More intriguingly is the role of Isu1p and Isu2p. Those proteins are scaffold for the mitochondrial Fe/S clusters assembly. Their presence is necessary for cytoplasmic tRNA modification, but not for mitochondrial ones. A possible explanation is related to the Nfs1p localization: clearly mitochondrial, also if recently was localized to the nucleus too (Naamati *et al.* 2009). Nfs1p desulfurase activity in Fe/S is then performed in mitochondria, with the help of

Isu1p and Isu2p. Tum1p was shown to be both mitochondrial and cytoplasmatic and it could work as a shuttle protein between mitochondria and cytosol, receiving a persulfide in the former and delivering to Uba4p in the latter. Nfs1p would be used in both processes on the scaffold built of Isu1p and Isu2p, donating a persulfide to Isd11p or to Tum1p.

2.1.5 tRNA Import into Mitochondria

Being essential for life every organism has of course a complete set of tRNA genes, transcribed by RNA polymerase III. The number of genes varies greatly among different organism, from few hundreds (299 in *S. cerevisiae*) to thousands. Also organelles have sets of tRNA genes, but in this case many particularities can be found. Besides human and yeast mitochondrial genomes, that code for a complete set of tRNAs, many species are known to have incomplete sets of mitochondrially encoded tRNAs. As mitochondrial translation is a fundamental process, this lead to the conclusion that nuclear encoded tRNAs have to be imported in mitochondria. For instance kinetoplastids as *Leishmania* and *Trypanosoma* totally lack mitochondrial tRNAs and have to import the whole set (Rubio Mary Anne T. *et al.* 2011). Organisms like *Trypanosoma bruceii* are known to have a free procyclic stage, in which they parasitizes a vector like flies, and a bloodstream stage in a vertebrate host. Their metabolic necessities change in dependence to the stage and mitochondria can be completely transformed from a cristae-absent to cristae-rich organelles. Such an extensive remodeling process might be faster under a complete control of the nucleus thus justifying a complete migration of these genes from mitochondrial to nuclear DNA (Alfonzo *et al.* 2011). The first experimental proof of nuclear encoded tRNA import into mitochondria was given in 1967 in *Tetrahymena pyriformis* (Suyama 1967). To date tRNA import into mitochondria has been proven in a wide range of organisms, and recently also in mammals (Rubio M. A. *et al.* 2008). In organisms where a complete set of tRNAs is present in mitochondrial genome, the role of the imported ones is still in controversial. Only in last years some cases have been clarified, showing a functional importance of this process under particular stress conditions. This will be further discussed.

After proving the mitochondrial tRNA import, the next step has been to focus on the mechanism involved and on aspects like targeting, selectivity and regulation of the process. These processes are still largely unknown and with great variety from organism to organism, underlining a sort of evolutionary convergence of different mechanisms to a common essential event (Salinas *et al.* 2008).

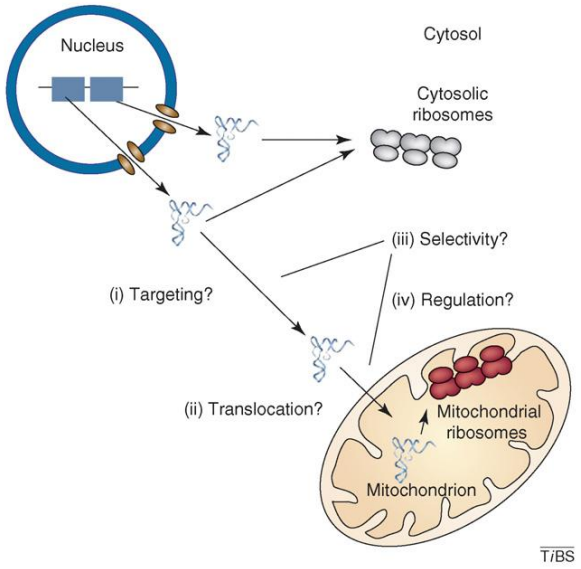

FIG 2.8: Critical steps in mitochondrial tRNA import process. Image taken from Salinas T *et al.* 2008.

Last review from Rubio MAT and colleagues, separated in two broadly classes the import mechanisms: type A and type B (Rubio Mary Anne T. *et al.* 2011). Type A is based on the canonical protein import system (i.e. TOM/TIM complexes) and requires ATP, membrane potential and cytosolic factors (Tarassov *et al.* 1995). This class is based on the only known example: the yeast $tRNA^{Lys}_{CUU}$. *S. cerevisae* harbors three different Lys tRNAs named tRK1 ($tRNA^{Lys}_{CUU}$), tRK2 ($tRNA^{Lys}_{UUU}$) and tRK3 ($tRNA^{Lys}_{UUU}$). tRK1 and tRK3 are nuclear encoded and tRK2 mitochondrial. tRK3 is exclusively cytoplasmic while tRK1 can be partially imported. The mechanism by which tRK1 is imported is quite fascinating. After aminoacylation in the cytosol, tRK1 is specifically recognized by one of the two isoforms of glycolytic enzyme enolase (Eno2p). Eno2p is known to be part of a macro complex of the mitochondrial outer membrane thus working also as a specific targeting system for tRK1 (Brandina *et al.* 2006). On the mitochondrial outer membrane tRK1 is associated to the pre-mito LysRS (preMSK1p), enzyme responsible for the aminoacylation of tRK3 in the mitochondria. The complex is now translocated in the mitochondrial matrix *via* TOM/TIM translocases (Tarassov *et al.* 1995; Entelis N. S. *et al.* 1998; Entelis N. *et al.* 2006). Regulation of the process is interestingly associated with ubiquitin/26s proteasome system. Genetic analysis indeed identified three proteins interacting with tRK1 or preMSK1p: Rpn13p, Rpn8p and Doa1p. Inhibition of the proteasome cellular activity decreases tRNA import of tRK1 while deletion of either *RPN13* or *DOA1* stimulates it (Brandina *et al.* 2007).

Type B (figure 2.9) is referred to all the other mechanisms that work independently from TOM/TIM canonical complexes. This class is still the most controversial, in which experimental proofs are present, but the real mechanism still poorly

understood. In mammals, $tRNA^{Gln}_{CUG}$ and $tRNA^{Gln}_{UUG}$ are imported in mitochondria. This requires ATP but not the mitochondrial membrane potential. In plants the anion channel VDAC is necessary and in kinetoplastids a complicated system in the inner membrane (RIC) was identified, relying also on the Complex III Rieske protein RIC6 (in *Leishmania tropica* but not in *Tripanosoma bruceii*). An outer membrane complex for tRNA import of kinetoplastids is still lacking. See Rubio MAT *et al.* 2011 and Salinas T *et al.* 2008 for review.

To date *S. cerevisiae* is the only organism in which both A and B types of tRNA import are proven to coexist. $tRNA^{Gln}_{CUG}$ and $tRNA^{Gln}_{UUG}$ are imported in a type B fashion. Rinehart and coworkers demonstrated the import of two $tRNA^{Gln}$ isoforms with specific RT-PCR on purified mitochondrial tRNA. Again the import was observed *in vitro* on purified mitochondria, process relying on ATP but not on other cytosolic factors.

Although experimental proofs of the import exist, understanding biological significance of these events is still a great challenge. Why organisms like *S. cerevisiae* and *Homo sapiens* still import tRNAs from cytosol to mitochondria when harboring a complete mitochondrial set? The only case totally understood is $tRNA^{Lys}_{CUU}$ in yeast and involves wobbling rules at anticodon base U_{34}. As previously described *S. cerevisiae* has three $tRNA^{Lys}$ genes: tRK1 ($tRNA^{Lys}_{CUU}$, cytosolic and mitochondrial), tRK2 ($tRNA^{Lys}_{UUU}$, cytosolic) and tRK3 ($tRNA^{Lys}_{UUU}$, mitochondrial). tRK3, exclusively mitochondrial, harbors a UUU anticodon with an $mnm^5s^2U_{34}$ modification thus being able to decode AAA lysine codon and wobbling to AAG. At 37˚C tRK3 is not correctly modified provoking a translational deficit in mitochondrial proteins with AAG codons (Var1p and Cox2p). Become clear the essential role of tRK1 import at 37˚C that complements the decoding deficiencies of hypomodified tRK3 allowing the correct translation of Var1p and Cox2p (Kamenski *et al.* 2007). Conversely is not clear which role $tRNA^{Gln}_{CUG}$ and $tRNA^{Gln}_{UUG}$ isoforms have in yeast and mammals mitochondria after import. At least in yeast was demonstrated that $tRNA^{Gln}_{CUG}$ is used in mitochondrial protein synthesis. Creating a nuclear suppressor $tRNA^{Gln}_{CUA}$ a mitochondrial *cox2-114*^{UAG} allele (harboring a non sense mutation) was suppressed. Presence of translated protein was confirmed by western blot but strangely no complementation of RD phenotype was observed (Rinehart 2005).

FIG 2.9: Type A and Type B of tRNA mitochondrial import. Image taken from Rubio MAT *et al.* 2011.

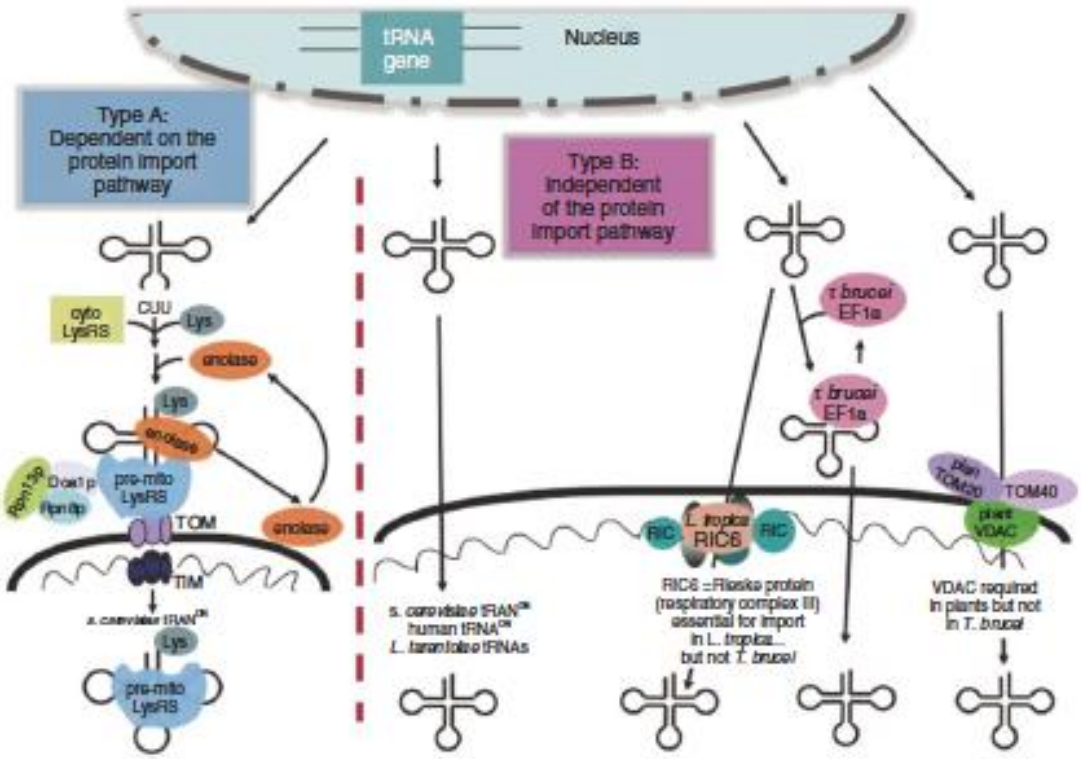

Of remarkable interest in tRNA import mechanism is how selectivity and targeting are achieved. In these cases probably we have the most variability among different species. Among different examples, excellently reviewed in Salinas *et al.* 2008, very intriguingly is $tRNA^{Glu}_{UUC}$ and $tRNA^{Gln}_{UUG}$ in *Leishmania tarantolae*. The selectivity here is based again on the chemical modification of wobble base U_{34}. Specific tRNAs from cytosol and mitochondria were isolated and characterized using mass spectrometry. The only difference that could be detected was the total absence of thiolation in U_{34} in the mitochondrial imported isoforms. In this specific genus the 2'-thiolation could therefore play an inhibitory role on tRNA import (Kaneko *et al.* 2003). On the other side, in the related kinetoplastids *Tripanosoma bruceii* it was shown that thiolated tRNAs are efficiently imported in mitochondria and dethiolated afterward (Bruske *et al.* 2009).

All these rules and examples show again how tRNA chemical modification is an important process, used not only for the expansion of decoding capacities but also to target and select tRNAs. This chemical targeting is very specific and variable among the evolution. One of the most intriguing aspects is how the process could be

regulated and integrated in the cellular network. Recent findings strongly suggest that tRNA chemical modification can be an essential response to extracellular and intracellular stresses. Modification could be reprogrammed during stresses, fine-tuning the performance of translation *via* tRNAs structure, decoding capacity or subcellular localization. A recent high-throughput analysis of *S. cerevisiae* tRNAs chemical modification under four different stresses (MMS, H_2O_2, $NaAsO_2$ and NaOCl) strongly support this idea (Chan *et al.* 2010).

2.2 Results and Discussion

2.2.1 Cytoplasmic tRNAs Chemical Modification is Essential for Mitochondrial Function at 37˚C

A genome wide screening focused on mitochondrial biogenesis at 37˚C was performed and results are described in Chapter 1 of this dissertation. Briefly 4688 *S. cerevisiae* haploid strains were tested for growth on non-fermentable carbon source ethanol, at 30 and 37˚C. A total of 488 strains resulted defective and 177 were selected as new candidates. Those genes were never related to mitochondrial biogenesis or their function at the moment of the screening was yet poorly understood. Their OXPHOS phenotype was later confirmed on different carbon sources. Cytochrome spectra profiles and respiratory rates were analyzed at 37˚C and used as parameters to organize deletants in phenotypic classes. Four classes were created accordingly to phenotype severity, ranging from A (very severe phenotype) to D (no evident defects).

Gene Ontology analysis on the mentioned datasets allowed identifying enriched functional classes. Strikingly among 88 new candidates (from 177 list) with a specific phenotype at 37˚C functional classes *"tRNA wobble uridine modification"* (child term of *"tRNA chemical modification"* and *"tRNA wobble base modification"*) and *"protein urmylation"* were significantly enriched (Table 2.1).

As described in section 2.1.3 wobble uridine (U34) in the anticodon of eleven cytoplasmic tRNAs is chemically modified. Carbamoylmethyl group (ncm) or a methoxycarbonylmethyl (mcm) are added in 5' position of U_{34}. $tRNA^{Lys}$, $tRNA^{Glu}$ and $tRNA^{Gln}$ are additionally modified with a thiol group in position 2' giving rise to the modified base $mcm^5s^2U_{34}$. Introduction of methyl and thiol groups was demonstrated to be necessary to modulate decoding capacities and fine-tuning tRNA performance. In some cases modification was essential in physiological conditions but different evidences associated this kind of modification to cellular stresses as DNA damage or oxidative stress (Begley *et al.* 2007; Chan *et al.* 2010).

Up to three steps are required for a complete modification: a first methylation catalyzed by Elongator complex, a second methylation by Trm9p/Trm112p and a final thiolation starting with cysteine desulfurase Nfs1p and concluding with functional pair Ncs2/Ncs6 that transfer the thio group to the final tRNA acceptor. At least 26 genes, reported in table 2.2, are clearly involved in the three steps. A detailed description of the mechanisms and reactions involved is provided in section 2.1.3.

TABLE 2.1: Biological Processes significantly enriched at 37˚C. For details see text in section 1.2.4 of this dissertation.

GO TERM	BIOLOGICAL PROCESS	p-value	genes
GO:0002097	tRNA wobble base modification	5.02E-11	9
GO:0002098	tRNA wobble uridine modification	5.02E-11	9
GO:0006400	tRNA modification	5.48E-07	9
GO:0032447	protein urmylation	1.45E-06	4
GO:0045324	late endosome to vacuole transport	1.12E-05	6
GO:0015031	protein transport	1.17E-05	21

TABLE 2.2: 26 genes involved in wobble base modification of cytoplasmic tRNAs. See 2.1.3 for details.

GENE	Note	YPE30˚C	YPE37˚C	LIST	OXPHOS	CLASS	R. EFF%
ELP1	Elongator Complex	0	HS	177	yes	C	36
ELP2	Elongator Complex	0	HS	177	yes	B	30
ELP3	Elongator Complex	0	MS	177	yes	B	50
ELP4	Elongator Complex	0	HS	177	yes	A	8
*ELP5**	Elongator Complex						
ELP6	Elongator Complex	0	HS	177	yes	B	29
*KTI11**	Elongator Complex						
KTI12	Elongator Complex	0	MS	177	yes	C	41
KTI13	Elongator Complex						
*KTI14**	Elongator Complex						
*SAP185***	Elongator Complex						
*SAP190***	Elongator Complex						
SIT4	Elongator Complex	MS	HS	488			
TRM9	Trm9p/Trm112p	0	MS	177	yes	B	43
*TRM112**	Trm9p/Trm112p						
TUM1	Thiolation Step						
UBA4	Thiolation Step	0	MS	177	yes	B	33
URM1	Thiolation Step	0	LS	488			
NCS2	Thiolation Step						
NCS6	Thiolation Step	0	MS	177	yes	D	81
*NFS1**	mt/cy Fe/S Cluster						
*ISU1***	mt/cy Fe/S Cluster						
*ISU2***	mt/cy Fe/S Cluster						
*CFD1**	cy Fe/S Cluster						
*CIA1**	cy Fe/S Cluster						
*NBP35**	cy Fe/S Cluster						

*deletant not present in the haploid deletants collection used.
**only double mutants show phenotype (*sap185Δsap190Δ* and *isu1Δisu2Δ*)
underlined genes were found to be not sensitive in tested condition.

Out of 26 mentioned genes 11 were identified in the mentioned screening as essential for mitochondrial biogenesis at 37˚C.

Among 15 genes of the pathway not identified, 8 corresponding null mutants were not present in the collection used for the screening (*ELP5, KTI11, KTI14, TRM112, NFS1, CFD1, CIA1, NBP35*). For five of those the corresponding null mutant is unviable. The three others were not included in the deletion project for reason unknown.

Relatively to *ISU1/ISU2* and *SAP185/SAP190* was demonstrated a concerted role in tRNA modification and impairments in the pathway could be observed only in corresponding double deletants (Nakai *et al.* 2007; Huang *et al.* 2008). Eventually only three null mutants corresponding to genes of the pathway were found to be not sensitive in the tested conditions (*KTI13*, *TUM1* and *NCS2*).

For 9 out of 11 identified mutants an OXPHOS impairment under stress condition was demonstrated for the first time and all displayed a specific severe phenotype (MS or HS). For 2 genes, *SIT4* and *URM1*, a role in mitochondrial biogenesis was already reported even if related to aspects different from tRNA chemical modification. Indeed *URM1* is yet involved in urmylation process, an ubiquitin-related protein modification, and its deletion was already identified in mitochondria genome-wide analysis (Luban *et al.* 2005). Targets of this non-canonical modifier are also involved in oxidative stress and apoptosis in both *S. cerevisiae* and mammalian cell lines (Van der Veen *et al.* 2011; Wang F. *et al.* 2011).

A deletion in *SIT4*, a 2A type serine-threonine phosphatase, was already shown to cause a defective growth in glycerol media at 30˚C (Dimmer 2002), confirmed also in the present screening. The defect was subsequently addressed and related to a carbohydrate metabolism shift toward a futile glycogenesis with consequent deprivation of Krebs cycle intermediates, detrimental for the cell (Jablonka *et al.* 2006). Independently, other mitochondrial related phenotypes were also observed in *sit4* mutants as oxidative stress sensitivity or cytoskeleton abnormalities (SGD).

As just mentioned the identified pathway targets cytoplasmic tRNAs. Many organisms are known to import cytosolic tRNAs in mitochondria with a role in some cases totally proven and obvious and in others only hypothetical or totally unknown. As pointed out in 2.1.5 some *species* do not harbor a complete set of mitochondrial tRNAs and import from cytosolic pool is obviously essential for mitochondrial protein synthesis. However genus like *H. sapiens* and *S. cerevisiae* harbor complete sets of mitochondrial tRNAs but still import cytosolic ones. In *S. cerevisiae* $tRNA^{Lys}_{CUU}$, $tRNA^{Gln}_{CUG}$ and $tRNA^{Gln}_{UUG}$ import have been clearly demonstrated and at least for

$tRNA^{Lys}_{CUU}$ the mitochondrial function is clear (Martin *et al.* 1979; Rinehart 2005; Rubio M. A. *et al.* 2008). Furthermore $tRNA^{Gln}_{CUG}$ and $tRNA^{Gln}_{UUG}$ are imported also in mammal mitochondria but the functional role of this event remains unclear (Rubio M. A. *et al.* 2008).

Out of the three cytosolic tRNAs found in mitochondria only $tRNA^{Gln}_{UUG}$ is modified through all the three steps of the aforementioned pathway (i.e. contains an $mcm^5s^2U_{34}$ wobble base). The role of this pathway and importance of the modification in fine-tuning the performance of tRNAs suggests that mitochondrial protein synthesis (MPS) could be the target from which depends a correct mitochondrial biogenesis at 37˚C. To this end different hypotheses can be proposed regarding the mechanisms underlying.

The first hypothesis concern a direct role of the modification pathway in MPS mediated uniquely by the imported cytosolic $tRNA^{Gln}_{UUG}$ whose role in mitochondria is still unknown.

The second hypothesis concern the import and a direct role of few other cytosolic tRNAs modified by the pathway rather then the unique $tRNA^{Gln}_{UUG}$. In this case import in mitochondria of these tRNAs would be still unproven.

The third scenario involves an indirect effect of these tRNAs on MPS *via* cytoplasmic defects. It is possible that loss of these modifications could impair cytoplasmic translation of proteins functional to the correct MPS. To this concern has to be noted that a similar effect was proposed to mediate *trm9Δ* sensitivity to DNA damage agents (Begley *et al.* 2007).

In order to shed some light into these hypotheses mitochondrial protein synthesis in mutants of the pathway was considered an essential experimental investigation. Three representative mutants were chosen resembling each of the essential steps in the modification pathway: ***elp3Δ*** (first methylation), *trm9Δ* (second methylation) and *ncs6Δ* (thiolation). Interestingly the three corresponding genes are conserved: *NCS6* is the yeast ortholog of human *CTU1,* which in combination with *CTU2* (*NCS2* in yeast) performs the same reaction (Dewez *et al.* 2008; Schlieker *et al.* 2008). *TRM9* is the yeast ortholog of *ALKBH8* and its functional partner *TRM112* is conserved too (ortholog of *TRMT112).* Also *ELP3,* coding the catalytic subunit of Elongator complex, is conserved in all *phyla.*

2.2.2 Phenotypical Analysis of ncs6Δ, trm9Δ and elp3Δ Null Mutants

Phenotypes relative to oxidative growth, cytochrome spectra profiles, oxygen consumption and mitochondrial DNA stability in *ncs6Δ*, *trm9Δ* and *elp3Δ* strains are reported in figure 2.10.

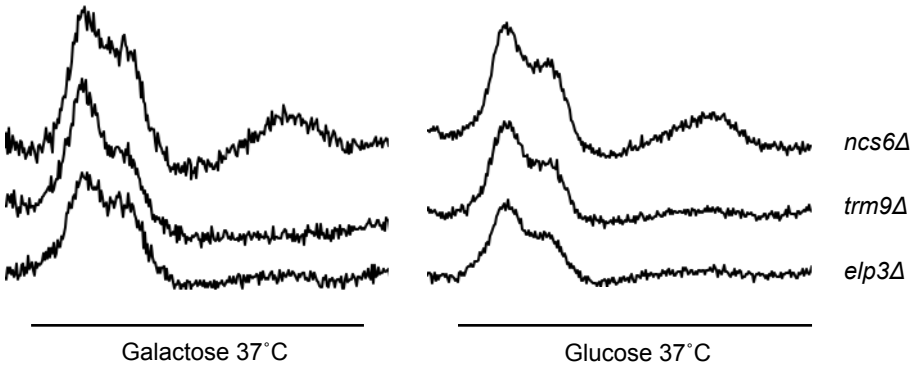

NAME	YPE 30˚C	YPE 37˚C	CLASS	R. EFF% Gal	R. EFF% Glu	petites (Gal)
NCS6	0	MS	D	86%	81%	1.4
TRM9	0	MS	B	43%	43%	1.1
ELP3	0	MS	B	55%	50%	1.5

FIG 2.10: Cytochrome spectra profiles and respiratory rates recorded in glucose and galactose media after 24hrs of incubation at 37˚C. Frequency % of spontaneous petite mutants in the population was assayed after growth of 24hrs at 37˚C in complete galactose media. Fold-values of frequency increase compared to wild type are reported for each mutant.

Growth phenotypes on oxidative carbon sources were similar for all the mutants at 37˚C, scored as medium sensitive (MS). Cytochrome spectra profiles recorded after growth in non-repressing glucose (0.6%) at 37˚C (as described in 4.2.3) allowed classification of *trm9Δ* and *elp3Δ* as class B mutants thus showing both qualitative and quantitative defects in mitochondrial respiratory chain. On the other hand *ncs6Δ* mutants displayed a cytochrome profile similar to a wild type strain (class D).

Oxygen consumption was markedly reduced in *trm9Δ* and *elpΔ* mutants, with efficiency rate of 43% and 50% of the wild type strain respectively. This decrease was less pronounced in *ncs6Δ* mutant, with efficiency as high as 81%.

Mutants were also assayed for cytochromes profiles and respiratory efficiencies after growth in complete galactose media under thermal stress. These analyses were performed to rule out any possible influence of this not-repressive fermentable carbon source usually implemented in MPS experiments. Cytochrome profiles at

37˚C in galactose media are comparable to that in low glucose even if slight differences could be observed. After growth in glucose *trm9Δ* strain displayed a small peak at about 603nm resembling residual COX complex that totally disappeared in galactose media. Nevertheless phenotypical classes are confirmed and respiratory efficiencies totally comparable thus concluding that the carbon source utilized could not influence final interpretation of the results.

Analysis of *petite* mutants accumulation was instead performed to exclude any correlation between observed MRC defects and potential instability of mitochondrial DNA in conditions used for cytochrome spectra analysis, oxygen consumption recording and MPS. *Petite* mutants indeed arise from spontaneous events of mitochondrial genome alteration as point mutation or recombination (with partial or total deletions) giving rise to ρ^- and ρ^0 genomes. To evaluate *petite* frequency the same cultures used for cytochrome spectra and respiratory efficiency evaluation has been used. Therefore 10ml pre-inoculations in YP galactose media are performed with strains previously purified of accumulated RD mutants. After over-night (o/n) incubation at 30˚C 150ml flasks of YP Gal 2% are inoculated and incubated for 24hrs at 37˚C in constant shacking at 120rpm. *Petite* frequency was estimated on aliquots from 150ml flasks. After serial dilutions 300 colonies are plated in fifth replicates on complete media containing ethanol 2% and 0.25% glucose. RD mutants grow until glucose is totally consumed, conversely wild type can shift to ethanol metabolism and continues to divide; *petite* mutants can therefore be distinguished by colony size.

As reported in figure 2.10 the *petite* frequency accumulation is very similar among the mutants with 1.1, 1.4 and 1.5 fold-increases for *trm9Δ, elp3Δ* and *ncs6Δ* respectively. Concerning *ncs6Δ* mutant appears clear that a *petite* accumulation 1.4 times higher then wild type is not index of extensive mtDNA damage as proven by a wild type cytochrome spectra profile. On these bases it is reasonable that structural defects observed in *trm9Δ* and *elp3Δ* mutants, showing petite accumulation comparable or even lower to *ncs6Δ*, should not be due to mtDNA mutations.

Interesting is the observation that *petite* frequency is quite different for both mutants and wild type in glucose and galactose media with a significantly higher accumulation in galactose media (data not shown).

2.2.3 Mitochondrial Protein Synthesis Is Impaired in elp3 and trm9 Null Mutants

Mitochondrial protein synthesis can be directly evaluated in a pulse experiment with ^{35}S-methionine in the presence of cycloheximide (inhibitor of cytoplasmatic translation). The protocol used (reported in section 4.2.5) requires normally cells grown in galactose media. Neo-synthetized products of mitochondrial translation were directly labeled with ^{35}S-methionine as described in 4.2.5 from cells grown at both 30 and 37˚C. Proteins were precipitated with TCA, resolved in SDS-page and transferred to nitrocellulose membrane.

A first analysis is reported in figure 2.11 and no differences could be observed at permissive temperature of 30˚C, results expected as none of the mutants displayed an OXPHOS negative phenotype in this condition. At 37˚C no evident reduction was observed in *ncs6Δ*. This leads to the conclusion that the enzymatic step impaired in ncs6Δ mutant, i.e. thiolation, does not have effects on MPS *per se*. This is in good agreement with the observed wild type cytochrome spectra profile.

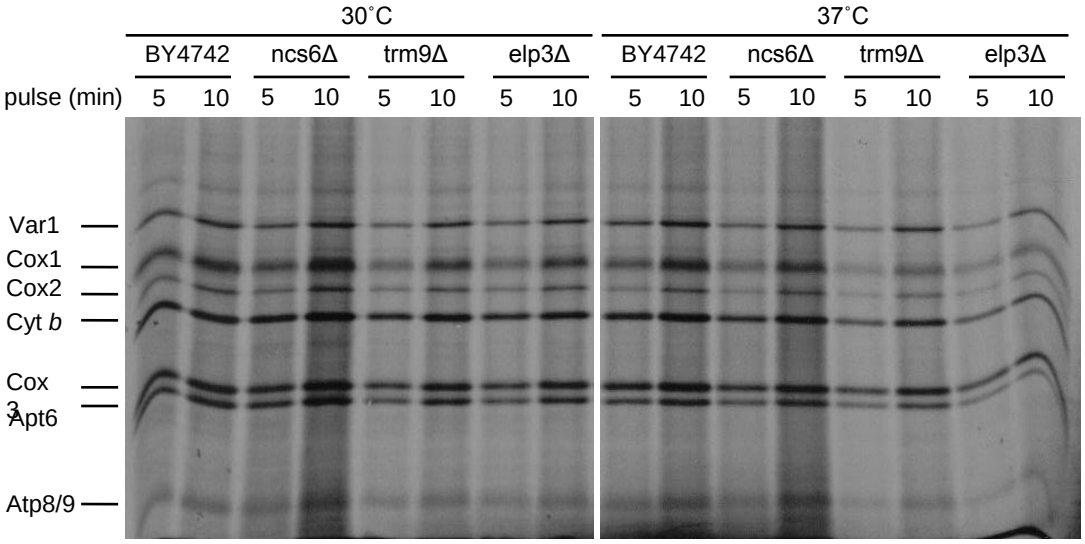

FIG 2.11: MPS analysis. Mitochondrial products of translation are labeled with ^{35}S-methionine in presence of cycloheximide, inhibitor of cytoplasmic translation. An equivalent of 0.6OD of cells was labeled for 5 and 10 minutes and total protein extracted, precipitated with TCA and resolved in SDS page (as described in 4.2.5). Autoradiography of MPS analysis carried out on cells grown at 30˚ and 37˚C for about 15 hrs is shown.

These results point out that OXPHOS negative phenotype observed at 37˚C for *ncs6Δ* mutant is not due to MPS defects. However it is known that *NCS6* plays a role not only in tRNA thiolation but in other processes like urmylation, a common ubiquintin-related post translational modification not involved in promoting proteolysis

but rather in nutrient sensing, budding and recently in oxidative stress response in *S. cerevisiae* (Goehring *et al.* 2003; Petroski *et al.* 2011). Also in the present screening, as reported in table 2.1, "*protein urmylation*" was among biological processes specifically enriched at 37˚C. Moreover different evidences indicate that *NCS6* gene product could be localized also in mitochondria without its functional partner Ncs2p (Huh *et al.* 2003; Nakai *et al.* 2008). Seems reasonable that Ncs6p in mitochondria could play a distinct role from tRNAs thiolation, may related to protein urmylation, whose defect is cause of the OXPHOS phenotype observed. This is also in agreement with the observation that *ncs2Δ* did not displayed any OXPHOS defects in the present screening. At this point "protein urmylation" pathway could be essential for mitochondrial biogenesis at 37˚C for its role in post-translational modification and not in modification of cytoplasmic tRNAs, as initially thought.

On the other hand extensive impairments were observed in *trm9Δ* and *elp3Δ* strains. Given the running distortions in *elp3Δ* lanes of the SDS-page (clear in the right panel in fig 2.11) to confirm the role of *TRM9* and *ELP3* in mitochondrial protein synthesis and better compare the effects on the single mitochondrial products two additional experiments were performed. Also the thermal stress was slightly increased performing growth and labeling at 38˚C to stress differences; results are shown in figure 2.12. Each protein band was afterwards quantified in both independent experiments for *trm9Δ* and *elp3Δ* strains and mean values were normalized to the synthesis rate of corresponding protein in wild type strain. The band intensities were thus converted in synthesis efficiencies (% of wild type) and results are shown in figure 2.12 panel b and c.

Autoradiography shows a decrease in MPS in *trm9Δ* strain especially in some mitochondrial products. Quantification reveals that: i) synthesis of Var1p and Atp6p (after 10 minutes of labeling) is comparable with that of wild type; ii) Cox1p and Cox2p result the most impaired products with synthesis efficiencies of about 55% and 65% respectively: iii) Cyt*b* and Cox3p are synthetized at about 70% and 80% of a wild type level respectively.

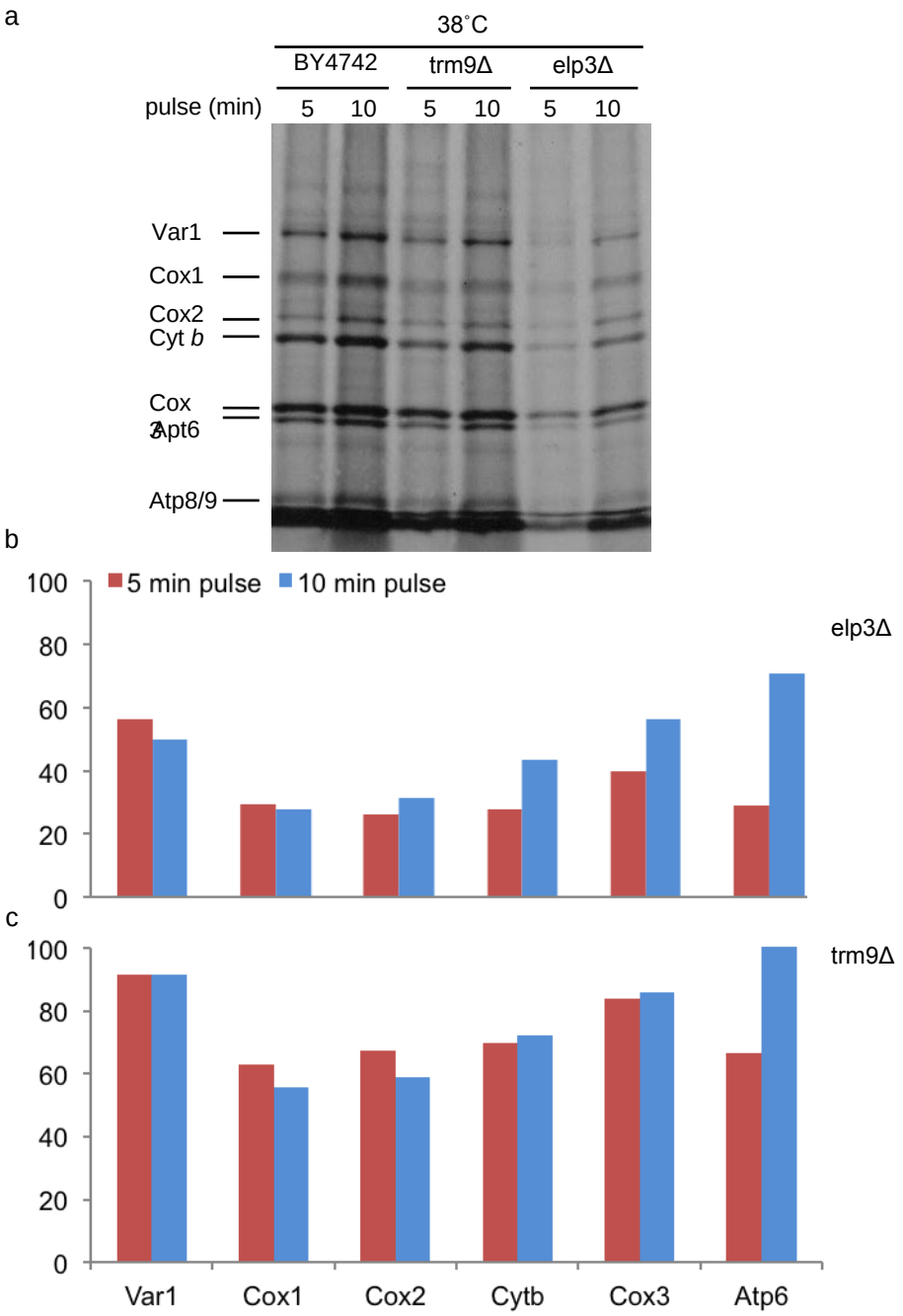

FIG 2.12: (a) Labeling of mitochondrial translation products with ^{35}S-methionine in presence of cycloheximide. Cells were grown about 15hrs at 38˚C on complete galactose media. An equivalent of 0.6OD of cells was labeled for 5 and 10 minutes and total protein extracted, precipitated with TCA and resolved in SDS page (as described in 4.2.5). **(b)(c)** Each band was quantified in two independent experiments (QuantityOne software). Mean values were calculated for each protein and then normalized to wild type (= 100%).

To rule out which of the proposed hypotheses is compatible with results obtained in MPS analysis a codon usage analysis was carried out. Frequency values for each codon whose corresponding tRNA is modified by the identified pathway (i.e. 11 different tRNAs) were calculated for the whole mitochondrial genome. A table (table

2.3) was then composed reporting for principal products of mitochondrial translation the frequency of each codon in the gene normalized to the overall mitochondrial genome occurrence. A value >100 means that a particular codon is over-represented in a gene, compared to the whole genome. Conversely a value <100 means low-occurrence of a particular codon in a given gene, always reported to the overall genome frequency. A 0.0 value mean that that particular codon in a gene is totally absent. If lack of a particular modification affects directly decoding of a particular codon it can be expected that proteins enriched in that codon could be specifically affected. This was previously demonstrated for tRK3 that being hypomodified at 37˚C was not able anymore to decode UUG lysine codons (Kamenski *et al.* 2007).

On the basis of codon frequencies the first hypothesis, focused a direct role in MPS of the sole cytosolic $tRNA^{Gln}_{UUG}$, can be discarded. Indeed Gln codons are equally distributed among principal products of MPS, and given this distribution an equal impairment in all the mitochondrial proteins was expected. For instance *Cyt* b is among the most impaired products while from its Gln codon distribution would suggest an opposite effect. The analysis for the other four codons susceptible of Trm9p modification revealed that the only tRNA for which codon frequency is compatible with experimental results is $tRNA^{Gly}_{UCC}$. Indeed Cox1p and Cox2p harbor significant over representation of Gly GGA codons and in MPS appeared as the most affected proteins. Conversely Var1p, that harbors no Gly GGA codons, is synthetized efficiently. These results would suggest that the second or the third hypothesis could be true: a direct participation of a cytosolic tRNA in MPS (cyt $tRNA^{Gly}_{UCC}$) or an indirect effect mediated through proteins translated in the cytosol.

More in general, effects of *TRM9* deletion are less severe then ones observed in *elp3* null mutation. A more diffused impairment in mitochondrial protein synthesis is indeed observed: i) Cox1p and Cox2p are the most affected proteins, synthetized at only about 28% and 31% of a wild type level; ii) Cyt*b*, Var1p and Cox3p are synthetized at 43, 50 and 56% of a wild type level; iii) a marked decreased in Atp6p synthesis was observed after 5 minutes of labeling, but the translation reached 70% of wild type at 10 minutes. The observation of a strong impairment in Var1p synthesis support the presence of other mechanisms involved rather then import of the unique cyt $tRNA^{Gly}_{UCC}$. However is difficult to imagine a direct role for all the remaining Elongator modified tRNAs based on an import mechanism still totally not supported. To this end a realistic interpretation could be that the identified pathway could affect MPS *via* a totally indirect effect, or based on a combination of a direct effect mediated by one or few imported tRNAs and indirect one.

TABLE 2.3: Mitochondrial genome codon usage analysis was performed in concern to 11 codons whose corresponding tRNA is chemically modified. Boxes are highlighted in light blue if a particular modification is present. Identity of chemical group added change in accordance: ncm^5 (first methylation only), mcm^5 (first and second methylation) and mcm^5s^2 (first, second methylation and thiolation). For each mitochondrial gene frequency of each codon are reported, normalized to mitochondrial genome occurrence. Boxes are highlighted in yellow for significant over representations.

tRNA	**Ala**	**Glu**	**Gly**	**Lys**	**Leu**	**Pro**	**Gln**	**Arg**	**Ser**	**Thr**	**Val**
codon	*GCA*	*GAA*	*GGA*	*AAA*	*TTA*	*CCA*	*CAA*	*AGA*	*TCA*	*ACA*	*GTA*
I°methyl.	*yes*	*yes*	*yes*	*yes*	*yes*	*yes*	*yes*	*yes*	*yes*	*yes*	*yes*
II°methyl.		*yes*	*yes*	*yes*			*yes*	*yes*			
thiolation		*yes*		*yes*			*yes*				
ATP6	60.2	85.6	88.1	104.2	103.1	137.9	87.7	113.3	131.4	102.7	114.6
ATP8	0.0	0.0	0.0	104.2	103.1	184.8	109.6	113.3	71.1	180.1	92.4
COB	150.6	114.1	97.9	104.2	101.9	129.6	73.5	113.3	122.8	75.6	105.4
COX1	144.5	101.6	161.6	104.2	101.9	121.3	97.6	113.3	140.0	135.1	122.0
COX2	120.4	107.3	122.4	91.7	104.2	126.9	97.6	113.3	116.3	113.5	68.4
COX3	123.5	114.1	102.8	104.2	103.1	91.0	109.6	113.3	94.8	84.6	110.9
OLI1	120.4	114.1	97.9	104.2	103.1	137.9	109.6	113.3	215.4	180.1	153.4
VAR1	0.0	114.1	0.0	99.0	99.7	0.0	109.6	68.0	40.9	23.4	37.0

The more severe effects observed in elp3Δ mutant in comparison to trm9Δ is compatible with the higher number of modified tRNAs that in turn can affect an higher number of proteins translated in the cytoplasm. Nevertheless it cannot be excluded that this worsening could be due to a different importance that ELP3 and TRM9 modifications might have on tRNAs biology. Is therefore known that tRNA chemical remodeling could be used to fine-tune tRNAs translation performances affecting directly decoding capacities, thermostability and folding properties. Different kind of cellular stresses (as oxidative stress and DNA damage) were shown to cause a significant change in tRNA chemical profile, favoring particular modifications (Chan *et al.* 2010).

Obtained results allowed demonstration that, in *S. cerevisiae,* Elongator and Trm9/Trm112 complex regulate mitochondrial protein synthesis under stress condition (37°C). Remain to be demonstrated which cytoplasmic proteins mediate this effect and/or other cytoplasmic tRNAs that could directly take part in mitochondrial protein synthesis process at 37°C.

2.3 References

Agris PF, Vendeix FAP and Graham WD (2007). "tRNA's Wobble Decoding of the Genome: 40 Years of Modification." Journal of Molecular Biology **366**(1): 1-13.

Alfonzo JD and Lukeš J (2011). "Assembling Fe/S-clusters and modifying tRNAs: ancient co-factors meet ancient adaptors." Trends in Parasitology **27**(6): 235-238.

Andersson DI, Bohman K, Isaksson LA and Kurland CG (1982). "Translation rates and misreading characteristics of rpsD mutants in Escherichia coli." Mol Gen Genet **187**(3): 467-472.

Arnez JG and Moras D (1997). "Structural and functional considerations of the aminoacylation reaction." Trends Biochem Sci **22**(6): 211-216.

Begley U, Dyavaiah M, Patil A, Rooney JP, DiRenzo D, Young CM, . . . Begley TJ (2007). "Trm9-Catalyzed tRNA Modifications Link Translation to the DNA Damage Response." Molecular Cell **28**(5): 860-870.

Bjork GR, Jacobsson K, Nilsson K, Johansson MJ, Bystrom AS and Persson OP (2001). "A primordial tRNA modification required for the evolution of life?" EMBO J **20**(1-2): 231-239.

Brandina I, Graham J, Lemaitre-Guillier C, Entelis N, Krasheninnikov I, Sweetlove L, . . . Martin RP (2006). "Enolase takes part in a macromolecular complex associated to mitochondria in yeast." Biochim Biophys Acta **1757**(9-10): 1217-1228.

Brandina I, Smirnov A, Kolesnikova O, Entelis N, Krasheninnikov IA, Martin RP and Tarassov I (2007). "tRNA import into yeast mitochondria is regulated by the ubiquitin-proteasome system." FEBS Lett **581**(22): 4248-4254.

Bruske EI, Sendfeld F and Schneider A (2009). "Thiolated tRNAs of Trypanosoma brucei are imported into mitochondria and dethiolated after import." J Biol Chem **284**(52): 36491-36499.

Butler AR, White JH, Folawiyo Y, Edlin A, Gardiner D and Stark MJ (1994). "Two Saccharomyces cerevisiae genes which control sensitivity to G1 arrest induced by Kluyveromyces lactis toxin." Mol Cell Biol **14**(9): 6306-6316.

Butler AR, White JH and Stark MJ (1991). "Analysis of the response of Saccharomyces cerevisiae cells to Kluyveromyces lactis toxin." J Gen Microbiol **137**(7): 1749-1757.

Chan CT, Dyavaiah M, DeMott MS, Taghizadeh K, Dedon PC and Begley TJ (2010). "A quantitative systems approach reveals dynamic control of tRNA modifications during cellular stress." PLoS Genet **6**(12): e1001247.

Chen C, Huang B, Anderson JT and Bystrom AS (2011). "Unexpected accumulation of ncm(5)U and ncm(5)S(2) (U) in a trm9 mutant suggests an additional step in the synthesis of mcm(5)U and mcm(5)S(2)U." PLoS One **6**(6): e20783.

Chen C, Tuck S and Bystrom AS (2009). "Defects in tRNA modification associated with neurological and developmental dysfunctions in Caenorhabditis elegans elongator mutants." PLoS Genet **5**(7): e1000561.

Cochella L and Green R (2005). "Fidelity in protein synthesis." Curr Biol **15**(14): R536-540.

Crick FH (1966). "Codon--anticodon pairing: the wobble hypothesis." J Mol Biol **19**(2): 548-555.

Dewez M, Bauer F, Dieu M, Raes M, Vandenhaute J and Hermand D (2008). "The conserved Wobble uridine tRNA thiolase Ctu1-Ctu2 is required to maintain genome integrity." Proc Natl Acad Sci U S A **105**(14): 5459-5464.

Dimmer KS (2002). "Genetic Basis of Mitochondrial Function and Morphology in Saccharomyces cerevisiae." Molecular Biology of the Cell **13**(3): 847-853.

Entelis N, Brandina I, Kamenski P, Krasheninnikov IA, Martin RP and Tarassov I (2006). "A glycolytic enzyme, enolase, is recruited as a cofactor of tRNA targeting toward mitochondria in Saccharomyces cerevisiae." Genes Dev **20**(12): 1609-1620.

Entelis NS, Kieffer S, Kolesnikova OA, Martin RP and Tarassov IA (1998). "Structural requirements of tRNALys for its import into yeast mitochondria." Proc Natl Acad Sci U S A **95**(6): 2838-2843.

Esberg A, Huang B, Johansson MJO and Byström AS (2006). "Elevated Levels of Two tRNA Species Bypass the Requirement for Elongator Complex in Transcription and Exocytosis." Molecular Cell **24**(1): 139-148.

Frohloff F, Fichtner L, Jablonowski D, Breunig KD and Schaffrath R (2001). "Saccharomyces cerevisiae Elongator mutations confer resistance to the Kluyveromyces lactis zymocin." EMBO J **20**(8): 1993-2003.

Furukawa K, Mizushima N, Noda T and Ohsumi Y (2000). "A protein conjugation system in yeast with homology to biosynthetic enzyme reaction of prokaryotes." J Biol Chem **275**(11): 7462-7465.

Gavin AC, Bosche M, Krause R, Grandi P, Marzioch M, Bauer A, . . . Superti-Furga G (2002). "Functional organization of the yeast proteome by systematic analysis of protein complexes." Nature **415**(6868): 141-147.

Goehring AS, Rivers DM and Sprague GF, Jr. (2003). "Urmylation: a ubiquitin-like pathway that functions during invasive growth and budding in yeast." Mol Biol Cell **14**(11): 4329-4341.

Goodman HM, Abelson J, Landy A, Brenner S and Smith JD (1968). "Amber suppression: a nucleotide change in the anticodon of a tyrosine transfer RNA." Nature **217**(5133): 1019-1024.

Goto Y, Nonaka I and Horai S (1990). "A mutation in the tRNA(Leu)(UUR) gene associated with the MELAS subgroup of mitochondrial encephalomyopathies." Nature **348**(6302): 651-653.
Goto Y, Nonaka I and Horai S (1991). "A new mtDNA mutation associated with mitochondrial myopathy, encephalopathy, lactic acidosis and stroke-like episodes (MELAS)." Biochim Biophys Acta **1097**(3): 238-240.
Greenwood C, Selth LA, Dirac-Svejstrup AB and Svejstrup JQ (2008). "An Iron-Sulfur Cluster Domain in Elp3 Important for the Structural Integrity of Elongator." Journal of Biological Chemistry **284**(1): 141-149.
Huang B, Johansson MJ and Bystrom AS (2005). "An early step in wobble uridine tRNA modification requires the Elongator complex." Rna **11**(4): 424-436.
Huang B, Lu J and Bystrom AS (2008). "A genome-wide screen identifies genes required for formation of the wobble nucleoside 5-methoxycarbonylmethyl-2-thiouridine in Saccharomyces cerevisiae." Rna **14**(10): 2183-2194.
Huh WK, Falvo JV, Gerke LC, Carroll AS, Howson RW, Weissman JS and O'Shea EK (2003). "Global analysis of protein localization in budding yeast." Nature **425**(6959): 686-691.
Ikeuchi Y, Shigi N, Kato J, Nishimura A and Suzuki T (2006). "Mechanistic insights into sulfur relay by multiple sulfur mediators involved in thiouridine biosynthesis at tRNA wobble positions." Mol Cell **21**(1): 97-108.
Jablonka W, Guzman S, Ramirez J and Montero-Lomeli M (2006). "Deviation of carbohydrate metabolism by the SIT4 phosphatase in Saccharomyces cerevisiae." Biochim Biophys Acta **1760**(8): 1281-1291.
Jablonowski D, Frohloff F, Fichtner L, Stark MJR and Schaffrath R (2001). "Kluyveromyces lactis zymocin mode of action is linked to RNA polymerase II function via Elongator." Molecular Microbiology **42**(4): 1095-1105.
Johansson MJO, Esberg A, Huang B, Bjork GR and Bystrom AS (2008). "Eukaryotic Wobble Uridine Modifications Promote a Functionally Redundant Decoding System." Molecular and Cellular Biology **28**(10): 3301-3312.
Kalhor HR and Clarke S (2003). "Novel Methyltransferase for Modified Uridine Residues at the Wobble Position of tRNA." Molecular and Cellular Biology **23**(24): 9283-9292.
Kamenski P, Kolesnikova O, Jubenot V, Entelis N, Krasheninnikov IA, Martin Robert P and Tarassov I (2007). "Evidence for an Adaptation Mechanism of Mitochondrial Translation via tRNA Import from the Cytosol." Molecular Cell **26**(5): 625-637.
Kaneko T, Suzuki T, Kapushoc ST, Rubio MA, Ghazvini J, Watanabe K and Simpson L (2003). "Wobble modification differences and subcellular localization of tRNAs in Leishmania tarentolae: implication for tRNA sorting mechanism." EMBO J **22**(3): 657-667.
Kirino Y and Suzuki T (2005). "Human mitochondrial diseases associated with tRNA wobble modification deficiency." RNA Biol **2**(2): 41-44.
Kobayashi Y, Momoi MY, Tominaga K, Momoi T, Nihei K, Yanagisawa M, . . . Ohta S (1990). "A point mutation in the mitochondrial tRNA(Leu)(UUR) gene in MELAS (mitochondrial myopathy, encephalopathy, lactic acidosis and stroke-like episodes)." Biochem Biophys Res Commun **173**(3): 816-822.
Kruger MK, Pedersen S, Hagervall TG and Sorensen MA (1998). "The modification of the wobble base of tRNAGlu modulates the translation rate of glutamic acid codons in vivo." J Mol Biol **284**(3): 621-631.
Lewin B (2004). Genes 8, Pearson Prentice Hall.
Liger D, Mora L, Lazar N, Figaro S, Henri J, Scrima N, . . . Graille M (2011). "Mechanism of activation of methyltransferases involved in translation by the Trm112 'hub' protein." Nucleic Acids Res **39**(14): 6249-6259.
Lu J (2005). "The Kluyveromyces lactis -toxin targets tRNA anticodons." Rna **11**(11): 1648-1654.
Luban C, Beutel M, Stahl U and Schmidt U (2005). "Systematic screening of nuclear encoded proteins involved in the splicing metabolism of group II introns in yeast mitochondria." Gene **354**: 72-79.
Martin RP, Schneller JM, Stahl AJ and Dirheimer G (1979). "Import of nuclear deoxyribonucleic acid coded lysine-accepting transfer ribonucleic acid (anticodon C-U-U) into yeast mitochondria." Biochemistry **18**(21): 4600-4605.
Mazauric MH, Dirick L, Purushothaman SK, Bjork GR and Lapeyre B (2010). "Trm112p is a 15-kDa zinc finger protein essential for the activity of two tRNA and one protein methyltransferases in yeast." J Biol Chem **285**(24): 18505-18515.
Motorin Y and Helm M (2010). "tRNA Stabilization by Modified Nucleotides." Biochemistry **49**(24): 4934-4944.
Naamati A, Regev-Rudzki N, Galperin S, Lill R and Pines O (2009). "Dual targeting of Nfs1 and discovery of its novel processing enzyme, Icp55." J Biol Chem **284**(44): 30200-30208.
Nakai Y, Nakai M and Hayashi H (2008). "Thio-modification of yeast cytosolic tRNA requires a ubiquitin-related system that resembles bacterial sulfur transfer systems." J Biol Chem **283**(41): 27469-27476.

Nakai Y, Nakai M, Lill R, Suzuki T and Hayashi H (2007). "Thio Modification of Yeast Cytosolic tRNA Is an Iron-Sulfur Protein-Dependent Pathway." Molecular and Cellular Biology **27**(8): 2841-2847.
Nishimura S and Watanabe K (2006). "The discovery of modified nucleosides from the early days to the present: a personal perspective." J Biosci **31**(4): 465-475.
Noma A, Sakaguchi Y and Suzuki T (2008). "Mechanistic characterization of the sulfur-relay system for eukaryotic 2-thiouridine biogenesis at tRNA wobble positions." Nucleic Acids Research **37**(4): 1335-1352.
Numata T, Ikeuchi Y, Fukai S, Suzuki T and Nureki O (2006). "Snapshots of tRNA sulphuration via an adenylated intermediate." Nature **442**(7101): 419-424.
Paraskevopoulou C, Fairhurst SA, Lowe DJ, Brick P and Onesti S (2006). "The Elongator subunit Elp3 contains a Fe4S4 cluster and binds S-adenosylmethionine." Mol Microbiol **59**(3): 795-806.
Petroski MD, Salvesen GS and Wolf DA (2011). "Urm1 couples sulfur transfer to ubiquitin-like protein function in oxidative stress." Proc Natl Acad Sci U S A **108**(5): 1749-1750.
Purushothaman SK, Bujnicki JM, Grosjean H and Lapeyre B (2005). "Trm11p and Trm112p are both required for the formation of 2-methylguanosine at position 10 in yeast tRNA." Molecular and Cellular Biology **25**(11): 4359-4370.
Rinehart J (2005). "Saccharomyces cerevisiae imports the cytosolic pathway for Gln-tRNA synthesis into the mitochondrion." Genes & Development **19**(5): 583-592.
Rubio MA, Rinehart JJ, Krett B, Duvezin-Caubet S, Reichert AS, Soll D and Alfonzo JD (2008). "Mammalian mitochondria have the innate ability to import tRNAs by a mechanism distinct from protein import." Proc Natl Acad Sci U S A **105**(27): 9186-9191.
Rubio MAT and Hopper AK (2011). "Transfer RNA travels from the cytoplasm to organelles." Wiley Interdisciplinary Reviews: RNA **2**(6): 802-817.
Salinas T, Duchêne A-M and Maréchal-Drouard L (2008). "Recent advances in tRNA mitochondrial import." Trends in Biochemical Sciences **33**(7): 320-329.
Sasarman F, Antonicka H, Horvath R and Shoubridge EA (2011). "The 2-thiouridylase function of the human MTU1 (TRMU) enzyme is dispensable for mitochondrial translation." Hum Mol Genet.
Schlieker CD, Van der Veen AG, Damon JR, Spooner E and Ploegh HL (2008). "A functional proteomics approach links the ubiquitin-related modifier Urm1 to a tRNA modification pathway." Proc Natl Acad Sci U S A **105**(47): 18255-18260.
Shi H and Moore PB (2000). "The crystal structure of yeast phenylalanine tRNA at 1.93 A resolution: a classic structure revisited." Rna **6**(8): 1091-1105.
Shoffner JM, Lott MT, Lezza AMS, Seibel P, Ballinger SW and Wallace DC (1990). "Myoclonic Epilepsy and Ragged-Red Fiber Disease (Merrf) Is Associated with a Mitochondrial-DNA Transfer Rnalys Mutation." Cell **61**(6): 931-937.
Simpson CL, Lemmens R, Miskiewicz K, Broom WJ, Hansen VK, van Vught PWJ, . . . Al-Chalabi A (2008). "Variants of the elongator protein 3 (ELP3) gene are associated with motor neuron degeneration." Human Molecular Genetics **18**(3): 472-481.
Slaugenhaupt SA and Gusella JF (2002). "Familial dysautonomia." Curr Opin Genet Dev **12**(3): 307-311.
Studte P, Zink S, Jablonowski D, Bar C, von der Haar T, Tuite MF and Schaffrath R (2008). "tRNA and protein methylase complexes mediate zymocin toxicity in yeast." Mol Microbiol **69**(5): 1266-1277.
Suyama Y (1967). "The origins of mitochondrial ribonucleic acids in Tetrahymena pyriformis." Biochemistry **6**(9): 2829-2839.
Suzuki T and Nagao A (2011). "Human mitochondrial diseases caused by lack of taurine modification in mitochondrial tRNAs." Wiley Interdiscip Rev RNA **2**(3): 376-386.
Suzuki T, Wada T, Saigo K and Watanabe K (2002). "Taurine as a constituent of mitochondrial tRNAs: new insights into the functions of taurine and human mitochondrial diseases." EMBO J **21**(23): 6581-6589.
Svejstrup JQ (2007). "Elongator complex: how many roles does it play?" Current Opinion in Cell Biology **19**(3): 331-336.
Tarassov I, Entelis N and Martin RP (1995). "An intact protein translocating machinery is required for mitochondrial import of a yeast cytoplasmic tRNA." J Mol Biol **245**(4): 315-323.
Tarassov I, Entelis N and Martin RP (1995). "Mitochondrial import of a cytoplasmic lysine-tRNA in yeast is mediated by cooperation of cytoplasmic and mitochondrial lysyl-tRNA synthetases." EMBO J **14**(14): 3461-3471.
Tumaitis TD and Lane BG (1970). "Differential labelling of the carboxymethyl and methyl substituents of 5-carboxymethyluridine methyl ester, a trace nucleoside constituent of yeast transfer RNA." Biochim Biophys Acta **224**(2): 391-403.
Umeda N, Suzuki T, Yukawa M, Ohya Y, Shindo H and Watanabe K (2005). "Mitochondria-specific RNA-modifying enzymes responsible for the biosynthesis of the wobble base in mitochondrial tRNAs. Implications for the molecular pathogenesis of human mitochondrial diseases." J Biol Chem **280**(2): 1613-1624.

Van der Veen AG, Schorpp K, Schlieker C, Buti L, Damon JR, Spooner E, . . . Jentsch S (2011). "Role of the ubiquitin-like protein Urm1 as a noncanonical lysine-directed protein modifier." Proc Natl Acad Sci U S A **108**(5): 1763-1770.

Versées W, De Groeve S and Van Lijsebettens M (2010). "Elongator, a conserved multitasking complex?" Molecular Microbiology **76**(5): 1065-1069.

Wang F, Liu M, Qiu R and Ji C (2011). "The dual role of ubiquitin-like protein Urm1 as a protein modifier and sulfur carrier." Protein Cell **2**(8): 612-619.

Wang X, Yan Q and Guan M-X (2009). "Mutation in MTO1 involved in tRNA modification impairs mitochondrial RNA metabolism in the yeast Saccharomyces cerevisiae." Mitochondrion **9**(3): 180-185.

Wang X, Yan Q and Guan M-X (2010). "Combination of the Loss of cmnm5U34 with the Lack of s2U34 Modifications of tRNALys, tRNAGlu, and tRNAGln Altered Mitochondrial Biogenesis and Respiration." Journal of Molecular Biology **395**(5): 1038-1048.

Winkler GS (2001). "RNA Polymerase II Elongator Holoenzyme Is Composed of Two Discrete Subcomplexes." Journal of Biological Chemistry **276**(35): 32743-32749.

Yarian C (2002). "Accurate Translation of the Genetic Code Depends on tRNA Modified Nucleosides." Journal of Biological Chemistry **277**(19): 16391-16395.

Chapter 3:

Functional Characterization of YIR024C Gene Product, a Hypothetical Adrenodoxin Reductase Physical Interactor

3.1 Introduction

3.1.1 ARH1 and YAH1 Roles in Fe/S Clusters and Heme A Biosynthesis

3.1.2 YIR024C Gene: State of Art

3.2 Results and Discussion

3.2.1 Confirmation of yir024cΔ Phenotypes

3.2.2 Yir024cΔ Harbors Several Mitochondrial Respiratory Chain Defects

3.2.3 Yir024cp-3HA Localizes to Mitochondrial Inner Membrane and Faces the IMS

3.2.4 Yir024cp-3HA Resides in a 250Kda Complex without Arh1p

3.3 References

3.1 Introduction

3.1.1 ARH1 and YAH1 Roles in Fe/S Clusters and Heme A Biosynthesis

The functional pair Arh1p/Yah1p was extensively characterized around the year 2000 with a substantial timing overlap. *ARH1* was identified as first but major contribution to the characterization of this functional pair came from *YAH1* gene.

Cytochrome P450 system receives electrons from the pair Adrenodoxin (ADX) and Adrenodoxin Reductase (ADR) during conversion of cholesterol into pregnenolone, common precursor of all steroid hormones. Existence in yeast of a protein with ADR was suggested observing that mitochondrial directed bovine Cytochrome P450 along with Adrenodoxin (ADX) alone were able to perform in yeast mitochondria the same reaction catalyzed in mammals (Dumas *et al.* 1996). Looking for a possible homolog a partially sequenced gene on chromosome IV was shown to code for a protein with similarity to ADR. This gene was found to be neighbor of *BCS1*, starting from its 5' with opposite direction (Nobrega F. G. *et al.* 1992). Named systematically *YDR376W* after genome sequencing was confirmed to be the yeast homolog of ADR and therefore called *ARH1*, Adrenodoxin Reductase Homolog 1 (Lacour *et al.* 1996; Lacour *et al.* 1998). The protein was demonstrated to be mitochondrial, associated to the inner membrane and containing a FAD and a NADPH binding domain. Extensive studies of *ARH1* were presented in 1998 when it was totally sequenced and demonstrated to be an essential gene in yeast (Manzella *et al.* 1998). Although in mammals *ARH1* is involved in sterol biosynthesis, effects of *ARH1* downregulation failed to be complemented with different sterols supplementation ruling out this possibility and opening the horizon to the other processes involved (Manzella *et al.* 1998). Being an essential gene almost all experimental data were obtained using a conditional allele driven by *GAL1* promoter. Also under repressing conditions the *GAL1-ARH1* expressing strain was viable, allowing a deeper study of phenotypes. Initially the most interesting observations were made in connection to iron metabolism. Indeed Arh1p depleted cells showed a total lack of iron homeostasis control with a cellular and subsequent mitochondrial iron overload (Li 2000). Moreover upon depletion of Arh1p defects in Fe/S clusters proteins (both mitochondrial and cytoplasmic as Aco1p and Leu3p) and heme containing proteins as Cyc1p and Cyt1p (Li 2000). These two impairments can be considered as the two first hints into the principal Arh1p roles in yeast mitochondria: Fe/S clusters and heme A biosynthesis.

Both these roles, as mentioned previously, are played with the functional and physical interactor Yah1p. Arh1p indeed takes electrons from NADH or NADPH that are then shuttled via cofactor FAD to the acceptor Yah1p. Although *YAH1* was identified later then *ARH1*, all the hints about function of this pair of proteins in S. cerevisiae come from its characterization. *YAH1* is coded at *YPL252C* locus, in chromosome XVI, and was demonstrated to be the homolog of human Adrenodoxin and thus called Yeast Adrenodoxin Homologue 1 (Barros *et al.* 1999). *YAH1,* as *ARH1,* is an essential gene and was studied in a conditional mutant. Yah1p localization was analyzed and confirmed to be mitochondrial soluble protein of the matrix and upon its depletion impairments in mitochondrial respiratory chain were observed (Barros *et al.* 1999). Accordingly to the phenotypes shown for Arh1p depleted cells, also in this case iron homeostasis defects were observed with a 30-fold increase of mitochondrial iron (Lange *et al.* 2000). Moreover Yah1p was the first protein from ferredoxins family (low molecular weight proteins with a Fe/S cluster as active site) with a characterized role in Fe/S cluster biosynthesis, role later demonstrated also for Yah1p bacterial counterpart Fdx. Yah1p depleted cells showed strong decay in activity of proteins containing Fe/S clusters such as Aconitase, Complex II and Complex III although protein levels were constant. This effect was also exploited in cytoplasmic Fe/S proteins such as Leu1p and resembled the same phenotype observed after *ARH1* repression. Measurements of ^{55}Fe incorporation in Fe/S proteins is used as index for a good synthesis and incorporation of these prosthetic groups; the direct role of Yah1p in this process was demonstrated in *GAL1-YAH1* strains, failing to detect any ^{55}Fe in a mitochondrial version of Leu1p upon establishment of repressive conditions (Lange *et al.* 2000). This role was further demonstrated studying the role of Isu1/Isu2 scaffold proteins, essential for Fe/S cluster biosynthesis. This scaffold is a protein structure where the rising Fe/S is assembled starting from sulfur obtained by Nfs1p desulfurase activity and iron from Yfh1p (Frataxin). If defects in these enzymatic activities are present, ^{55}Fe incorporated in the scaffold will be very low. On the other hand if later steps are defective ^{55}Fe will be accumulated. A lack of accumulation of iron in the scaffold was observed upon depletion of Yah1p, like in Yfh1p and Nfs1p depleted cells (Muhlenhoff *et al.* 2003). This not only confirmed the role of Yah1p in Fe/S cluster assembly but also shifted the main interest on the first steps of the process.

Arh1p and Yah1p thus generate an electron flow that is clearly used in Fe/S cluster biosynthesis. Although the role is clear, the molecular details are still lacking. Indeed the real acceptor of electrons from Yah1p is not known. Actually the electron flow is

proposed to start from Arh1p passing two electrons to Yah1p that in turn transfers to S^0 formed in the desulfurase activity of Nfs1p from the donor cysteine. In this way the sulfur is reduced to S^{2-}, the form found in Fe/S clusters. The preferential electron donor for the couple Arh1p/Yah1p is NADH (Muhlenhoff *et al.* 2002), but probably also the phosphorylated form is used. Indeed Arh1p has a NADPH binding domain and levels of this cofactor were found to influence clusters synthesis: a pos5Δ strain, lacking the sole mitochondrial NADH kinase, cannot accumulate NADPH in the mitochondria with consequent failure in assembling clusters (Pain *et al.* 2010).

A role for *YAH1* and consequently for *ARH1* in heme biosynthesis came mostly from the study of *COX15*, already shown to be essential for cytochrome c oxidase assembly (Glerum *et al.* 1997). Heme biosynthesis starts in mitochondria from succinyl-CoA and glycine that *via* multiple enzymatic steps are converted in a porphyrin ring (catalyzed by Hem1p to Hem4p). This is in turn converted with three enzymatic steps, catalyzed by Hem12p, Hem13p and Hem14p into protoporphyrin IX (SGD, KEGG). The final addition of $iron^{2+}$ is catalyzed by ferrochelatase Hem15p giving rise to heme B (protoheme). Defects in early steps cause a complex set of pathologies called “porphyrias” in human. Mitochondrial heme B is inserted in complex III or modified in different forms to be inserted in other mitochondrial respiratory chain (MRC) complexes. In the IMS two different lyases, namely Cyc3p and Cyt2p, covalently attach heme B to cytochrome c and cytochrome c_1 respectively. Heme A, present only in complex IV, is synthetized in the matrix modifying heme B structure in two positions: carbon C-2 is farnesylated and carbon C-8 is formylated (Moraes *et al.* 2004). The first modification occurs in C-2 producing heme O and is catalyzed by *COX10* gene product, already characterized for its role in COX biogenesis and subsequently in heme A biosynthesis (Nobrega M. P. *et al.* 1990; Tzagoloff *et al.* 1993). A mutant in *COX15* was also shown to harbor defects in mitochondrial heme profile. In particular it showed an accumulation of heme O and undetectable heme A (Barros *et al.* 2001). This suggested a monoxygenase role for Cox15p on C-8. In *Schizosaccharomyces pombe COX15* coding frame is fused with *YAH1* giving rise to a fusion product and leading to the conclusion that they could act in the same enzymatic pathways. The same fusion product can be obtained starting from S. cerevisiae genes and it is able to be localized in mitochondria and complements specific defects of both *COX15* and *YAH1* mutants (Barros *et al.* 2001). Furthermore *yah1* temperature sensitive mutants were shown to have decreased level of heme A but still detectable heme O and being unable to efficiently incorporate radioactive δ-aminolevulinic acid (product of glycine and succinyl-CoA condensation) into heme A

(Barros 2002). Thus a direct role for Yah1p in heme O to heme A conversion was demonstrated. The reaction was proposed to involve a first hydroxylation on C-8, catalyzed by the three-component monooxygenase Cox15p, Yah1p and Arh1p. The subsequently conversion of the alcohol to aldehyde would be catalyzed by a yet unknown protein (Barros *et al.* 2001; Barros *et al.* 2002).

3.1.2 YIR024C Gene: State of Art

YIR024C gene is located on chromosome nine with a coding sequence of 651bp (Churcher *et al.* 1997). It codes for a verified polypeptide of 216 amino acids with theoretical mass of 24.597Da. The protein was localized to mitochondria in high-throughput analyses (Huh *et al.* 2003; Sickmann *et al.* 2003). As no experimental evidences on functional role of Yir024cp exist, no GO functional classes are related and up to date is still classified as gene product with molecular function and biological process unknown. However among several genome-wide screenings performed on deletants collection, *YIR024C* gene was related to mitochondrial biogenesis. It is indeed included in the database created by Hess DC and colleagues, already described in section 1.1.3. Briefly a complex iterative algorithm was used to predict genes involved in mitochondrial function, with subsequent experimental confirmation. Hess DC implemented extensive analyses on petites frequency, respiratory growth rate and mitochondrial inheritance. Although *YIR024C* was among the predicted genes, no evident phenotypes could be observed in the null mutant (Hess *et al.* 2009). *YIR024C* was for the first time associated to a mitochondrial phenotype in genome-wide screening described in Chapter 1 of this dissertation. As mentioned previously, total results (488 genes identified as oxidative growth defective) were compared with existing literature. *YIR024C* was initially filtered as already reported in Hess DC screening, but subsequently retained as gene with uncharacterized function. Deletion in *YIR024C* gene caused a low sensitive phenotype in ethanol containing media at 30˚C, exacerbated at 37˚C. Spectra analysis and oxygen consuming revealed a Class A mutant with respiratory efficiency of 13%, thus strongly impaired (figure 3.1).

One interesting aspect in *YIR024C* limited literature is found among physical interactors. Indeed it was found to be a positive match with Adrenodoxin Reductase Homolog (Arh1p) in a double hybrid assay. Using Arh1p as bait (fused with DNA binding domain) and Yir024Cp as prey (fused with a transactivator domain) authors were able to detect reporter activity (Uetz *et al.* 2000). Although double-hybrid is considered a “non-physiological” assay especially for mitochondrial proteins, it is widely used and represents a solid research approach.

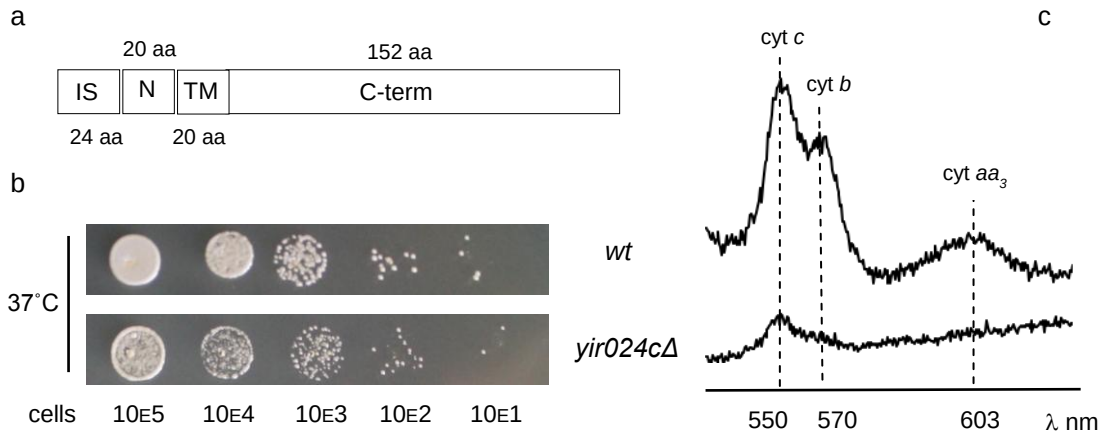

FIG 3.1: (a) Cartoon representation of Yir024Cp features. IS import sequence, N n-terminus, TM predicted trans-membrane domain. **(b)** Original phenotype in high-throughput screening at 37˚C in YPE media. **(c)** Cytochromes spectra profile of yir024cΔ strain. Profile was classified as class A and respiratory efficiency was 13% of a wild type.

Arh1p along with its functional partner Yah1p, plays an important role in at least two essential cellular processes: heme biosynthesis and Fe/S clusters assembly.

Heme is a prosthetic group widely used in nature, from bacteria to humans with roles not only as cofactor in respiratory complexes. Three different forms of mitochondrial heme are embedded in respiratory complexes allowing electron transport through mitochondrial inner membrane. Moreover it is a versatile molecule used both in yeast and human to regulate cellular responses to oxygen availability: yeast Hap1p and mammal Bach1 transcription factors activities are regulated by heme and in turn they activate or repress nuclear genes (Mense *et al.* 2006). Fe/S clusters are essential prosthetic groups used for redox processes, catalysis and also for structural purposes. Many mitochondrial proteins use different forms of clusters, ranging from simple rhombic 2Fe/2S to complex combination of three and more clusters chemically linked. Synthesis of these essential cofactors is carried out in mitochondria but they are also exported to be used in the cytosol. Fe/S cluster biosynthesis is in fact one of the mitochondrial functions essential for the cell besides respiratory metabolism. Indeed many of the genes required for Fe/S cluster biosynthesis are essential for cell viability (Lill *et al.* 2006; Lill 2008). Very recently also a role in coenzyme Q biosynthesis for Arh1p/Yah1p pair was characterized (Pierrel *et al.* 2010).

Despite the extensive study of this essential processes some aspects are still not completely characterized, moreover in the steps in which Arh1p and Yah1p take part. A hypothetical physical interactor could therefore represent an interesting research focus although no homologs exist in upper eukaryotes. Therefore a functional characterization of *YIR024C* gene product was undertaken and will be the focus of this chapter.

3.2 Results and Discussion

3.2.1 Confirmation of yir024cΔ Phenotypes

Coming from a high-throughput analysis, the first step towards a single gene functional characterization consists of confirming the originally reported phenotypes. A suitable approach includes the transfer of the deletion cassette to a different genetic context and retests these phenotypes. In the aforementioned screening, a BY4742 haploid deletants collection was used, each carrying a single gene disruption achieved with PCR created *KanMX4* cassette, coding a resistance determinant for geneticin (G418). Although this collection was widely used in genomic-wide screenings focused on mitochondrial biogenesis, the BY4742 genetic bacgkround is not ideal for mitochondrial studies. This background carries a mutant allele for the *HAP1* gene, coding for a transcription factor essential for gene regulation in response to oxygen and heme levels (Mortimer *et al.* 1986). For this reason, the *YIR024C::KanMX4* cassette was amplified from *BY4742 yir024cΔ* and transferred to the W303 genetic context. The cassette was PCR-amplified from a genomic DNA preparation by using two external primers (FWYIR024c and RVYIR024c, sequences reported in Appendix 6). Identity of amplification product was granted with a restriction enzyme digestion control as KanMX4 harbors a unique *Hind*III restriction site. A wild-type W303-1B strain was transformed with 1µg of purified *YIR024C::KanMx4* and transformants selected on media containing geneticin. Twenty independent clones were patched on selective media and on five random additional controls were performed. Integration at the correct locus was checked with a PCR strategy. Using an additional upstream forward primer specific for *YIR024C* locus (A1YIR024c) and a reverse primer internal to the *KanMX4* gene (K3), an amplification product could be obtained only if the disruption cassette was at the correct locus. This was confirmed in four out of five strains. Eventually, a *W3031b YIR024c::KanMX4* strain was obtained and used for all the further analysis that will be described below. This approach granted the correct profile of the new deletant strain and at the same time the identity of original *BY4742* deletant strain present in the collection thus confirming that *yir024cΔ* was responsible for the observed phenotypes.

Respiratory growth in spot assay, cytochrome spectra and oxygen consumption were analyzed in W303 *yir024cΔ*. As showed in figure 3.2 all the original phenotypes were confirmed. The analysis was extended to 30˚C for cytochromes spectra and oxygen consumption. The same protocols, reported in sections 4.2.3 and 4.2.4 were used (Ferrero *et al.* 1981). Generally, defects were observed on complete media only at 37˚C,

as expected. Indeed cytochrome profile was scored as class A, although wild-type W30-1B in the same condition was altered to a certain extent in comparison with the results obtained at 30°C. The absence of cytochromes in the *yir024cΔ* mutant at 37°C was consistent with a reduction in oxygen consumption efficiency that was of 15% of wild-type. Conversely, on complete media at 30˚C no such defects were observed. Cytochromes were indeed classified as D profile with respiratory efficiency of 85% at 30˚C. To analyze respiratory growth, we performed a serial dilutions growth test in both complete and synthetic minimum media at 30 and 37˚C. As expected from original phenotypes (low sensitive in complete media at 30˚C and 37˚C) in complete media, only a slightly deficient phenotype was observed at 30˚C, which was exacerbated at 37˚C. This is a controversial aspect among *yir024cΔ* phenotypes as cytochrome spectra and oxygen consuming in the same condition would suggest more evident defects. If respiratory growth is analyzed in a minimum synthetic media, phenotypes are strongly exacerbated with almost total impairment at 30˚C too.

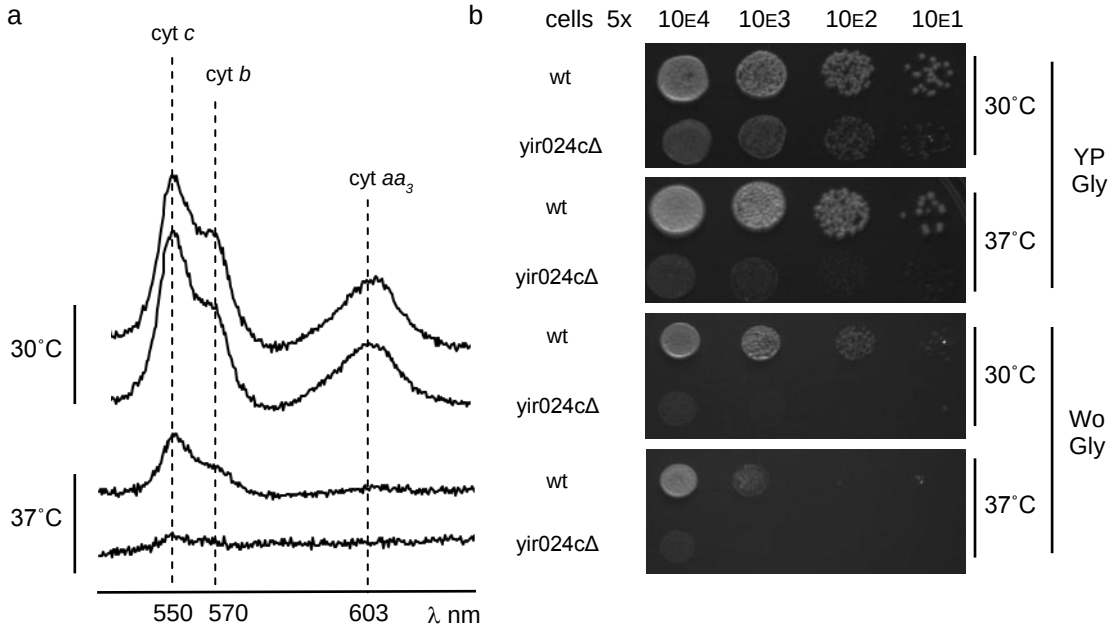

FIG 3.2: (a) Cytochromes spectra profile recorded on whole cells after growth in complete media. Analysis was carried out at both 30 and 37˚C. **(b)** Spot assay of serial dilutions in complete YP or synthetic minimal (Wo). Plates were incubated at indicated temperatures for 3 days

Trying to explore the controversial aspect of *yir024cΔ* phenotypes, cytochrome content was analyzed directly on isolated mitochondria to allow a more sensitive analysis. Mitochondria with intact outer membrane were isolated from *yir024cΔ* and wild-type strains grown in complete media containing galactose at 30 and 37˚C (see section 4.3.1). Total cytochromes were extracted and analyzed spectrophotometrically as described in section 4.3.3 (Ferrero *et al.* 1981). As shown in figure 3.3, no evident defects were observed at 30˚C, as expected. Cytochrome spectra profile at 37˚C on purified mitochondria displayed strong defects in cyt *b* and a shift in absorbance peak for cyt aa_3 (COX). Absorbance of complex IV depends on the coordinated heme A prosthetic group that in COX environment shows a maximum at λ of 603nm. The observed absorbance shift is indicative of heme A absorption in a non-native environment, already shown in other mutants such as *cyc3Δ*, lacking the cyt c heme lyase (Barros *et al.* 2002). Interestingly, the profile observed on purified mitochondria is quite different from the one recorded on whole cells. This profile is in better agreement with the observed growth defect and it is still in accordance with a very low efficiency in oxygen consuming. Indeed qualitative and quantitative defects were recorded for cyt *b* and cyt aa_3.

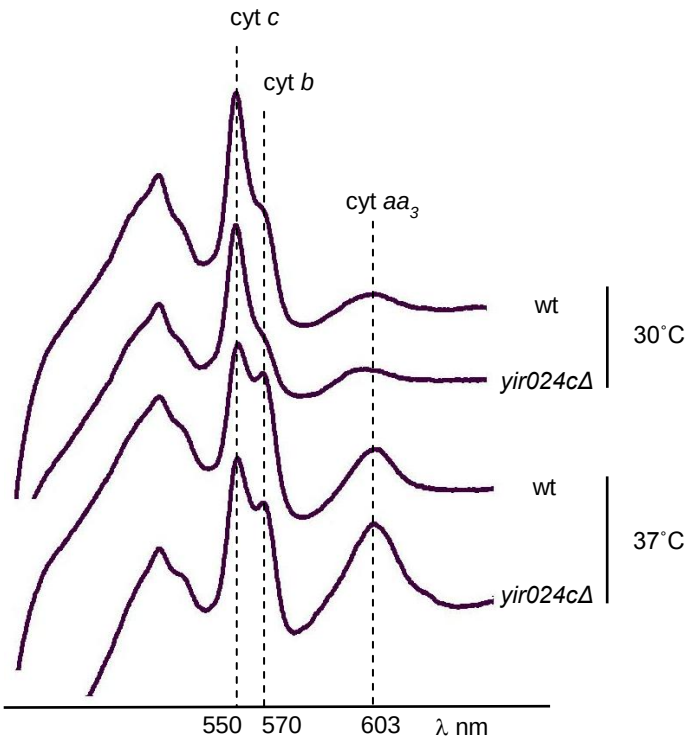

FIG 3.3: Cytochrome spectra profile recorded on isolated mitochondria. An equivalent of 2.5mg of mitochondrial proteins were used.

Following the confirmation of the original phenotypes also in W303 genetic context we have established that *YIR024C* gene product plays a role in some uncharacterized aspect of mitochondrial biogenesis. A better functional characterization of mitochondrial phenotypes and extensive biochemical analyses of the gene product were undertaken as described below.

3.2.2 Yir024cΔ Harbors Several Mitochondrial Respiratory Chain Defects

In order to obtain a comprehensive characterization of defects in mitochondrial respiratory chain (MRC) of a *yir024cΔ* strain, we performed an extensive biochemical analysis of respiratory complexes. Mitochondria with intact outer membrane were isolated from *yir024cΔ* and wild type strains grown at 30 and 37˚C in complete media supplemented with galactose. An equivalent of 40µg of mitochondrial proteins were resolved in 12% SDS-page and transferred to nitrocellulose membrane, as described in section 4.1.8. Membranes were immuno-decorated with primary antibodies against following MRC proteins: Cox1p, Cox2p, Cox3p, Cox4p, Cyt*b*, Rip1p, Cyt*c*, Sdh1p and βATPase for complex V. Results are shown in figure 3.4.

Among the tested subunits of complex IV, the steady state levels of Cox1p, Cox2p and Cox3p were substantially affected in *yir024cΔ* at 37˚C. Interestingly these three subunits are mitochondrial DNA-encoded and form the catalytic core of the enzyme, which is unstable in the absence of holoenzyme assembly. No decrease was observed in Cox4p steady state level at 37˚C, although both strains show defects compared to the counterparts at 30˚C. The substantial decrease of Cox1p, common to all *bona fide* COX mutants, could also explain the peak shift observed in cytochromes profile. Probably the heme A environment is changed thus affecting its coordination and absorbance properties (Barros *et al.* 2002).

Also complex III was found affected at 37˚C, with a marked decrease in Cyt*b* in *yir024Δ* at 37˚C. Conversely, for rieske-protein Rip1p (ubiquinol-cytochrome-c reductase), Cyt*c* and βATPase no changes in steady state levels were detected. Complex II behavior was initially unexpected: Sdh1p subunit appeared substantially increased in *yir024cΔ* strain at 37˚C. To further address this phenotype the level of fully assembled complex II was assessed. An equivalent of 200µg of mitochondrial proteins were resolved in one dimension BN-page as described elsewhere (Cruciat *et al.* 2000), western blot and immune-decoration using antibody against Sdh2p were then performed. As shown in figure 3.4 panel b, the level of fully assembled complex was totally comparable in all the conditions. Furthermore the steady state level of Sdh2p subunit in SDS-page was constant and no changes in SDH specific enzymatic activity could be recorded (data not shown). Therefore, it can be concluded that the detected increase in Sdh1p subunit in *yir024cΔ* at 37˚C might be an unpecific event.

Enzymatic activities of Complex IV (COX) and ComplexIII+NADH dehydrogenase (NCCR) were recorded on isolated mitochondria at 30 and 37˚C (see sections 4.3.4 and 4.3.6). COX and NCCR specific activities at 37˚C were reduced of about 80% and 50% respectively. Conversely, no defects were observed on mitochondria isolated after growth at 30˚C. This is in general accordance with observed steady state levels of MRC chain subunits.

.

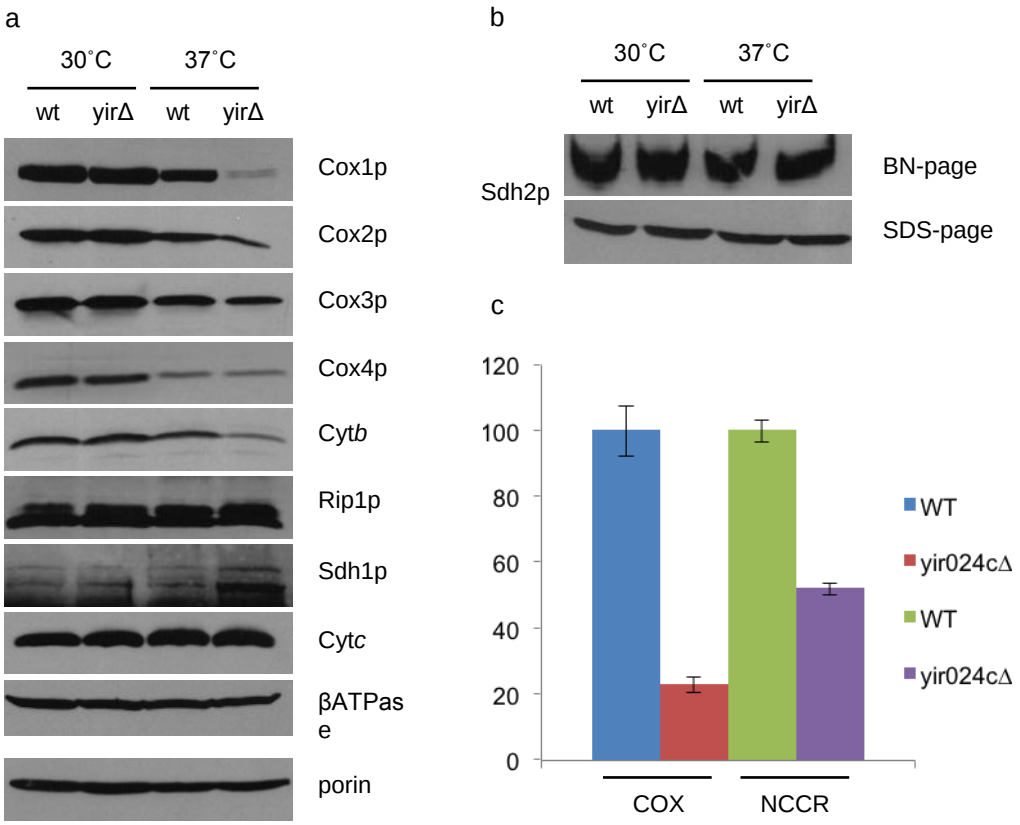

FIG 3.4: (a) 40µg of mitochondrial proteins were resolved in 12% SDS-page. Western blot were immune-decorated with primary antibodies against indicated proteins. Suitable secondary antibodies and ECL based chemistry were used for developing. Porin was used as loading control. **(b)** 200µg of mitochondrial proteins were analyzed is 1D BN-page and fully assembled complex II was visualized with antibody against Sdh2p. SDS-page and western blot with antibody against Sdh2p was also included. **(c)** COX and NCCR enzymatic activities recorded on mitochondria isolated from cells grown at 37˚C. Three replicates for each sample were assayed and mean values considered. Wild type activity is considered as 100%

In summary, deletion in *YIR024C* gene causes several MRC defects. Mitochondrial encoded subunits of complex IV (Cox1p, Cox2p and Cox3p) were markedly decreased at 37˚C, with a concomitant reduction of enzymatic specific activity to 20% of wild type. Complex III was similarly affected with evident diminution in Cyt*b* steady state level and NCCR activity reduction to 50% of the wild type. All the performed assays used mitochondria isolated from cells grown in complete media supplemented with galactose and results are in general accordance with the physiological analyses described previouslyThe interesting aspect of Yir024cp physical interaction with Arh1p suggested that some defects in heme metabolism could also be present. Therefore, 2mg of total mitochondrial proteins isolated at 30˚C and 37˚C were used for HPLC analysis of total heme content (see section 4.3.7) and results are shown in figure 3.5. In strain harboring *YIR024C* deletion defects in heme metabolism could be observed at 37˚C, compared to a wild type strain. As expected no such changes were detected at 30˚C (data not shown).

Specific enzymatic defects in heme biosynthesis can be postulated from profiles of total mitochondrial heme resolved in C18 reverse phase HPLC in acetonitrile gradient (Barros *et al.* 2001). For instance a *cox10Δ* strain has neither heme A nor heme O, but a normal level of heme B (Tzagoloff *et al.* 1993). *Cox15Δ* and *yah1Δ* instead accumulate (to different extents) heme O with no detectable levels of heme A. Defects in different steps can be postulated observing accumulation in different mitochondrial heme species and was the principal observation used to propose the enzymatic roles of Cox10p, Cox15p and Yah1p. In *yir024cΔ* strain no specific changes in A and O ratios were observed at 37˚C thus no specific enzymatic defects in the steps involving heme B to Heme A conversion could be postulated. Nevertheless, in the mutant all the three species of heme were about half of the wild-type counterpart. In particular, a lower content of heme B could cause the corresponding decrease in heme A and heme O. Thus if a direct role of Yir024cp in heme biosynthesis exists it is likely played in a different step then biosynthesis of heme A starting from heme B or heme O. For instance it could be involved in the conversion of porphyrin ring to heme B in mitochondria.

The role of *YIR024C* gene in heme metabolism remains still unclear and requires further investigations.

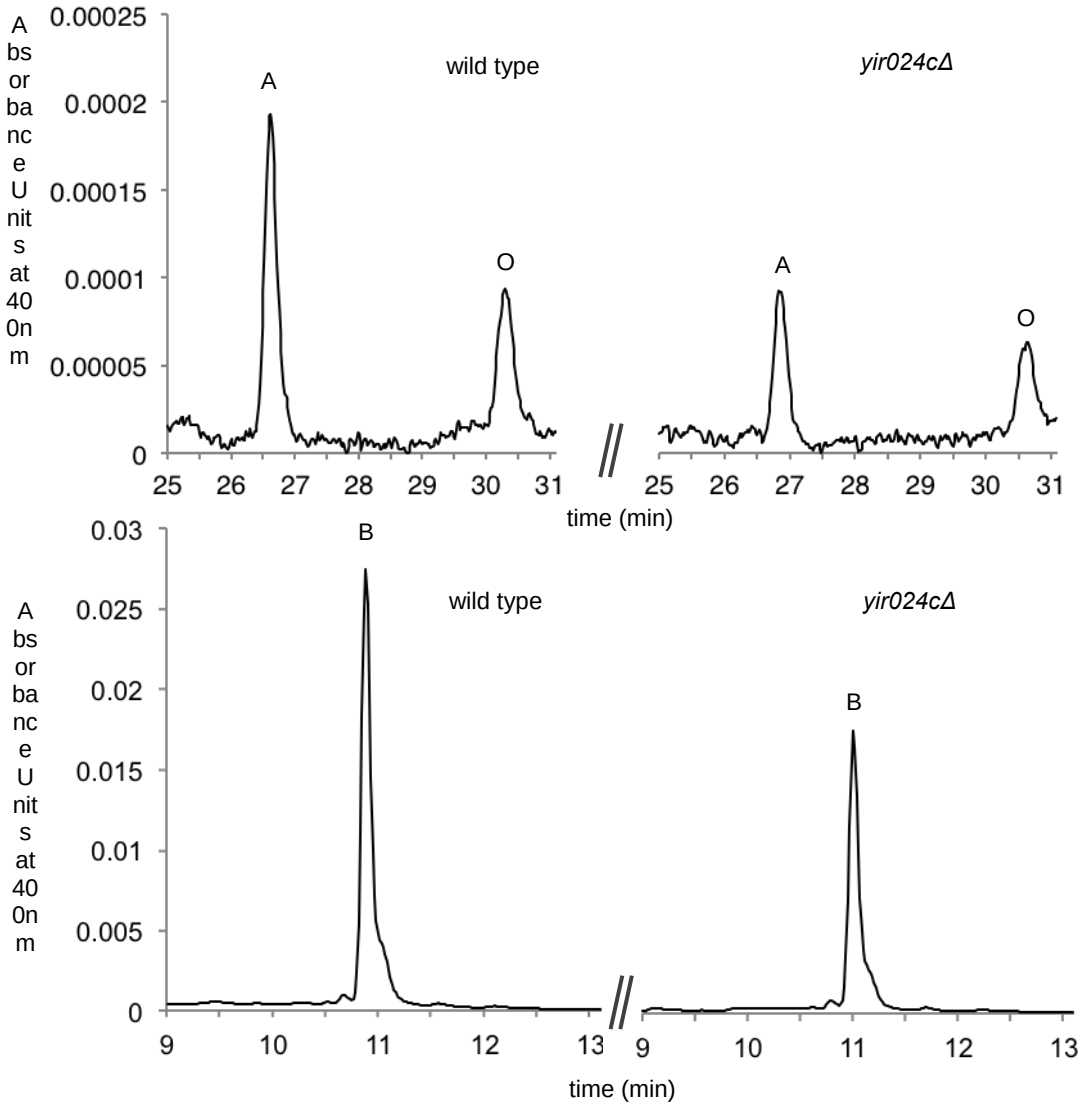

FIG 3.5: HPLC analysis of total heme content on 2mg of mitochondrial proteins as described previously (Barros *et al.* 2001). Mitochondria were isolated at 37˚C. Heme A and O are shown in the upper panel with retention time of about 26-27 min and 30-31 min respectively. Heme B profile is shown in the lower panel with retention time of about 11 minutes

3.2.3 Yir024cp-3HA Localizes to Mitochondrial Inner Membrane and Faces the IMS

To better understand the functional role of Yir024cp in mitochondria, we created a strain expressing an epitope tagged version of the protein. From wild type W303 genomic DNA *YIR024C* gene was amplified using the primers Y024CFWBam and Y024CHA3RVPst (sequences reported in Appendix 6). The former was designed to create a *BamHI* restriction site and the latter to introduce a triple Hemagglutinin tag (3HA) in frame with the coding sequence along with a *PstI* restriction site. The expected product of 1350bp was purified and cloned as *BamHI-PstI* in *YIplac211* integrative vector. The construct *YIplac211-YIR024C3HA* was then sequenced to confirm the correct in frame tagging. The shuttle vector *YIplac211* harbors *TRP1* gene as selectable marker that can be used to direct a locus specific integration in *S. cerevisiae* (Rothstein 1983). Using the unique *AarI* restriction site in *TRP1* gene the construct was linearized and used to transform *yir024cΔ* strain. Selection of *YIR024C::KanMX4 trp1-1::YIplac211-YIR024C3HA* strain was performed on minimum media without Trp. Complementation of *YIR024C* deletion phenotype by tagged version of the protein was confirmed by a serial dilutions growth test on minimum media with Gly (data not shown). Additionally, the presence of HA-tag was confirmed in SDS-page on total cellular extracts followed by western blot and immuno-detection using an antibody against HA. HA signal was detected at expected size of about 30 kDa (data not shown). Total cellular extracts were obtained as described in 4.2.6.

All existing Yir024cp localization data published so far were obtained with high-throughput approaches and therefore the subcellular localization was experimentally tested using the strain expressing the HA-tagged Yir024c protein. Equivalent of 40µg of purified mitochondrial proteins and post mitochondrial supernatant (PMS, cytoplasmic fraction) of Yir024cp3HA expressing strain were resolved in 12% SDS-page followed by western blot. The membranes were probed with an antibody against HA and as cytoplasmic and mitochondrial controls Pgk1p and Cox2p. Cox2p was localized in mitochondrial fraction and Pgk1p mostly in PMS. Also mitochondrial fraction was positive to Pgk1p detection indicating some cytoplasmic contamination. Nevertheless being the HA signal exclusively mitochondrial the subcellular localization of Yir024cp3HA was confirmed (fig 3.6 panel a).

Although mitochondrial localization was expected from previous results and phenotypes observed, no data existed on sub-mitochondrial localization and topology of the protein.

Sub-localization of a protein in mitochondrial compartments can be determined from its solubility after sonication and extraction under alkaline conditions as described in 4.3.9. Mitochondria for a total of 200µg proteins were sonicated to allow separation of mitochondrial soluble proteins (S) from membrane fraction proteins. Carbonate extraction of membrane fraction is used to achieve further separation of integral in membrane (CP) and membrane-associated proteins (CS). Equivalents of 40µg for each fraction were resolved in SDS-page followed by western blot and immune detection (fig 3.6 panel b). Soluble proteins such as Cytb_2 were predominant in S fraction and conversely Cox2p, which has several transmembrane domains, exclusively in the CP fraction. Mss51p is known to be a peripheral protein of the mitochondrial inner membrane (Siep *et al.* 2000) and it is usually enriched in CS fraction compared to S. Same fractions were probed with antibody against HA and signal was exclusively revealed in CP fraction. Yir024Cp3HA is indeed a mitochondrial integral membrane protein. Its presence in the membrane fraction is in accordance with the predicted N-terminal trans-membrane domain of 20 amino acids. Treatment of mitochondria and mitoplasts obtained by hypotonic swelling with proteinase K can give hints in proteins topology. Indeed a matrix protein is protected from proteinase digestion in both mitochondria and mitoplasts. A protein residing or facing the IMS is instead digested when outer membrane is disrupted by hypotonic swelling, but protected in intact mitochondria. Yir024cp3HA behavior was comparable to that of Cmc2p, an IMS protein, and Cox2p a protein facing the matrix. As shown in figure 3.6 panel c, like Cmc2p HA was detected only when outer membrane was intact. Taken together, these results indicate that Yir024cp is a mitochondrial integral membrane protein that faces the IMS. Moreover, it can be postulated that Yir024cp is inserted in the mitochondrial inner membrane and not in the outer membrane. Indeed the position of the unique predicted hydrophobic trans-membrane leaves only a short N-terminal portion on one side, and the major C-terminal with HA tag on the other. With this topology if Yir024cp had been in the outer membrane it would not have been protected in intact mitochondria.

Given that only twenty amino acids would be residing in the mitochondrial matrix, justifying a physical interaction between Yir024cp and Arh1p, a soluble protein of the mitochondrial matrix, become challenging. However this cannot be excluded and therefore native size determination and co-immunoprecipitation studies were undertaken to determine whether Yir024cp resides in a complex and if it contains or not the predicted interactor Arh1p.

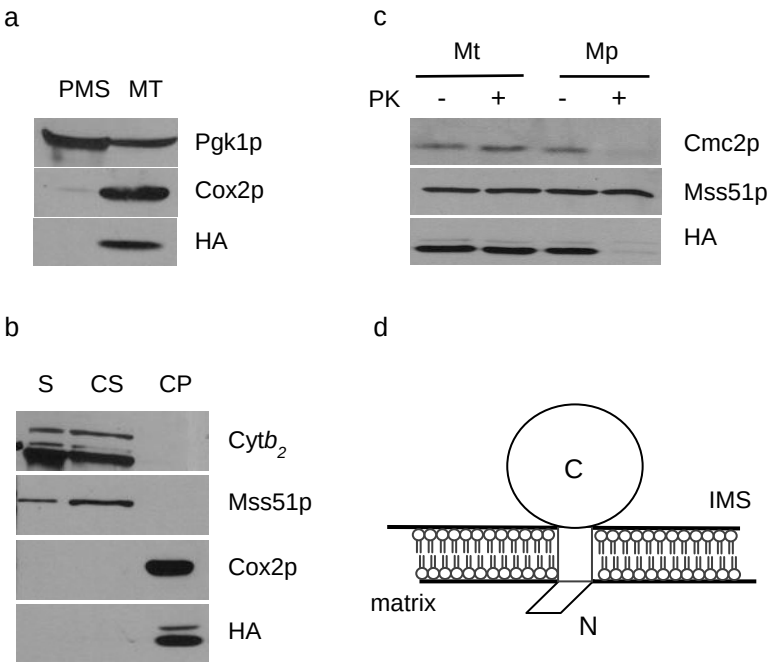

FIG 3.6: Localization and topology analysis of Yir024cp3HA protein. **(a)** Mitochondrial proteins (MT) and post mitochondrial supernatant (PMS) were isolated as described in 4.3.1. **(b)** 200µg of mitochondrial protein were subjected to sonic irradiation as described in 4.3.9 to separate soluble proteins (S) from membrane fraction. Alkaline treatment of membrane fraction allowed separation of membrane bound proteins (CS) and integral membrane proteins (CP). **(c)** Mitochondria and mitoplasts obtained by hypotonic swelling were treated with proteinase K as described in 4.3.8. **(d)** Cartoon representing topology of Yir024cp. A small N-terminus of 20aa is the mitochondrial matrix and the remaining globular part faces intermembrane space (IMS).

3.2.4 Yir024cp-3HA Resides in a 250Kda Complex without Arh1p

Determination of native size is a very indicative analysis of physiological protein state. Indeed in denaturing conditions of SDS-page destroy all the physical interactions and is not possible to determine if a protein is physiologically in mono or oligomeric forms and if it normally forms a complex. Sedimentation properties of a protein in a density gradient are indicators of its native size. To perform this kind of analysis it is necessary to extract the protein in native conditions from isolated mitochondria. Extraction conditions are a crucial parameter: strong detergents efficiently solubilize proteins but also disrupt physical interactions among partners. Thus, it is necessary to start by finding the mildest extraction conditions that are able to solubilize most of the protein. Key components of the extraction buffer are type and concentration of detergent and salt concentration. Different detergents have different properties and each protein needs a unique condition for efficient solubilization. Salt increases in a dose-dependent fashion the efficiency but also impairs ionic interactions among proteins, being then able to disrupt complexes. To test the extraction conditions, 50µg of mitochondrial proteins from Yir024cp3HA expressing strain were treated with different detergents and KCl concentration as described in section 4.3.10. After a clarification step with high-speed centrifugation, solubilized proteins are found in the supernatant fraction (S) and retained proteins in pellet (P). Equivalent amounts of S and P fraction were loaded and resolved in SDS-page followed by western blot and immune-detection with antibody against HA epitope and results are shown in figure 3.7. At least 90% of Yir024cp3HA was efficiently solubilized with lauryl-maltoside at 0.5%. KCl addition showed no efficiency increase. These conditions were used in all subsequent analyses.

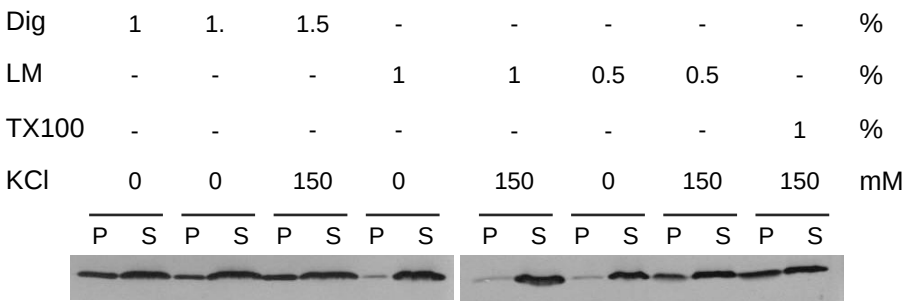

FIG 3.7: Selection of extraction conditions tested. 50µg of protein were treated with indicated conditions. Digitonin, lauryl-maltoside and triton X100 were tested with or without KCl 150mM.

Sedimentation properties of Yir024cp3HA were assessed in a linear 7-20% sucrose gradient and compared with those of known markers used to calibrate the gradient (LDH=130Kda and Hemoglobin=67Kda). Mitochondrial extracts were solubilized with 0.5% digitonin and gradient was performed as described in 4.3.11 with 12hrs centrifugation at 28000rpm, 4˚C. Fractions were recovered and Yir024cp3HA distribution assayed by western blot with antibodies against HA epitope. Estimated native molecular weight was calculated as 250Kda suggesting that it relies in a complex across the inner mitochondrial membrane. To address whether Arh1p is a physical interactor residing in this complex, the same fractions were assayed with Arh1p antibody provided by Dr. Alexander Tzagoloff (Manzella *et al.* 1998). As shown in figure 3.8, no evident co-localization of the two signals was observed suggesting that in these conditions Arh1p is not part of the complex. However, weak signals showed co-localization is heavy weight fractions, indicating that a possible not predominant, labile or transient interaction could exist. Being most of the phenotypes observed at high temperature it was reasoned that interaction of the two proteins could exist only under thermal stress. Mitochondria from Yir024cp3HA expressing strain were isolated after growth at 37˚C and sedimentation properties tested in the same conditions, however no co-localization was observed and the native size of Yir024cp3HA was still of 250Kda. This led to the conclusion that Arh1p is not residing in the same complex than Yir024cp3HA. The Y2H assay results reported by Huh and colleagues could thus be a false positive; alternative, the interaction could just be transient. To be sure of this conclusion a final confirmation was obtained with co-immunoprecipitation analysis (CoIP) performed as described in 4.3.12. Equivalent of 4mg of mitochondrial proteins were solubilized with 0.5% digitonin and incubated with agarose-HA affinity matrix to retain Yir024cp3HA and physical interactors. Unbound material was recovered and matrix washed prior final elution with SDS-page loading buffer. Retained proteins and unbound material were resolved in SDS-page and assayed with western blot using antibodies against HA, Arh1p and also Yah1p, provided by Dr. Mario Barros (Barros *et al.* 1999). As shown in figure 3.8, Yir024cp3HA was absorbed in the matrix with efficiency of at least 90% but Arh1p and Yah1p signals were exclusively in the unbound fraction. At this point a simple model of physical interaction between the short N terminal matrix domain of Yir024cp and Arh1p has to be excluded. Still a transient and very unstable interaction not detectable in the conditions used might exist. For instance the 250Kda complex were Yir024cp resides, working like a scaffold, could bridge this interaction. However is unlikely that the same complex could have mediated the interaction also in the nuclear environment in which the Y2H assay is performed.

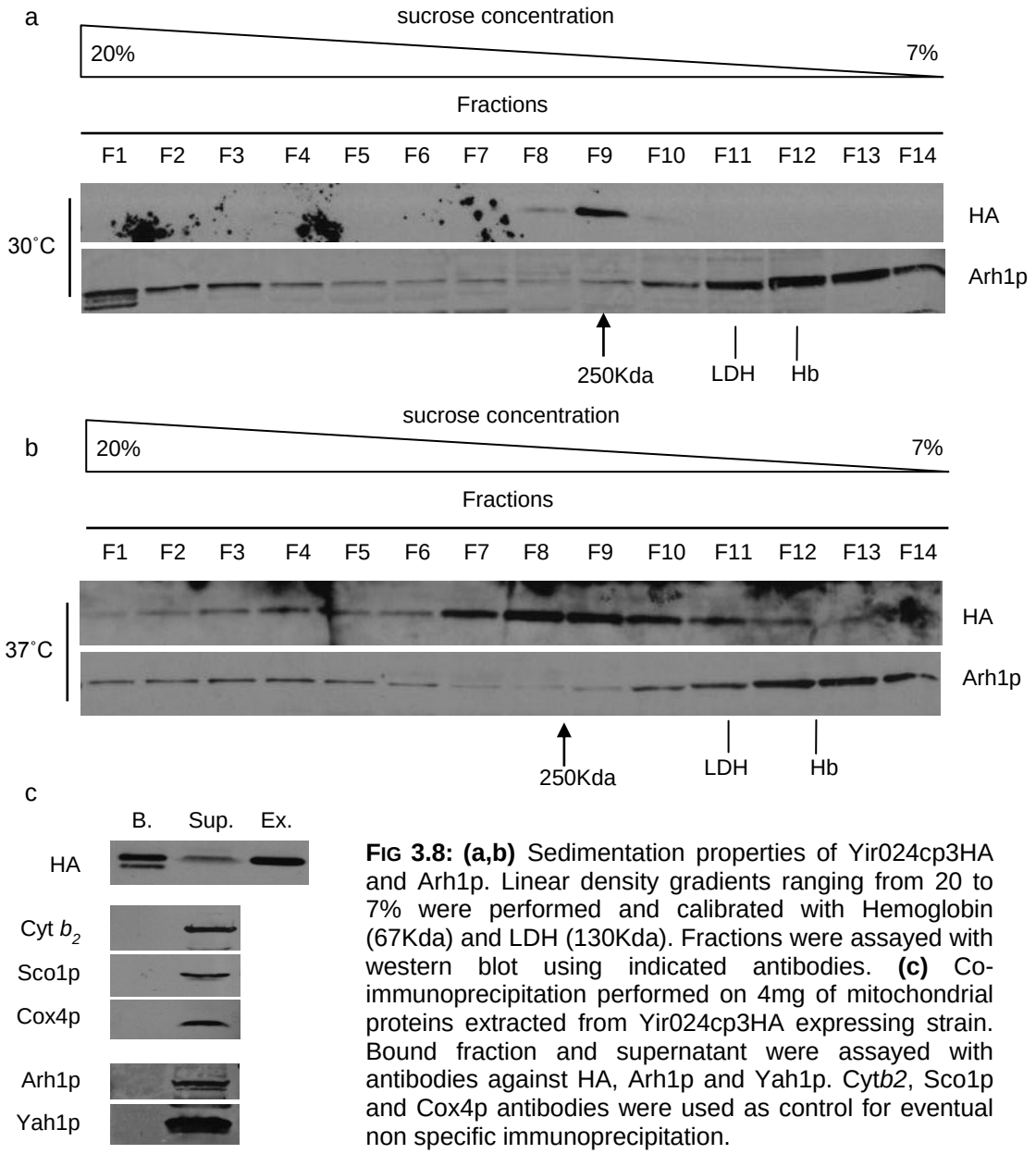

FIG 3.8: (a,b) Sedimentation properties of Yir024cp3HA and Arh1p. Linear density gradients ranging from 20 to 7% were performed and calibrated with Hemoglobin (67Kda) and LDH (130Kda). Fractions were assayed with western blot using indicated antibodies. **(c)** Co-immunoprecipitation performed on 4mg of mitochondrial proteins extracted from Yir024cp3HA expressing strain. Bound fraction and supernatant were assayed with antibodies against HA, Arh1p and Yah1p. Cyt*b2*, Sco1p and Cox4p antibodies were used as control for eventual non specific immunoprecipitation.

Although Yir024cp is not a physical interactor of Arh1p, its role remains unclear and interesting. Indeed it has an uncommon topology in the mitochondrial compartments, with a small N terminal of 20 amino acids exposed to the mitochondrial matrix and a big globular domain of 152 amino acids in the IMS. Not many proteins are known to share this kind of topology. Some of those are involved in different steps of complex IV maturation like Sco1p, Cox11p, Pet100p and Pet191p or complex III like Bca1p (Glerum *et al.* 1996; Forsha *et al.* 2001; Carr *et al.* 2005; Khalimonchuk *et al.* 2008; Mathieu *et al.* 2011). A defect in such processes could explain the observed phenotypes of *yir024cΔ*

that could therefore represent an ancillary assembly factor for respiratory complexes. Some others proteins with same topology are involved in mitochondrial morphology, as Fmp30p (Kuroda *et al.* 2011), or inner membrane organization. Strikingly three independent studies, published within few days in October 2011, completely characterized the same six protein complex of mitochondrial inner membrane needed for *cristae* organization (named MICOS, MINOS and MitOS). The complex contained Mitofillin/Fcj1 plus Aim5p, Aim37p, Aim13p, Mos1p and Mos2p. All these proteins except Aim13p and Mos2p were demonstrated to share the same topology of Yir024cp3HA (Harner *et al.* 2011; Hoppins *et al.* 2011; von der Malsburg *et al.* 2011). None of these approaches identified Yir024cp as a component of this complex but would be interesting to analyze mitochondrial morphology in *yir024cΔ* looking for *cristae* defects or other morphological phenotypes. It is indeed known that defects in *cristae* formation can cause respiratory deficiency like in mutants of the aforementioned complex. Also, it would be interesting to understand if Yir024cp function resides in its localization anchored to the inner membrane. To address this point a strain expressing only the globular domain along with an import sequence should be created and phenotypes compared with those of the mutant strain.

Certainly, one of the most direct ways to shed light into functional role of this protein in the inner membrane is to characterize the complex in which it resides. In order to do that the 250Kda complex was purified. Six linear 7-20% sucrose gradients were prepared for a total of 24mg of mitochondrial proteins treated and all the corresponding fractions were pooled together and assayed with western blot. The three fractions with most intense HA signal were used as starting material for a co-immunoprecipitation with agarose-HA affinity matrix. The final elution was successfully achieved with SDS loading buffer. Elute was loaded in 12% SDS-page and protein bands were stained with Coomassie blue. Different bands with a molecular weight of about 60-70Kda were identified. Some bands were cut from the gel and submitted to mass-spectrometry analysis. Identification of 250Kda complex partners should give precise hints in the function of this uncharacterized protein. Unfortunately no proteins were identified in the bands we sent for sequencing, but only background interference. This analysis should be repeated with large amounts of starting material.

3.3 References

Barros MH (2002). "Mitochondrial Ferredoxin Is Required for Heme A Synthesis in Saccharomyces cerevisiae." Journal of Biological Chemistry **277**(12): 9997-10002.

Barros MH, Carlson CG, Glerum DM and Tzagoloff A (2001). "Involvement of mitochondrial ferredoxin and Cox15p in hydroxylation of heme O." FEBS Lett **492**(1-2): 133-138.

Barros MH and Nobrega FG (1999). "YAH1 of Saccharomyces cerevisiae: a new essential gene that codes for a protein homologous to human adrenodoxin." Gene **233**(1-2): 197-203.

Barros MH and Tzagoloff A (2002). "Regulation of the heme A biosynthetic pathway in Saccharomyces cerevisiae." FEBS Lett **516**(1-3): 119-123.

Carr HS, Maxfield AB, Horng YC and Winge DR (2005). "Functional analysis of the domains in Cox11." J Biol Chem **280**(24): 22664-22669.

Churcher C, Bowman S, Badcock K, Bankier A, Brown D, Chillingworth T, . . . et al. (1997). "The nucleotide sequence of Saccharomyces cerevisiae chromosome IX." Nature **387**(6632 Suppl): 84-87.

Cruciat CM, Brunner S, Baumann F, Neupert W and Stuart RA (2000). "The cytochrome bc1 and cytochrome c oxidase complexes associate to form a single supracomplex in yeast mitochondria." J Biol Chem **275**(24): 18093-18098.

Dumas B, Cauet G, Lacour T, Degryse E, Laruelle L, Ledoux C, . . . Achstetter T (1996). "11 beta-hydroxylase activity in recombinant yeast mitochondria. In vivo conversion of 11-deoxycortisol to hydrocortisone." Eur J Biochem **238**(2): 495-504.

Ferrero I, Viola AM and Goffeau A (1981). "Induction by glucose of an antimycin-insensitive, azide-sensitive respiration in the yeast Kluyveromyces lactis." Antonie Van Leeuwenhoek **47**(1): 11-24.

Forsha D, Church C, Wazny P and Poyton RO (2001). "Structure and function of Pet100p, a molecular chaperone required for the assembly of cytochrome c oxidase in Saccharomyces cerevisiae." Biochem Soc Trans **29**(Pt 4): 436-441.

Glerum DM, Muroff I, Jin C and Tzagoloff A (1997). "COX15 codes for a mitochondrial protein essential for the assembly of yeast cytochrome oxidase." J Biol Chem **272**(30): 19088-19094.

Glerum DM, Shtanko A and Tzagoloff A (1996). "SCO1 and SCO2 act as high copy suppressors of a mitochondrial copper recruitment defect in Saccharomyces cerevisiae." J Biol Chem **271**(34): 20531-20535.

Harner M, Korner C, Walther D, Mokranjac D, Kaesmacher J, Welsch U, . . . Neupert W (2011). "The mitochondrial contact site complex, a determinant of mitochondrial architecture." EMBO J **30**(21): 4356-4370.

Hess DC, Myers CL, Huttenhower C, Hibbs MA, Hayes AP, Paw J, . . . Caudy AA (2009). "Computationally driven, quantitative experiments discover genes required for mitochondrial biogenesis." PLoS Genet **5**(3): e1000407.

Hoppins S, Collins SR, Cassidy-Stone A, Hummel E, DeVay RM, Lackner LL, . . . Nunnari J (2011). "A mitochondrial-focused genetic interaction map reveals a scaffold-like complex required for inner membrane organization in mitochondria." The Journal of Cell Biology **195**(2): 323-340.

Huh WK, Falvo JV, Gerke LC, Carroll AS, Howson RW, Weissman JS and O'Shea EK (2003). "Global analysis of protein localization in budding yeast." Nature **425**(6959): 686-691.

Khalimonchuk O, Rigby K, Bestwick M, Pierrel F, Cobine PA and Winge DR (2008). "Pet191 is a cytochrome c oxidase assembly factor in Saccharomyces cerevisiae." Eukaryot Cell **7**(8): 1427-1431.

Kuroda T, Tani M, Moriguchi A, Tokunaga S, Higuchi T, Kitada S and Kuge O (2011). "FMP30 is required for the maintenance of a normal cardiolipin level and mitochondrial morphology in the absence of mitochondrial phosphatidylethanolamine synthesis." Mol Microbiol **80**(1): 248-265.

Lacour T, Achstetter T and Dumas B (1998). "Characterization of recombinant adrenodoxin reductase homologue (Arh1p) from yeast. Implication in in vitro cytochrome p45011beta monooxygenase system." J Biol Chem **273**(37): 23984-23992.

Lacour T and Dumas B (1996). "A gene encoding a yeast equivalent of mammalian NADPH-adrenodoxin oxidoreductases." Gene **174**(2): 289-292.

Lange H, Kaut A, Kispal G and Lill R (2000). "A mitochondrial ferredoxin is essential for biogenesis of cellular iron-sulfur proteins." Proc Natl Acad Sci U S A **97**(3): 1050-1055.

Li J (2000). "Adrenodoxin Reductase Homolog (Arh1p) of Yeast Mitochondria Required for Iron Homeostasis." Journal of Biological Chemistry **276**(2): 1503-1509.

Lill R (2008). "Maturation of Iron-Sulfur Proteins in Eukaryotes: Mechanisms, Connected Processes, and Diseases." Annual Review of Biochemistry.

Lill R and Mühlenhoff U (2006). "Iron-Sulfur Protein Biogenesis in Eukaryotes: Components and Mechanisms." Annual Review of Cell and Developmental Biology **22**(1): 457-486.

Manzella L, Barros MH and Nobrega FG (1998). "ARH1 of Saccharomyces cerevisiae: a new essential gene that codes for a protein homologous to the human adrenodoxin reductase." Yeast **14**(9): 839-846.

Mathieu L, Marsy S, Saint-Georges Y, Jacq C and Dujardin G (2011). "A transcriptome screen in yeast identifies a novel assembly factor for the mitochondrial complex III." Mitochondrion **11**(3): 391-396.

Mense SM and Zhang L (2006). "Heme: a versatile signaling molecule controlling the activities of diverse regulators ranging from transcription factors to MAP kinases." Cell Res **16**(8): 681-692.
Moraes CT, Diaz F and Barrientos A (2004). "Defects in the biosynthesis of mitochondrial heme c and heme a in yeast and mammals." Biochim Biophys Acta **1659**(2-3): 153-159.
Mortimer RK and Johnston JR (1986). "Genealogy of principal strains of the yeast genetic stock center." Genetics **113**(1): 35-43.
Muhlenhoff U, Gerber J, Richhardt N and Lill R (2003). "Components involved in assembly and dislocation of iron-sulfur clusters on the scaffold protein Isu1p." EMBO J **22**(18): 4815-4825.
Muhlenhoff U, Richhardt N, Gerber J and Lill R (2002). "Characterization of iron-sulfur protein assembly in isolated mitochondria. A requirement for ATP, NADH, and reduced iron." J Biol Chem **277**(33): 29810-29816.
Nobrega FG, Nobrega MP and Tzagoloff A (1992). "BCS1, a novel gene required for the expression of functional Rieske iron-sulfur protein in Saccharomyces cerevisiae." EMBO J **11**(11): 3821-3829.
Nobrega MP, Nobrega FG and Tzagoloff A (1990). "COX10 codes for a protein homologous to the ORF1 product of Paracoccus denitrificans and is required for the synthesis of yeast cytochrome oxidase." J Biol Chem **265**(24): 14220-14226.
Pain J, Balamurali MM, Dancis A and Pain D (2010). "Mitochondrial NADH kinase, Pos5p, is required for efficient iron-sulfur cluster biogenesis in Saccharomyces cerevisiae." J Biol Chem **285**(50): 39409-39424.
Pierrel F, Hamelin O, Douki T, Kieffer-Jaquinod S, Mühlenhoff U, Ozeir M, . . . Fontecave M (2010). "Involvement of Mitochondrial Ferredoxin and Para-Aminobenzoic Acid in Yeast Coenzyme Q Biosynthesis." Chemistry & Biology **17**(5): 449-459.
Rothstein RJ (1983). "One-step gene disruption in yeast." Methods Enzymol **101**: 202-211.
Sickmann A, Reinders J, Wagner Y, Joppich C, Zahedi R, Meyer HE, . . . Meisinger C (2003). "The proteome of Saccharomyces cerevisiae mitochondria." Proc Natl Acad Sci U S A **100**(23): 13207-13212.
Siep M, van Oosterum K, Neufeglise H, van der Spek H and Grivell LA (2000). "Mss51p, a putative translational activator of cytochrome c oxidase subunit-1 (COX1) mRNA, is required for synthesis of Cox1p in Saccharomyces cerevisiae." Curr Genet **37**(4): 213-220.
Tzagoloff A, Nobrega M, Gorman N and Sinclair P (1993). "On the functions of the yeast COX10 and COX11 gene products." Biochem Mol Biol Int **31**(3): 593-598.
Uetz P, Giot L, Cagney G, Mansfield TA, Judson RS, Knight JR, . . . Rothberg JM (2000). "A comprehensive analysis of protein-protein interactions in Saccharomyces cerevisiae." Nature **403**(6770): 623-627.
von der Malsburg K, Muller JM, Bohnert M, Oeljeklaus S, Kwiatkowska P, Becker T, . . . van der Laan M (2011). "Dual role of mitofilin in mitochondrial membrane organization and protein biogenesis." Dev Cell **21**(4): 694-707.

Material and Methods

4.1 Miscellanea

4.1.1 Strains Used

4.1.2 Media And Growth Conditions

4.1.3 Nuclei Acids Manipulation

4.1.4 E. Coli Transformation

4.1.5 S. Cerevisiae Transformation

4.1.6 Polymerase Chain Reaction

4.1.7 Protein Separation with SDS-Page

4.1.8 Western Blotting and Ig-Detection

4.2 Whole Cell Analysis

4.2.1 Growth Analyses of BY4742 Knock Out Collection

4.2.2 Serial Dilution Growth Test (Spot Assay)

4.2.3 Cytochromes Spectra Absorption

4.2.4 Oxygen Consumption

4.2.5 In Vivo Labeling of Mitochondrial Products with ^{35}S-met

4.2.6 Crude Total Protein Extraction

4.3 Mitochondrial Analysis

4.3.1 Preparation of Yeast Mitochondria with Intact Outer Membrane

4.3.2 Quantification of Total Mitochondrial Proteins

4.3.3 Extraction of Total Mitochondrial Cytochromes

4.3.4 NADH Cytochrome C Reductase (NCCR) Enzymatic Activity

4.3.5 Succinate Dehydrogenase (SQDR) Enzymatic Activity

4.3.6 Cytochrome C Oxidase (COX) Enzymatic Activity

4.3.7 HPLC Analysis of Total Heme Content

4.3.8 Mitochondrial Protein Localization

4.3.9 Solubility Assay (Alkaline Carbonate Extraction)

4.3.10 Solubilization of Mitochondrial Proteins

4.3.11 Sucrose Density Gradients

4.3.12 Co-Immunoprecipitation Analysis with HA Affinity Matrix

4.4 References

4.1 Miscellanea

4.1.1 Strains used

NAME	GENOTYPE	REF
BY4742	*MATα his3Δ1 leu2Δ0 lys2Δ0 ura3Δ0*	(Brachmann *et al.* 1998)
BY4739	*MATα leu2Δ0 lys2Δ0 ura3Δ0*	(Brachmann *et al.* 1998)
W303-1a	*MATa leu2-3112 trp1-1 can1-100 ura3-1 ade2-1 his3-*	(Brachmann *et al.* 1998)
W303-1b	*MATα leu2-3112 trp1-1 can1-100 ura3-1 ade2-1 his3-*	(Brachmann *et al.* 1998)
elp3Δ	*BY4742 elp3::KANMX4*	(Giaever *et al.* 2002)
trm9Δ	*BY4742 trm9::KANMX4*	(Giaever *et al.* 2002)
ncs6Δ	*BY4742 ncs6::KANMX4*	(Giaever *et al.* 2002)
yir024cΔ	*BY4742 yir024c::KANMX4*	(Giaever *et al.* 2002)
yir024cΔ	*W303-1b yir024c::KANMX4*	this study
yir024c3HA	*W303-1b yir024c::KANMX4 ura3-1::YIR024C3HA*	this study

To perform the genome-wide screening the *S. cerevisiae* Genome Deletion Project collection was used (Giaever *et al.* 2002). It was purchased from Open Biosystems (Huntsville, AL) and rearranged in 13 24x16 plates, each with eight empty fixed positions as contaminations control. One copy of each 384 plate is maintained in liquid medium YPD 15% glycerol (see above for composition) at -80˚C as stab culture.
As bacterial system the strain *DH10B* (Brachmann *et al.* 1998) was used.

4.1.2 Media and growth conditions

For yeast the following media were used: YP (1% peptone, 0.5% yeast extract), YPA (2% peptone, 1% yeast extract, 7.5mg/ml adenine), YNB (YNB ForMedium™ w/o aminoacids w/o NH_4SO_4 1,9 g/L, NH_4SO_4 5 g/L). Minimum media was enriched with drop-out powder (Kaiser *et al.* 1994). If necessary singles aminoacids could be excluded from complete drop-out to maintain selective pressure. As solidifying agent agar ForMedium™ 2% was added.
Carbon sources were added at final concentration of 2% if not specified differently. The following sources were used: Glucose (D), Ethanol (E), Glycerol (G), Potassium Acetate (KAc), Lactate (L).
S. cerevisiae was cultured at 30˚C, in constant shacking 120 rpm if liquid media was used. To induce heat stress, cultures were incubated at 37˚C in thermostat or water bath.

For *E. coli* LB media was used (1% bacto tryptone Difco™, 0.5% yeast extract Difco™, 0.5% NaCl, pH 7.2-7.5). Agar 2% and ampicillin (Sigma-Aldrich®) 100mg/ml were added if needed. For α-complementation selection 80µl of 5-bromo-4-chloro-3-indolyl-b-D-galactopyranoside (Xgal) 2% (dissolved in dimethilformamide) and 40µl isopropyl-beta-D-thiogalactopyranoside (IPTG) 23,8 mg/ml were added. Cultures were incubated at 37˚C in constant shacking if necessary.

4.1.3 Nucleic Acids manipulation

All the manipulations were carried out with standard techniques (Maniatis *et al.* 1982). Plasmid DNA was extracted from *E. coli* with Wizard® Plus SV Minipreps, Wizard® Plus Minipreps (©Promega) or following standard procedures (Maniatis *et al.* 1982). DNA recovery from agarose gel and purification of PCR products were carried out with Wizard® SV Gel and PCR Clean-up System (©Promega) commercial kit.

Genomic DNA from *S. cerevisiae* was extracted as previously described (Hoffman *et al.* 1987; Looke *et al.* 2011).

Enzymatic manipulations (restriction, ligation, dephosphorylation) were carried out following manufacturer indications (New England Biolabs® *Inc.* NEB, Invitrogen™).

Sequencing was performed with external services (©Eurofins-MWG for Europe, Genewiz® *Inc.* for United States).

4.1.4 E. coli transformation

E. coli transformation was achieved with electroporation. Competent cells were prepared as previously described (Dower *et al.* 1988). Transformation was carried out with 1-3µl of plasmid DNA or ligation product. One mm or 2 mm cuvettes were used, applying respectively a current of 1.75KV, 25 µF 200 Ω or 2KV, 25 µF 200 Ω.

Alternatively, $CaCl_2$ competent cells were prepared and transformed with standard techniques (Maniatis *et al.* 1982).

4.1.5 S. cerevisiae transformation

Yeast transformation was carried out with Lithium Acetate (LiAc) as described by Gietz *et al.* If a greater efficiency was desired, the long protocol was applied (Gietz *et al.* 2002).

For the one-step gene disruption and episomic plasmids integration (Rothstein 1983) the protocol used was modified from Schiestl *et al.* method (Schiestl *et al.* 1989) and performed as follows:

1. Inoculate strain to be transformed in 10ml YPD and grow o/n at 30˚C
2. Inoculate from overnight batch into fresh 10ml YPD to OD_{600} of about 0.1
3. Grow cells at 30˚C until OD_{600} reaches 0.6 to 1
4. Harvest 1ml of culture centrifuging 2000-3000rpm for 1-2 minutes. Resuspend in 1ml of TEL solution and centrifuge 2000-3000rpm for 5 minutes.

   TEL solution: 10mM TrisHCl pH 7.5
   1mM EDTA pH 8
   0.1M LiAc
5. Resuspend pellet in 0.1ml TEL and transfer to a clean sterile eppendorf tube. Add transforming DNA (1-10µg) and 5µl of 10mg/ml salmon sperm DNA solution (previously denatured for 5 minutes at 95˚C and cooled 2 minutes on ice). Mix and incubate 30 minutes at room temperature without shacking
6. Add 0.7ml of 40% PEG4000 in TEL buffer and mix by pipetting. Incubate 45-60 minutes at room temperature without shacking
7. Heat shock at 42˚C for 10 minutes and incubate on ice 2-5 minutes
8. Pellet for 1 minute and wash once in 0.2ml of TE (10mM TrisHCl pH 7.5, 1mM EDTA pH 8). Pellet again for 1 minute ad resuspend in 100µl of sterile water. Plate on selective medium.

4.1.6 Polymerase Chain Reaction

All the reactions were performed following manufacturer indications. For analytical purpose *Taq* DNA polymerase 2X master mix (NEB) or GoTaq® DNA polymerase (©Promega) were used. Preparative reactions (for gene cloning, cassette transfer, sequencing) were performed with a high fidelity polymerase. KOD HiFi DNA polymerase was used (Novagen®).

4.1.7 Protein separation with SDS-page

Protein separation with SDS-page was performed with classical Laemmli system (Laemmli 1970). Separating gels were prepared at 12% polyacrylamide (30:0.8 acrylamide-bis), stacking gel at 6%. Running was performed for 1hr 30' at 100-120volts.

4.1.8 Western Blotting and Ig-detection

Separated proteins were transferred to nitrocellulose membrane by electroblot for 1hr 15' at 200mA. Semi-dry blotting system was used. Quality of the blot was assessed with Ponceau S staining.

Transfer Buffer: 200mM glycine
25 mM Tris
20% methanol

Membranes were blocked 1hr with 5% non-fat dry milk prepared in washing buffer and incubated o/n with appropriate primary antibody (mono or polyclonal).

Washing Buffer: TBS 1%
tween 0.1%

Blocked membranes were washed 2 times 15 min with washing buffer prior incubation with suitable secondary antibodies, conjugated with horseradish peroxidase (1:10000 in 5% milk if anti rabbit Ig, 1.5% milk if anti mouse). After 1hr incubation membranes were washed as above and developed with ECL based immune revelation. If greater sensitivity was necessary SuperSignal West Femto or Pico commercial kits were implemented (© Thermo Scientific).

4.2 Whole Cell Analysis

4.2.1 Growth Analysis of BY4742 Knock Out Collection (primary screening)

To perform genome-wide growth analysis a pin-replica strategy was used. A multi-blot replicator VP384S2A (V&P Scientific, Inc.) and a semiautomatic device (designed and built in c/o Department of Genetics, University of Parma) were used (Fig 4.1). All replication steps were carried out under sterile hood flux.

a b c

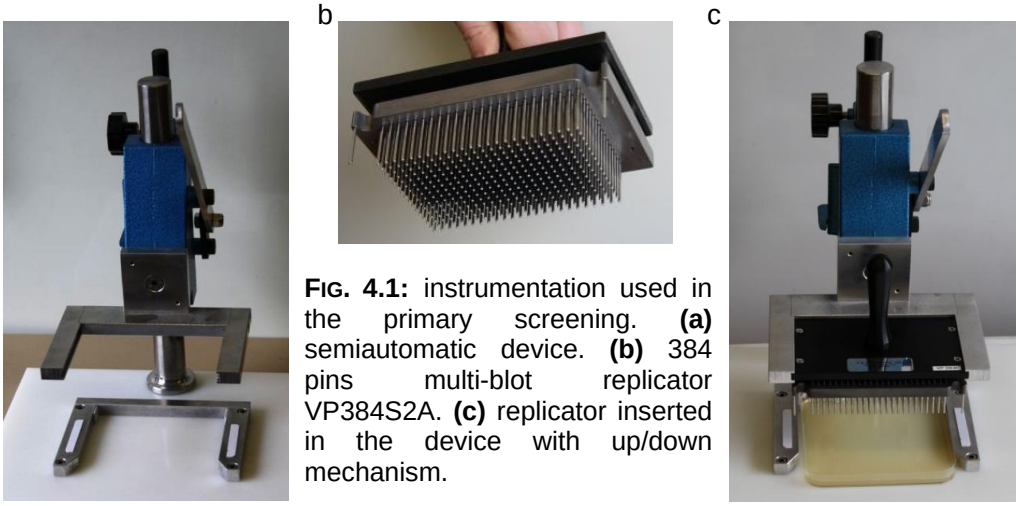

FIG. 4.1: instrumentation used in the primary screening. **(a)** semiautomatic device. **(b)** 384 pins multi-blot replicator VP384S2A. **(c)** replicator inserted in the device with up/down mechanism.

Each 384-well format plate of the knock out collection (See Strains section) is maintained at -80˚C as stab culture. To work on fresh cells a first replica from stab culture to solid media was performed as follows:

- The multi-blot replicator is sterilized washing sequentially in bleach 10% (no more than 30''), twice in sterile water and finally in propan-2-ol (Sigma-Aldrich®) for 1 minute. The replicator is left hanging for five minutes to let the propanol dry. Between each wash replicator pins are dried on a piece of blotting paper. Using the up/down mechanism of semiautomatic device the replicator pins are dipped in the thawed stab and subsequently printed on a fresh YPD medium plus 200µg/ml G418 plate. The new 384-well plate is incubated at 30˚C for 48hrs.

For growth analysis each collection plate was used to create new plates for conditions of interest (different media or growth temperature):

- Sterile replicator is used to pick up cells from a fresh plate prepared from stab culture as described. Before printing a new agar plate is necessary to dilute and normalize the number of cells on every pin. To this purpose the replicator is

dipped up/down 20 times in a 384-well plate, each well filled with 70µl of sterile water. Afterward a new plate is printed and incubated in condition of interest (for instance 37˚C). After 48hrs a picture is taken of every plate and semi-quantitative growth scores are attributed to each clone, comparing to opportune controls.

4.2.2 Serial Dilution Growth Test (Spot Assay)

Spot assay is a classical phenotypic analysis used to test growth of single strains in different condition. The principle is a 10-fold serial dilution from a starting culture at 1*10e7 cells/ml, performed then three or four times. From these suspensions a fixed volume is spotted in ordered rows on agar plates then incubated for at least 48hrs.

Spot assay was used as secondary screening during high-throughput analysis. A total number of 16 strains (14 null mutants plus WT and ρ^0) were managed in a single experiment. The first column and the seventh of a 96-well plate were filled with 150µl of YPD and strains inoculated with sterile toothpick. After incubation at 30˚C o/n the OD_{600} was measured for each strain. The second column was used to dilute each strain to a concentration of 1 OD (1*10e7). Other 4 columns were used for four 10-fold serial dilutions, using a multichannel pipette. From each column 4µl were spotted in YPD and YPE plates, in conditions resembling the primary screening.

Comparing to WT and ρ^0 ones strains were classified as low sensitive (LS), medium sensitive (MS) or high sensitive (HS), as shown in Fig. 4.2.

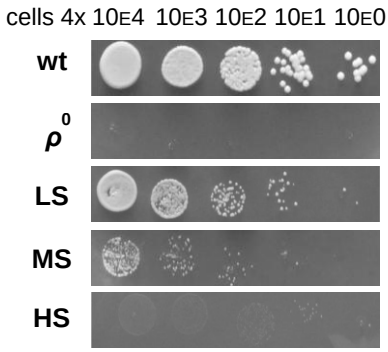

Fig. 4.2. Examples of spot assay of serial dilutions ranging from 4*10e4 to 4*10 cells.

Spot assay was performed using the same principles for single strains. Dilutions were carried out in eppendorf tubes and 10 or 5µl of suspensions were spotted in ordered rows on agar plates in conditions of interest. After 48 or 72hrs images of the plates were taken.

4.2.3 Cytochromes Spectra Absorption

Mitochondrial respiratory chain intactness can be assessed recording the cytochromes absorption profile on whole cells. All the experiments were carried out with a *Cary 300Scan* UV-vis spectrophotometer (Varian Inc.), recording continuously from 630 to 540nm. The following general protocol was used:

1. Strains are pre inoculated in 10ml YPD plus G418 200µg/ml and incubated o/n 30˚C
2. Inoculate 2.5ml in 150ml of YPD 0.6% and incubate 24hrs at 37˚C
3. After checking that glucose is finished (to be sure that any repression is affecting the cells) harvest cells centrifuging 5000rpm 10 minutes, 4˚C
4. Resuspend in water proportionally to the cells humid wet (to normalize concentration among different strains)
5. Register the spectra oxidized versus reduced.

Raw data were processed using Excel functions (Microsoft® Office). WT strain was included in each analysis.

4.2.4 Oxygen Consumption

Oxygen consumption was recorded using Oxygraph system from Hansatech, composed of a S1 Clark electrode core controlled with Oxygraph Plus software (Hansatech Instruments Ltd.).

Cells were obtained as described for cytochromes spectra recording. One hundred µl were added to 900µl of K-ftalate 0.1M pH5 in the chamber. Oxygen decrease was recorded for at least 1 minute.

Five hundred µl of cell suspension were exsiccated at 37˚C for 48hrs and dry wet estimated. Absolute oxygen consumption rate was expressed as nmol O_2 for minute for mg of cells (nmol/min mg).

4.2.5 In Vivo Labeling of Mitochondrial Products with ^{35}S-met

1. Grow strains on YP Gal plates and inoculate at very low concentration in 10ml of synthetic minimum media with galactose and auxotrophic requirements. This step can also be performed in YP Gal media. Grow until OD_{600} is 0.6 – 2 maximum.
2. Harvest equivalent of 0.6 OD in eppendorf tube. Centrifuge 1 minute 6000-8000rpm
3. Wash the pellet with 500µl of 40mM phosphate pH 6, galactose 2% (Important: repeat twice this step if cells were grown in complete media to eliminate any residual methionine). Resuspend cells in 500µl of the same buffer
4. Add 10µl of freshly prepared cycloheximide (10mg/ml in water), mix and incubate 2.5 minutes at 30˚C (or the temperature at which the cells were grown)
5. Add 2.5-4µl of ^{35}S-methionine (10Ci/ml). Mix and incubate for a definite time depending on the experiment (usually 5 to 15 minutes)
6. Centrifuge 1 minute at maximum speed and resuspend cells in 75µl of Rodel Mix (protect stock solution from light). Immediately add 500µl of bidistilled H_2O. Add 575µl of 50% tri-chloroacetic acid (TCA). Incubate at least 15 minutes on ice. Centrifuge 15000rpm, 10 minutes

   Rodel Mix: 5.56ml 5M NaOH
   1.11ml ß-mercaptoethanol
   6.84ml H_2O
   1.5ml 0.1M PMSF
7. Wash pellet once without resuspending with 0.5M Tris-Base (no pH adjusted) to neutralize TCA. Wash once without resuspending with bi-distilled H_2O.
8. Resuspend in 25µl of 1X Loading Buffer without heating. Load on 17.5% SDS-PAGE (10X15cm separating gel at least)

   Loading Buffer 1X: 2% SDS
   10% Glycerol
   60mM Tris-HCl, pH 6.8
   2.5% ß-mercaptoethanol
   bromophenol blue
9. Run until blue reaches the bottom, without exiting the gel. Maximum 40mA.
10. Semidry transfer to nitrocellulose membrane for 1hr 30minutes at 200mA. Let the membrane dry for few minutes at 37˚C and perform a first exposition of about 24 hrs.

Buffers and Gel composition

Solution	Separating Gel 17.5%	Stacking Gel 5%
30% acrylamide 0.2 bis-acrylamide	12.61ml	1.079ml
1.825M TrisHCl pH 8.8	4.55ml	-
0.6M TrisHCl pH 6.8	-	0.650ml
water	4.55ml	4.620ml
SDS 10%	217µl	65µl
APS 10%	109µl	32.5µl
TEMED	7.8µl	6.5µl
final volume	22.1ml	6.5ml

Running Buffer: 50mM Tris-HCl, pH 8.3
384mM glycine
0.1% SDS

Prepare a 5X stock solution (30gr Tris-Base, 144gr glycine, 5gr SDS for 1 liter). Dilute to 1X and adjust the pH precisely to pH 8.3. The pH is crucial for optimal proteins resolution. Check frequently the pH of 1X running buffer.

4.2.6 Crude Total Protein Extraction

1. Grow cells overnight to 0.7-1.2 OD
2. Harvest the equivalent of 1.2OD of cells by centrifugation 1min 6000-8000rpm
3. Wash once with water and resuspend the pellet in 75µl of Rodel mix (see above)
4. Add 500µl of water
5. Add 575µl of TCA50%
6. Incubate on ice at least 15 minutes. Centrifuge 15000rpm 10min
7. Wash pellet once with 0.5M Tris-base without resuspending (about 1ml)
8. Wash pellet once with water without resuspending (about 1ml)
9. Resuspend in 25µl of 1X LB and add few µl of Tris-base if the color is yellowish

4.3 Mitochondrial Analysis

4.3.1 Preparation of Yeast Mitochondria with Intact Outer Membrane

(Glick et al. 1995)

1. Cells are harvested at 2000-3500 rpm for 7 minutes and washed once with sorbitol 1.2M
2. Washed cells are suspended in digestion buffer at concentration of 1gr of cells in 3ml

   Digestion Buffer: 30ml 2M sorbitol
   3ml 1M phosphate buffer, pH 7.5
   0.1ml 0.5M EDTA pH 8
   0.5ml ß-mercaptoethanol
   50mg of zymolyase 20000
   16ml of water (Vf=50ml)

Incubate at 30˚C or 37˚C depending on the used growth conditions until most of the cells have been converted to spheroplasts.

3. Add cold Buffer A and immediately centrifuge 6000rpm for 10 minutes. Wash two additional times with Buffer A

   Buffer A: 1.2M deionized sorbitol (use BioRad® AG501-X8 resin)
   20mM KPO_4 pH 7.5

4. Washed spheroplasts are suspended in 0.6M sorbitol, 20mM KMES pH 6, 0.5mM PMSF at concentration of 1gr/3ml. Homogenize with and glass/Teflon pestle and overhead stirrer (Wheaton Science Products)
5. Centrifuge 3500rpm for 5 minutes to pellet debries. Collect the supernatant and centrifuge 10000rpm for 10 minutes to sediment mitochondria. The supernatant is the post mitochondrial fraction (PMS) and represent the cytosolic component
6. Mitochondria are briefly suspended with plastic sticks in 8ml of 0.6M sorbitol, 20mM KMES pH 6. Mitochondria are now suspended by gently homogenization in glass/Teflon pestle. Centrifuge at 3500rpm for 5 minutes to pellet broken mitochondria
7. Collect supernatant and centrifuge at 10000rpm for 10 minutes. Mitochondrial pellet is suspended in 2ml of 0.6M sorbitol, 20mM KMES and diluted with 20ml of 0.6M sorbitol, 20mM HEPES pH 7.4. Centrifuge 10000rpm for 10 minutes.
8. Suspend mitochondrial pellet in 0.6M sorbitol, 20mM HEPES accordingly to the pellet dimension. Mitochondria can be stored at -80˚C

4.3.2 Quantification of Total Mitochondrial Proteins

Quantification of protein concentration in mitochondrial extracts was performed with folin assay as follows:

1. Add 5 µl of proteins to 0.6ml of H_2O (two independent replicates for sample)
2. Add 3ml of Copper Reagent

   Copper Reagent: 0.5 ml 1% $CuSO_4$
   0.5 ml 2% K-Na tartrate
   49 ml 2% Na_2CO_3 in 0.1M NaOH
3. Incubate 10 min room temperature
4. Add 0.3ml of Folin&Ciocalteau's reagent (Sigma-Aldrich®) diluted 1:1 in water. Mix immediately vortexing briefly
5. Incubate at 90˚C for 2 min
6. Cool down on ice for 2 min
7. Measure absorbance at 750nm.

Absorbance values were converted in mg/ml concentrations fitting to a standard curve built with BSA standard solutions.

4.3.3 Extraction of Total Mitochondrial Cytochromes

(Tzagoloff *et al.* 1975)

Mitochondria were prepared with intact outer membrane. Following protocol was used:

1. Use 2.5 – 5mg of total mitochondrial proteins
2. Add 50mg of KCl and mix with plastic stick
3. Add water (to final volume of 1ml)
4. Add 50µl of 1M Tris-HCl pH 7.5
5. Add 100µl of 10% K deoxycholate

Centrifuge 40000rpm for 15 min 4˚C, transfer clear supernatant to a new tube and add 100µl of 20% K deoxycholate. Divide equally the solution in two cuvettes. The reference cuvette will be oxidized with few µl of a concentrate $KFeCN_3$ solution, the sample cuvette will be reduced adding few grains of Na-dithionite (add very small amount each time to avoid over reduction). Register the spectra continuously from 650 to 450nm.

Cytochromes can be quantified using following extinction coefficients (ε):

- cytochrome c+c_1 ε=18.7 (552 – 540 nm)
- cytochrome b ε=23.4 (560 – 575 nm)
- cytochrome a+a_3 ε=24.0 (605 – 630 nm)

and following formula: [(ΔOD/ε)*(1/mg)*1000] = nmol cyt / mg

4.3.4 NADH Cytochrome c Reductase (NCCR) Enzymatic Activity

This assay measures the combined activity of NADH dehydrogenase and complex III in yeast. Electron flux is from NADH-DH to complex III *via* ubiquinol to the final acceptor cytochrome c. Mitochondria were prepared as described and following protocol:

Solutions needed:
10mM K-phosphate pH 7.5
80mM KCN
1% cytochrome c (bovine or horse heart, Sigma-Aldrich®)
0.1M NADH in K-phosphate pH 7.5
0.5% Na-deoxycholate

Protocol: Prepare two cuvettes with 0.920ml of 10mM K-phosphate, 80µl of 1% cytochrome c, 5µl of KCN and 10µl of NADH. Use one of the two as reference and record the baseline for about 30'' at 550nm. Add solubilized mitochondria to the reaction and record for additional 1 minute (volume variable in accordance with concentration, usually 10-50µg).

To solubilize mitochondrial protein treat with 1 volume of Na-deoxycholate 0.5% (Na-DOC) just before the assay, pipetting up/down few times. For good statistical analyses repeat each sample three times solubilizing mitochondria once in a bigger volume (for instance 15µl of mitochondria plus 15µl of Na-DOC and neutralizing Na-DOC with 50µl of sorbitol HEPES EDTA solution.

Specific Activity: NCCR activity is calculated with cytochrome c ε of 18.5 and the following formula (ΔOD*ε/min mg).

4.3.5 Succinate Dehydrogenase (SQDR) enzymatic activity

This assay measures the rate of reduction of an artificial electron acceptor as dichlorophenolindophenol (DCPIP) by complex II. Mitochondria were prepared as described and following protocol:

Solutions needed:
10mM K-phosphate pH 7.4
0.4M succinate pH 7.4
80mM KCN
20mM phenazyne methosulfate (PMS)
20mM DCPIP
0.5% Na-DOC

Protocol: Add to a cuvette 900µl of K-phosphate, 40µl of succinate, 5µl of KCN and mitochondrial protein (about 25µg) previously solubilized. Incubate 3 minutes (this step is needed to release SDH from tight binding with oxaloacetate).

Add 50µl of PMS and finally start reaction with 5µl DCPIP. Record activity at 600nm.

Solubilization of mitochondrial protein is carried out 1 volume treatment of 0.5% Na-DOC.

Specific Activity: SQDR activity is calculated with ε of 22 and the following formula (ΔOD*ε/min mg).

4.3.6 Cytochrome c Oxidase (COX) Enzymatic Activity

This assay measures the rate of cytochrome c oxidation by complex IV in yeast. Mitochondria were prepared as described and following protocol:

Solutions needed:
20mM K-phosphate pH 7.5
1% cytochrome c in 20mM K-phosphate
0.5% Na-DOC

Protocol: Prepare two cuvettes with 920µl of K-phosphate and 80µl of cytochrome c reduced (with few grains of Na-dithionite). The reference cuvette will be oxidized with few drops of a concentrate $KFeCN_3$ solution. The difference in absorption between the two cuvettes should be 1OD. Add about 10µg of mitochondrial proteins previously solubilized to start reaction and record activity at 550nm. For computation of enzymatic rate it will be necessary also the zero value of absorbance (A_0).

Solubilization of mitochondrial proteins is achieved with 1 vol 0.5% Na-DOC treatment.

Specific activity: COX activity is calculated with cytochrome c ε of 18.5 and the following formula $[2.3\log(A_1/A_2)/(\varepsilon*mg*min)]*A_0$

4.3.7 Heme Analysis using High Pressure Chromatography (HPLC)

HPLC analysis of total heme was performed in reverse phase C18 column as described previously (Barros *et al.* 2001). Total mitochondria were extracted as described previously. Total heme was extracted in the following conditions:

1. Pellet 2mg of total mitochondria centrifuging 10000rpm 10 minutes, 4˚C
2. Resuspend pellet in 250µl of Acetone HCl 3% vortexing vigorously
3. Centrifuge 5 minutes, 14000rpm 4˚C
4. Prepare in a clean eppendorf 250µl of a 50% Acetonitrile 0.02% trifluoroacetic acid (TFA) solution
5. Transfer the supernatant of the centrifugation to the 50% Acetonitrile 0.02% TFA solution. Mix well
6. Centrifuge 7-10 minutes 14000rpm 4˚C
7. Collect supernatant and transfer to a clean tube
8. Add 25µl of 1.65M ammonium hydrochloride to adjust pH to 3.5
9. Mix well and centrifuge 5 minutes 14000rpm 4˚C
10. Load 400µl of the extract to an HPLC tube for analysis

4.3.8 Mitochondrial Protein Localization

Based on Glick BS procedure (Glick et al. 1995)

Mitochondria were prepared as describe. Following protocol was used:

1. Centrifuge 10000rpm, 10 minutes 4˚C to pellet mitochondria. Set up four different tubes with 200µg of total proteins
2. Wash sample 1 and 2 with 0.6M sorbitol, 20mM HEPES pH 7.4. Sample 3 and 4 with 20mM HEPES pH 7.4
3. Set up the following conditions:

	1	**2**	**3**	**4**
Mitochondria	200µg	200µg	200µg	200µg
0.6M sorbitol, HEPES 20 mM pH 7.4	250µl	250µl	-	-
HEPES 20 mM pH 7.4	-	-	250µl	250µl
Proteinase K (1:20 of a 0.63 mg/ml) solution)	-	5µl	-	5µl

4. Incubate samples on ice for 60 minutes
5. Add 5µl of 0.1M PMSF to stop reaction of Proteinase K
6. Centrifuge 20000rpm, 15 minutes 4˚C. Remove and keep supernatants
7. Pellet is resuspended in 0.1ml of 0.6M sorbitol, 20mM HEPES pH 7.4
8. Centrifuge 14000rpm, 5 minutes 4˚C
9. Dissolve pellets in 100µl of 1X SDS-page loading buffer (LB) and add 2µl of 0.1M PMSF
10. Load 20-30µl in 12% SDS-page and perform western against different mitochondrial proteins. Ideally use a control for each mitochondrial compartment

4.3.9 Solubility Assay (Alkaline Carbonate Extraction)

(Fujiki et al. 1982)

Mitochondria were prepared as previously described. Following protocol was used:

1. Pellet 200µg of total mitochondrial protein by centrifugation 10000rpm, 10minutes 4˚C
2. Suspend mitochondria in 100µl of 0.6M sorbitol 20mM HEPES and add 4µl of 0.1M PMSF
3. This mitochondrial suspension is sonicated 2 timed for 3 seconds, intensity 2 (conditions has to be optimized each time)
4. Sonicated mitochondria are centrifuged at 35000rpm, 15 minutes 4˚C
5. Supernatant is collected and centrifuged again to remove any additional insoluble portins that might have remained. Pellet is washed gently twice with 0.6M sorbitol

20mM HEPES without resuspending. This allow removal of any supernatant remained

6. The centrifuged again supernatant (S fraction) is mixed with SDS page loading buffer (75µl of S + 25µl of LB4X)
7. The pellet (not soluble fraction) is resuspended in 100µl of Na_2CO_3 100mM pH 11 (dissolved in water, the pH is critical) and incubated on ice 30 minutes
8. Centrifuge 35000rpm, 15 minutes 4˚C
9. The supernatant (CS fraction) is centrifuged again to remove any additional insoluble fraction and eventually mixed with LB4X to a final volume of 100µl
10. The pellet (CP fraction) is washed gently twice with carbonate without resuspending to remove any CS fraction that might have remained
11. CP fraction is resuspended in 100µl of LB1X
12. Load proportionally the three fractions on SDS page and perform western using controls for soluble proteins, integral membrane proteins and loosely bound membrane proteins

4.3.10 Solubilization of Mitochondrial Proteins

To solubilize mitochondrial tagged proteins (for following biochemical characterization) different extracting conditions were tested to find the mildest one. The following test protocol was used:

1. Pellet 0.5mg of total mitochondrial proteins centrifuging 10000rpm 4˚C
2. Discard supernatant and resuspend n 50µl of Extraction buffer

   Extraction buffer: 20mM HEPES
   0.5mM PMSF
   + detergent (digitonin, laurylmaltoside)
   + salt (KCl, NaCl)
   water to 100µl
3. Incubate 10 min on ince
4. Centrifuge 21000 rpm, 15 minutes 4˚C
5. Transfer 37.5µl of supernatant in a new tube and add 12.5µl of LB4X
6. Wash the pellet twice with 10mM HEPES without resuspending
7. Resuspend pellet in 50µl of LB1X

Equivalent µg from pellet and supernatant are loaded in SDS page to evaluate the extraction efficiency for protein of interest.

4.3.11 Sucrose Density Gradients

Linear sucrose density gradients were used to estimate native molecular size of tagged proteins and for co-sedimentation analysis. This general protocol was used:

Sample preparation: 4mg of total mitochondrial proteins are solubilized with previously tested conditions in a total volume of 400µl. Forty µl of supernatant are kept and used as positive control of extraction. Two mg of hemoglobin (Sigma-Aldrich®) and 60µg of lactate dehydrogenase resuspended in 40µl of extraction buffer are added to the clarified supernatant.

Gradient preparation: for a 5ml linear 7-20% sucrose gradient the following solutions were prepared

	7% sucrose	**20% sucrose**
sucrose powder	210 mg	600 mg
HEPES 1M	60 µl	60 µl
PMSF 0.1M	15 µl	15 µl
Detergent	1/10 of tested	1/10 of tested
water to final volume	3 ml	3 ml

Use 2.5ml of each solution to prepare a 5ml linear gradient with a gradient maker. Load the entire sample on the top of the gradient.

Spinning and fractioning: loaded gradients are spinned in a swinging-bucket rotor. Speed and time depend on the ranges of molecular weights (MW) and have to be optimized each time. Two standard conditions can be:

- CLASSICAL: 28000 rpm for 12hrs, 4˚C (high-medium MW)
- EXPANDED: 45000 rpm for 16hrs, 4˚C (low MW)

Gradients are recovered and fractioned in a variable number of fractions. For instance 5 ml gradients can give about 15 fractions of 350µl approx. Loading samples are prepared with 73µl of each fraction, 2µl of PMSF 0.1M and 25µl of LB4X. Separation is performed on 12% SDS-page loading 20-30µl of each sample.

Gradient calibration: To calibrate the gradient each fraction is tested for hemoglobin and LDH concentrations as follows:

- Hemoglobin: read at 409nm a 1:20 dilution in water of each fraction
- LDH: estimate the activity of LDH for 40'' at 340nm as follows
    - 865µl of 20mM K-phosphate pH 7.4
    - 100µl of 2mM NADH
    - 30µl of 10mM pyruvate
    - 5µl of fraction

Is possible to estimate roughly the molecular size of a protein/complex comparing with sedimentation behavior of known loading controls as hemoglobin (67Kda) and LDH (130Kda) (Martin *et al.* 1961; Barrientos *et al.* 2002).

4.3.12 Co-immunoprecipitation (CoIP) Analysis with HA Affinity Matrix

For CoIP studies an HA affinity matrix was used, consisting of purified HA.11 antibody immobilized on Sepharose™ beads (AFC-101P, Covance Inc.).

General protocol can be briefly summarized as follows:

Pre-cleaning: step required if starting from total mitochondria. If sucrose gradient fractions are used this can be avoided.

1. Pellet naked agarose beads (1/10 vol of the sample to process) 1000 rpm 1min 4˚C
2. Wash twice with 6 volumes of PBS pH 7.4
3. Add supernatant from mitochondrial protein solubilization (2-4mg)
4. Incubate 1hr, 4˚C in gently rotation

Binding:

1. Pellet appropriate volume of HA-beads and wash twice with PBS pH 7.4
2. Recover the supernatant from naked beads and transfer to HA-beads
3. Incubate 4hrs (up to o/n) at 4˚C, in gently rotation
4. Pellet beads at 1000 rpm 1 min 4˚C
5. Recover the supernatant (UNBOUND fraction)
6. Wash 4 times with PBS pH 7.4 (or with extraction buffer to lower stringency)

Elution: elution can be achieved in two ways.

1. Elution with SDS loading buffer 1X: this will remove all the proteins bound to the matrix but will also destroy physical interactions.
2. Competitive elution with HA peptide: a solution of HA peptide 400µg/ml in 50mM Tris-HCl (pH 7.5) 50mM NaCl, 1mM EDTA (pH 8) can be applied to the beads to release the HA-tagged proteins. This is a native elution that will not destroy interactions.

Volumes and timing have to be optimized. A standard condition can be 20-30 minutes in gently rotation at room temperature. Load equivalent quantities of UNBOUND and ELUTE fractions on SDS-page along with extraction control.

4.4 References

Barrientos A, Korr D and Tzagoloff A (2002). "Shy1p is necessary for full expression of mitochondrial COX1 in the yeast model of Leigh's syndrome." EMBO J **21**(1-2): 43-52.

Barros MH, Carlson CG, Glerum DM and Tzagoloff A (2001). "Involvement of mitochondrial ferredoxin and Cox15p in hydroxylation of heme O." FEBS Lett **492**(1-2): 133-138.

Brachmann CB, Davies A, Cost GJ, Caputo E, Li J, Hieter P and Boeke JD (1998). "Designer deletion strains derived from Saccharomyces cerevisiae S288C: a useful set of strains and plasmids for PCR-mediated gene disruption and other applications." Yeast **14**(2): 115-132.

Dower WJ, Miller JF and Ragsdale CW (1988). "High efficiency transformation of E. coli by high voltage electroporation." Nucleic Acids Res **16**(13): 6127-6145.

Fujiki Y, Hubbard AL, Fowler S and Lazarow PB (1982). "Isolation of intracellular membranes by means of sodium carbonate treatment: application to endoplasmic reticulum." J Cell Biol **93**(1): 97-102.

Giaever G, Chu AM, Ni L, Connelly C, Riles L, Veronneau S, . . . Johnston M (2002). "Functional profiling of the Saccharomyces cerevisiae genome." Nature **418**(6896): 387-391.

Gietz RD and Woods RA (2002). "Transformation of yeast by lithium acetate/single-stranded carrier DNA/polyethylene glycol method." Methods Enzymol **350**: 87-96.

Glick BS and Pon LA (1995). "Isolation of highly purified mitochondria from Saccharomyces cerevisiae." Methods Enzymol **260**: 213-223.

Hoffman CS and Winston F (1987). "A ten-minute DNA preparation from yeast efficiently releases autonomous plasmids for transformation of Escherichia coli." Gene **57**(2-3): 267-272.

Kaiser C, Michaelis S and Mitchell A (1994). Methods in yeast genetics: A Cold Spring Harbor Laboratory course manual. Cold Spring Harbor, NY, Cold Spring Harbor Laboratory Press

Laemmli UK (1970). "Cleavage of structural proteins during the assembly of the head of bacteriophage T4." Nature **227**(5259): 680-685.

Looke M, Kristjuhan K and Kristjuhan A (2011). "Extraction of genomic DNA from yeasts for PCR-based applications." Biotechniques **50**(5): 325-328.

Maniatis T, Fritsch E and Sambrook J (1982). Molecular cloning: A laboratory manual. Cold Spring Harbor, NY, Cold Spring Harbor Laboratory.

Martin RG and Ames BN (1961). "A method for determining the sedimentation behavior of enzymes: application to protein mixtures." J Biol Chem **236**: 1372-1379.

Rothstein RJ (1983). "One-step gene disruption in yeast." Methods Enzymol **101**: 202-211.

Schiestl RH and Gietz RD (1989). "High efficiency transformation of intact yeast cells using single stranded nucleic acids as a carrier." Curr Genet **16**(5-6): 339-346.

Tzagoloff A, Akai A and Needleman RB (1975). "Assembly of the mitochondrial membrane system. Characterization of nuclear mutants of Saccharomyces cerevisiae with defects in mitochondrial ATPase and respiratory enzymes." J Biol Chem **250**(20): 8228-8235.

Appendices

APPENDIX 1: Total list of 488 identified. Phenotypes in primary screening and filter parameter are reported.

ORF	GENE	ORF TYPE	Ethanol, 30°C	Ethanol, 37°C	FILTER
YAL002W	VPS8	VER	0	HS	**NEW**
YAL013W	DEP1	VER	MS	HS	**genome**
YAL021C	CCR4	VER	LS	LS	**NEW**
YAL039C	CYC3	VER	HS	HS	**genome**
YAL044C	GCV3	VER	MS	HS	**genome**
YAL046C	AIM1	VER	0	HS	**genome**
YAL047C	SPC72	VER	HS	HS	**genome**
YBL019W	APN2	VER	HS	HS	**genome**
YBL021C	HAP3	VER	HS	HS	**genome**
YBL031W	SHE1	VER	HS	HS	**genome**
YBL032W	HEK2	VER	HS	HS	**genome**
YBL036C		VER	HS	HS	**genome**
YBL038W	MRPL16	VER	HS	HS	**genome**
YBL045C	COR1	VER	HS	HS	**genome**
YBL046W	PSY4	VER	HS	HS	**genome**
YBL057C	PTH2	VER	HS	HS	**genome**
YBL079W	NUP170	VER	0	LS	**genome**
YBL080C	PET112	VER	HS	HS	**genome**
YBL082C	ALG3	VER	HS	HS	**genome**
YBL090W	MRP21	VER	HS	HS	**genome**
YBL099W	ATP1	VER	HS	HS	**genome**
YBR003W	COQ1	VER	HS	HS	**genome**
YBR021W	FUR4	VER	LS	HS	**NEW**
YBR026C	ETR1	VER	0	HS	**genome**
YBR044C	TCM62	VER	LS	MS	**pet only**
YBR081C	SPT7	VER	MS	MS	**NEW**
YBR084W	MIS1	VER	0	MS	**pet only**
YBR095C	RXT2	VER	LS	LS	**NEW**
YBR126C	TPS1	VER	0	MS	**NEW**
YBR127C	VMA2	VER	HS	HS	**genome**
YBR128C	ATG14	VER	HS	HS	**genome**
YBR146W	MRPS9	VER	HS	HS	**genome**
YBR179C	FZO1	VER	HS	HS	**genome**
YBR185C	MBA1	VER	LS	MS	**pet only**
YBR221C	PDB1	VER	LS	HS	**pet only**
YBR251W	MRPS5	VER	HS	HS	**genome**
YBR267W	REI1	VER	LS	0	**NEW**
YBR268W	MRPL37	VER	HS	HS	**genome**
YBR282W	MRPL27	VER	HS	HS	**genome**
YBR289W	SNF5	VER	MS	HS	**genome**
YBR298C	MAL31	VER	0	MS	**NEW**
YCL001W-A		UNC	0	LS	**genome**
YCL005W	LDB16	VER	0	MS	**NEW**
YCL008C	STP22	VER	0	HS	**NEW**
YCL010C	SGF29	VER	HS	HS	**genome**
YCR003W	MRPL32	VER	HS	HS	**genome**
YCR009C	RVS161	VER	0	HS	**genome**
YCR020C-A	MAK31	VER	LS	LS	**NEW**

ORF	GENE	ORF TYPE	Ethanol, 30°C	Ethanol, 37°C	FILTER
YCR024C	SLM5	VER	HS	HS	**genome**
YCR028C-A	RIM1	VER	HS	HS	**genome**
YCR046C	IMG1	VER	HS	HS	**genome**
YCR051W		UNC	0	LS	**NEW**
YCR077C	PAT1	VER	0	LS	**NEW**
YCR079W	PTC6	VER	0	LS	**pet only**
YDL005C	MED2	VER	MS	MS	**NEW**
YDL006W	PTC1	VER	0	HS	**genome**
YDL012C		VER	HS	HS	**genome**
YDL033C	SLM3	VER	HS	HS	**genome**
YDL039C	PRM7	VER	HS	HS	**genome**
YDL044C	MTF2	VER	HS	HS	**genome**
YDL045W-A	MRP10	VER	HS	HS	**genome**
YDL047W	SIT4	VER	MS	HS	**genome**
YDL056W	MBP1	VER	HS	HS	**genome**
YDL067C	COX9	VER	HS	HS	**genome**
YDL077C	VAM6	VER	HS	HS	**genome**
YDL088C	ASM4	VER	0	HS	**NEW**
YDL091C	UBX3	VER	HS	HS	**genome**
YDL104C	QRI7	VER	0	MS	**genome**
YDL119C		UNC	HS	HS	**genome**
YDL129W		UNC	HS	HS	**genome**
YDL157C		UNC	HS	HS	**genome**
YDL160C	DHH1	VER	LS	0	**genome**
YDL192W	ARF1	VER	HS	HS	**genome**
YDL198C	GGC1	VER	LS	HS	**genome**
YDL202W	MRPL11	VER	HS	LS	**genome**
YDL203C	ACK1	VER	0	LS	**NEW**
YDL204W	RTN2	VER	LS	LS	**NEW**
YDL232W	OST4	VER	0	MS	**NEW**
YDR005C	MAF1	VER	0	HS	**NEW**
YDR017C	KCS1	VER	LS	MS	**genome**
YDR065W	RRG1	VER	HS	HS	**genome**
YDR069C	DOA4	VER	0	HS	**genome**
YDR074W	TPS2	VER	LS	0	**NEW**
YDR079W	PET100	VER	HS	HS	**genome**
YDR114C		UNC	HS	HS	**genome**
YDR115W		UNC	HS	HS	**genome**
YDR116C	MRPL1	VER	HS	HS	**genome**
YDR129C	SAC6	VER	0	HS	**genome**
YDR140W	MTQ2	VER	0	LS	**NEW**
YDR162C	NBP2	VER	HS	HS	**NEW**
YDR175C	RSM24	VER	HS	HS	**genome**
YDR176W	NGG1	VER	MS	MS	**genome**
YDR178W	SDH4	VER	MS	0	**genome**
YDR194C	MSS116	VER	HS	HS	**genome**
YDR195W	REF2	VER	MS	HS	**genome**
YDR197W	CBS2	VER	HS	HS	**genome**
YDR202C	RAV2	VER	0	HS	**genome**
YDR204W	COQ4	VER	HS	HS	**genome**
YDR207C	UME6	VER	MS	HS	**NEW**
YDR226W	ADK1	VER	MS	MS	**genome**
YDR231C	COX20	VER	HS	HS	**genome**
YDR237W	MRPL7	VER	HS	HS	**genome**
YDR244W	PEX5	VER	HS	HS	**NEW**

ORF	GENE	ORF TYPE	Ethanol, 30°C	Ethanol, 37°C	FILTER
YDR264C	AKR1	VER	0	HS	**genome**
YDR270W	CCC2	VER	MS	MS	**genome**
YDR276C	PMP3	VER	0	HS	**NEW**
YDR293C	SSD1	VER	0	HS	**NEW**
YDR296W	MHR1	VER	HS	HS	**genome**
YDR298C	ATP5	VER	HS	HS	**genome**
YDR316W	OMS1	VER	0	LS	**genome**
YDR322W	MRPL35	VER	HS	HS	**genome**
YDR323C	PEP7	VER	MS	HS	**genome**
YDR332W	IRC3	VER	HS	HS	**genome**
YDR337W	MRPS28	VER	HS	HS	**genome**
YDR347W	MRP1	VER	HS	HS	**genome**
YDR349C	YPS7	VER	LS	MS	**NEW**
YDR350C	ATP22	VER	HS	HS	**genome**
YDR363W-A	SEM1	VER	0	MS	**NEW**
YDR368W	YPR1	VER	0	MS	**NEW**
YDR375C	BCS1	VER	HS	HS	**genome**
YDR388W	RVS167	VER	0	HS	**genome**
YDR403W	DIT1	VER	0	MS	**NEW**
YDR430C	CYM1	VER	0	MS	**genome**
YDR435C	PPM1	VER	0	HS	**NEW**
YDR443C	SSN2	VER	LS	LS	**NEW**
YDR458C	HEH2	VER	HS	HS	**genome**
YDR493W	MZM1	VER	HS	HS	**genome**
YDR495C	VPS3	VER	MS	HS	**genome**
YDR512C	EMI1	VER	MS	MS	**genome**
YDR523C	SPS1	VER	HS	HS	**genome**
YDR529C	QCR7	VER	HS	HS	**genome**
YEL007W		UNC	LS	MS	**NEW**
YEL024W	RIP1	VER	HS	HS	**genome**
YEL027W	VMA3	VER	HS	HS	**genome**
YEL038W	UTR4	VER	0	MS	**NEW**
YEL050C	RML2	VER	HS	HS	**genome**
YER050C	RSM18	VER	HS	HS	**genome**
YER058W	PET117	VER	HS	HS	**genome**
YER087W	AIM10	VER	MS	HS	**genome**
YER117W	RPL23B	VER	MS	HS	**NEW**
YER122C	GLO3	VER	HS	HS	**genome**
YER131W	RPS26B	VER	HS	HS	**genome**
YER145C	FTR1	VER	HS	HS	**genome**
YER154W	OXA1	VER	HS	HS	**genome**
YER155C	BEM2	VER	HS	HS	**genome**
YER178W	PDA1	VER	LS	HS	**pet only**
YFL025C	BST1	VER	LS	LS	**NEW**
YFL036W	RPO41	VER	HS	HS	**genome**
YFR019W	FAB1	VER	MS	HS	**genome**
YFR033C	QCR6	VER	0	MS	**pet only**
YGL012W	ERG4	VER	0	HS	**NEW**
YGL017W	ATE1	VER	HS	HS	**genome**
YGL045W	RIM8	VER	0	MS	**NEW**
YGL058W	RAD6	VER	LS	MS	**genome**
YGL062W	PYC1	VER	0	HS	**NEW**
YGL070C	RPB9	VER	HS	HS	**genome**
YGL071W	AFT1	VER	HS	HS	**genome**
YGL084C	GUP1	VER	0	LS	**genome**

ORF	GENE	ORF TYPE	Ethanol, 30°C	Ethanol, 37°C	FILTER
YGL095C	VPS45	VER	0	HS	**genome**
YGL129C	RSM23	VER	HS	HS	**genome**
YGL135W	RPL1B	VER	HS	HS	**genome**
YGL136C	MRM2	VER	LS	HS	**pet only**
YGL143C	MRF1	VER	HS	HS	**genome**
YGL167C	PMR1	VER	MS	HS	**genome**
YGL168W	HUR1	VER	HS	HS	**genome**
YGL173C	KEM1	VER	0	HS	**NEW**
YGL211W	NCS6	VER	0	MS	**NEW**
YGL212W	VAM7	VER	0	MS	**NEW**
YGL213C	SKI8	VER	0	LS	**NEW**
YGL226W	MTC3	VER	LS	LS	**genome**
YGL237C	HAP2	VER	HS	HS	**genome**
YGL244W	RTF1	VER	HS	HS	**genome**
YGL251C	HFM1	VER	LS	MS	**genome**
YGR036C	CAX4	VER	LS	0	**genome**
YGR062C	COX18	VER	HS	HS	**genome**
YGR076C	MRPL25	VER	HS	HS	**genome**
YGR084C	MRP13	VER	LS	MS	**pet only**
YGR092W	DBF2	VER	0	HS	**NEW**
YGR102C		VER	HS	HS	**genome**
YGR104C	SRB5	VER	LS	MS	**NEW**
YGR112W	SHY1	VER	HS	HS	**genome**
YGR127W		UNC	0	MS	**NEW**
YGR150C	CCM1	VER	HS	HS	**genome**
YGR155W	CYS4	VER	MS	HS	**genome**
YGR165W	MRPS35	VER	HS	HS	**genome**
YGR171C	MSM1	VER	HS	HS	**genome**
YGR174C	CBP4	VER	MS	HS	**genome**
YGR180C	RNR4	VER	HS	HS	**genome**
YGR183C	QCR9	VER	MS	HS	**genome**
YGR188C	BUB1	VER	MS	MS	**genome**
YGR200C	ELP2	VER	0	HS	**NEW**
YGR215W	RSM27	VER	HS	HS	**genome**
YGR220C	MRPL9	VER	HS	HS	**genome**
YGR222W	PET54	VER	HS	HS	**genome**
YGR229C	SMI1	VER	0	HS	**NEW**
YGR243W	FMP43	UNC	HS	HS	**genome**
YGR252W	GCN5	VER	0	MS	**genome**
YGR260W	TNA1	VER	0	HS	**NEW**
YHL012W		UNC	0	LS	**NEW**
YHL027W	RIM101	VER	0	HS	**NEW**
YHL038C	CBP2	VER	HS	HS	**genome**
YHR001W-A	QCR10	VER	0	MS	**pet only**
YHR006W	STP2	VER	HS	HS	**genome**
YHR008C	SOD2	VER	0	HS	**genome**
YHR009C		UNC	HS	HS	**genome**
YHR011W	DIA4	VER	HS	HS	**genome**
YHR013C	ARD1	VER	0	LS	**NEW**
YHR021C	RPS27B	VER	LS	LS	**NEW**
YHR026W	VMA16	VER	HS	HS	**genome**
YHR029C	YHI9	VER	MS	MS	**NEW**
YHR030C	SLT2	VER	0	MS	**NEW**
YHR038W	RRF1	VER	HS	HS	**genome**
YHR039C-A	VMA10	VER	MS	HS	**NEW**

ORF	GENE	ORF TYPE	Ethanol, 30°C	Ethanol, 37°C	FILTER
YHR041C	SRB2	VER	0	MS	**genome**
YHR049W	FSH1	VER	LS	LS	**NEW**
YHR051W	COX6	VER	HS	HS	**genome**
YHR067W	HTD2	VER	0	HS	**genome**
YHR091C	MSR1	VER	HS	HS	**genome**
YHR100C	GEP4	VER	LS	MS	**pet only**
YHR111W	UBA4	VER	0	MS	**NEW**
YHR116W	COX23	VER	HS	HS	**genome**
YHR120W	MSH1	VER	HS	HS	**genome**
YHR129C	ARP1	VER	0	MS	**NEW**
YHR147C	MRPL6	VER	HS	HS	**genome**
YHR168W	MTG2	VER	HS	HS	**genome**
YHR194W	MDM31	VER	0	MS	**genome**
YIL008W	URM1	VER	0	LS	**genome**
YIL039W	TED1	UNC	LS	MS	**NEW**
YIL093C	RSM25	VER	0	LS	**genome**
YIL157C	COA1	VER	HS	HS	**genome**
YIR021W	MRS1	VER	HS	HS	**genome**
YIR024C		VER	LS	LS	**genome**
YIR026C	YVH1	VER	LS	LS	**NEW**
YJL003W	COX16	VER	0	MS	**genome**
YJL063C	MRPL8	VER	HS	HS	**genome**
YJL095W	BCK1	VER	0	HS	**NEW**
YJL101C	GSH1	VER	0	MS	**genome**
YJL117W	PHO86	VER	MS	HS	**NEW**
YJL126W	NIT2	VER	0	HS	**NEW**
YJL131C	AIM23	VER	MS	MS	**genome**
YJL176C	SWI3	VER	LS	MS	**genome**
YJL183W	MNN11	VER	LS	MS	**NEW**
YJL189W	RPL39	VER	LS	LS	**NEW**
YJL209W	CBP1	VER	HS	HS	**genome**
YJR033C	RAV1	VER	0	HS	**NEW**
YJR040W	GEF1	VER	MS	HS	**genome**
YJR048W	CYC1	VER	LS	MS	**pet only**
YJR049C	UTR1	VER	0	LS	**NEW**
YJR074W	MOG1	VER	0	HS	**NEW**
YJR077C	MIR1	VER	HS	HS	**genome**
YJR079W		UNC	LS	MS	**NEW**
YJR102C	VPS25	VER	LS	HS	**genome**
YJR113C	RSM7	VER	HS	HS	**genome**
YJR120W		VER	HS	HS	**genome**
YJR121W	ATP2	VER	HS	HS	**genome**
YJR122W	IBA57	VER	HS	HS	**genome**
YJR144W	MGM101	VER	HS	HS	**genome**
YKL002W	DID4	VER	MS	HS	**genome**
YKL003C	MRP17	VER	HS	HS	**genome**
YKL006W	RPL14A	VER	LS	MS	**NEW**
YKL011C	CCE1	VER	0	MS	**NEW**
YKL016C	ATP7	VER	HS	HS	**genome**
YKL037W	AIM26	VER	MS	HS	**genome**
YKL054C	DEF1	VER	LS	HS	**genome**
YKL055C	OAR1	VER	HS	HS	**genome**
YKL067W	YNK1	VER	0	LS	**NEW**
YKL080W	VMA5	VER	HS	HS	**genome**
YKL087C	CYT2	VER	MS	HS	**genome**

ORF	GENE	ORF TYPE	Ethanol, 30°C	Ethanol, 37°C	FILTER
YKL109W	HAP4	VER	HS	HS	**genome**
YKL110C	KTI12	VER	0	MS	**NEW**
YKL134C	41183	VER	HS	HS	**genome**
YKL137W	CMC1	VER	MS	0	**genome**
YKL138C	MRPL31	VER	HS	HS	**genome**
YKL148C	SDH1	VER	0	MS	**genome**
YKL155C	RSM22	VER	HS	HS	**genome**
YKL167C	MRP49	VER	LS	MS	**genome**
YKL170W	MRPL38	VER	HS	HS	**genome**
YKL185W	ASH1	VER	LS	LS	**NEW**
YKL194C	MST1	VER	HS	HS	**genome**
YKL204W	EAP1	VER	0	MS	**NEW**
YKL208W	CBT1	VER	MS	HS	**genome**
YKL212W	SAC1	VER	LS	HS	**genome**
YKL213C	DOA1	VER	0	MS	**NEW**
YKR006C	MRPL13	VER	HS	HS	**genome**
YKR016W	FCJ1	VER	0	HS	**genome**
YKR035W-A	DID2	VER	0	MS	**NEW**
YKR052C	MRS4	VER	0	MS	**NEW**
YKR085C	MRPL20	VER	HS	HS	**genome**
YKR097W	PCK1	VER	LS	LS	**NEW**
YLL002W	RTT109	VER	LS	MS	**NEW**
YLL009C	COX17	VER	HS	HS	**genome**
YLL018C-A	COX19	VER	HS	HS	**genome**
YLL027W	ISA1	VER	HS	HS	**genome**
YLL033W	IRC19	VER	HS	HS	**genome**
YLL039C	UBI4	VER	0	HS	**NEW**
YLL041C	SDH2	VER	MS	MS	**genome**
YLL042C	ATG10	VER	HS	HS	**genome**
YLR015W	BRE2	VER	0	MS	**NEW**
YLR021W	IRC25	VER	0	LS	**NEW**
YLR025W	SNF7	VER	LS	HS	**genome**
YLR038C	COX12	VER	MS	HS	**genome**
YLR042C		UNC	0	MS	**NEW**
YLR055C	SPT8	VER	LS	LS	**NEW**
YLR056W	ERG3	VER	MS	HS	**genome**
YLR059C	REX2	VER	0	HS	**genome**
YLR067C	PET309	VER	HS	HS	**genome**
YLR069C	MEF1	VER	HS	HS	**genome**
YLR070C	XYL2	VER	HS	HS	**genome**
YLR079W	SIC1	VER	0	HS	**NEW**
YLR087C	CSF1	VER	LS	LS	**NEW**
YLR091W	GEP5	VER	HS	HS	**genome**
YLR114C	AVL9	VER	LS	HS	**genome**
YLR119W	SRN2	VER	LS	HS	**NEW**
YLR125W		UNC	HS	HS	**genome**
YLR139C	SLS1	VER	HS	HS	**genome**
YLR144C	ACF2	VER	HS	HS	**genome**
YLR148W	PEP3	VER	HS	HS	**genome**
YLR182W	SWI6	VER	LS	MS	**NEW**
YLR200W	YKE2	VER	0	HS	**NEW**
YLR201C	COQ9	VER	HS	HS	**genome**
YLR203C	MSS51	VER	HS	HS	**genome**
YLR218C	COA4	VER	MS	MS	**genome**
YLR260W	LCB5	VER	HS	HS	**genome**

ORF	GENE	ORF TYPE	Ethanol, 30°C	Ethanol, 37°C	FILTER
YLR270W	DCS1	VER	HS	HS	**genome**
YLR304C	ACO1	VER	LS	LS	**pet only**
YLR312W-A	MRPL15	VER	HS	HS	**genome**
YLR315W	NKP2	VER	0	HS	**NEW**
YLR320W	MMS22	VER	LS	MS	**NEW**
YLR357W	RSC2	VER	MS	HS	**NEW**
YLR362W	STE11	VER	0	HS	**NEW**
YLR377C	FBP1	VER	MS	MS	**genome**
YLR382C	NAM2	VER	HS	HS	**genome**
YLR384C	IKI3	VER	0	HS	**NEW**
YLR393W	ATP10	VER	HS	HS	**genome**
YLR417W	VPS36	VER	LS	HS	**NEW**
YLR439W	MRPL4	VER	HS	HS	**genome**
YML008C	ERG6	VER	0	MS	**genome**
YML009C	MRPL39	VER	0	HS	**pet only**
YML013W	UBX2	VER	0	MS	**NEW**
YML014W	TRM9	VER	0	MS	**NEW**
YML030W	AIM31	VER	0	MS	**genome**
YML061C	PIF1	VER	HS	HS	**genome**
YML081C-A	ATP18	VER	LS	LS	**genome**
YML087C	AIM33	VER	HS	HS	**genome**
YML112W	CTK3	VER	LS	HS	**genome**
YMR015C	ERG5	VER	HS	HS	**genome**
YMR021C	MAC1	VER	HS	HS	**genome**
YMR035W	IMP2	VER	HS	HS	**genome**
YMR054W	STV1	VER	0	MS	**genome**
YMR058W	FET3	VER	LS	MS	**genome**
YMR063W	RIM9	VER	MS	HS	**genome**
YMR064W	AEP1	VER	HS	HS	**genome**
YMR070W	MOT3	VER	HS	HS	**genome**
YMR072W	ABF2	VER	HS	HS	**genome**
YMR077C	VPS20	VER	HS	HS	**genome**
YMR097C	MTG1	VER	HS	HS	**genome**
YMR098C	ATP25	VER	HS	HS	**genome**
YMR116C	ASC1	VER	0	HS	**NEW**
YMR123W	PKR1	VER	MS	HS	**genome**
YMR125W	STO1	VER	0	HS	**NEW**
YMR142C	RPL13B	VER	LS	LS	**NEW**
YMR150C	IMP1	VER	HS	HS	**genome**
YMR154C	RIM13	VER	0	LS	**NEW**
YMR158W	MRPS8	VER	HS	HS	**genome**
YMR164C	MSS11	VER	0	HS	**NEW**
YMR179W	SPT21	VER	MS	LS	**NEW**
YMR188C	MRPS17	VER	HS	HS	**genome**
YMR193W	MRPL24	VER	HS	HS	**genome**
YMR198W	CIK1	VER	0	MS	**NEW**
YMR202W	ERG2	VER	LS	HS	**NEW**
YMR207C	HFA1	VER	0	HS	**genome**
YMR216C	SKY1	VER	LS	LS	**NEW**
YMR228W	MTF1	VER	HS	HS	**genome**
YMR231W	PEP5	VER	MS	HS	**genome**
YMR238W	DFG5	VER	LS	LS	**NEW**
YMR244C-A		UNC	MS	HS	**genome**
YMR256C	COX7	VER	HS	HS	**genome**
YMR257C	PET111	VER	HS	HS	**genome**

ORF	GENE	ORF TYPE	Ethanol, 30°C	Ethanol, 37°C	FILTER
YMR263W	SAP30	VER	0	LS	**genome**
YMR275C	BUL1	VER	0	HS	**NEW**
YMR282C	AEP2	VER	HS	HS	**genome**
YMR286W	MRPL33	VER	HS	HS	**genome**
YMR287C	DSS1	VER	HS	HS	**genome**
YMR293C	HER2	VER	HS	HS	**genome**
YMR312W	ELP6	VER	0	HS	**NEW**
YNL005C	MRP7	VER	HS	HS	**genome**
YNL052W	COX5A	VER	HS	HS	**genome**
YNL071W	LAT1	VER	LS	HS	**pet only**
YNL073W	MSK1	VER	HS	HS	**genome**
YNL079C	TPM1	VER	0	MS	**genome**
YNL081C	SWS2	VER	HS	HS	**genome**
YNL136W	EAF7	VER	0	HS	**NEW**
YNL159C	ASI2	VER	HS	HS	**genome**
YNL177C	MRPL22	VER	HS	HS	**genome**
YNL185C	MRPL19	VER	HS	HS	**genome**
YNL199C	GCR2	VER	LS	MS	**NEW**
YNL215W	IES2	VER	0	MS	**NEW**
YNL252C	MRPL17	VER	HS	HS	**genome**
YNL280C	ERG24	VER	HS	HS	**genome**
YNL298W	CLA4	VER	LS	HS	**NEW**
YNL320W		UNC	0	LS	**NEW**
YNR020C	ATP23	VER	HS	HS	**genome**
YNR037C	RSM19	VER	HS	HS	**genome**
YNR041C	COQ2	VER	HS	HS	**genome**
YNR045W	PET494	VER	HS	HS	**genome**
YNR052C	POP2	VER	MS	HS	**NEW**
YOL004W	SIN3	VER	LS	HS	**genome**
YOL008W	COQ10	VER	HS	HS	**genome**
YOL009C	MDM12	VER	HS	HS	**genome**
YOL012C	HTZ1	VER	0	LS	**NEW**
YOL023W	IFM1	VER	LS	MS	**genome**
YOL027C	MDM38	VER	MS	HS	**genome**
YOL033W	MSE1	VER	HS	HS	**genome**
YOL051W	GAL11	VER	HS	HS	**genome**
YOL071W	EMI5	VER	LS	MS	**genome**
YOL076W	MDM20	VER	0	HS	**genome**
YOL083W	ATG34	VER	HS	HS	**genome**
YOL087C		UNC	LS	MS	**NEW**
YOL091W	SPO21	VER	0	HS	**NEW**
YOL095C	HMI1	VER	HS	HS	**genome**
YOL096C	COQ3	VER	HS	HS	**genome**
YOL126C	MDH2	VER	0	LS	**NEW**
YOR014W	RTS1	VER	0	MS	**NEW**
YOR017W	PET127	VER	0	MS	**pet only**
YOR030W	DFG16	VER	0	MS	**NEW**
YOR036W	PEP12	VER	MS	HS	**genome**
YOR037W	CYC2	VER	LS	MS	**genome**
YOR065W	CYT1	VER	HS	HS	**genome**
YOR068C	VAM10	VER	0	MS	**NEW**
YOR106W	VAM3	VER	0	MS	**NEW**
YOR125C	CAT5	VER	HS	HS	**genome**
YOR127W	RGA1	VER	HS	HS	**genome**
YOR141C	ARP8	VER	0	HS	**genome**

ORF	GENE	ORF TYPE	Ethanol, 30°C	Ethanol, 37°C	FILTER
YOR150W	MRPL23	VER	HS	HS	**genome**
YOR155C	ISN1	VER	HS	HS	**genome**
YOR158W	PET123	VER	HS	HS	**genome**
YOR184W	SER1	VER	LS	MS	**NEW**
YOR187W	TUF1	VER	HS	HS	**genome**
YOR211C	MGM1	VER	HS	HS	**genome**
YOR221C	MCT1	VER	MS	HS	**genome**
YOR275C	RIM20	VER	0	HS	**NEW**
YOR286W	RDL2	VER	LS	0	**genome**
YOR322C	LDB19	VER	LS	MS	**NEW**
YOR323C	PRO2	VER	0	MS	**NEW**
YOR330C	MIP1	VER	HS	HS	**genome**
YOR334W	MRS2	VER	LS	MS	**genome**
YOR350C	MNE1	VER	MS	HS	**genome**
YOR358W	HAP5	VER	HS	HS	**genome**
YOR375C	GDH1	VER	HS	HS	**genome**
YPL002C	SNF8	VER	0	HS	**NEW**
YPL013C	MRPS16	VER	HS	HS	**genome**
YPL040C	ISM1	VER	HS	HS	**genome**
YPL051W	ARL3	VER	0	MS	**NEW**
YPL060W	MFM1	VER	MS	MS	**genome**
YPL065W	VPS28	VER	0	HS	**NEW**
YPL066W		UNC	LS	HS	**NEW**
YPL084W	BRO1	VER	0	HS	**NEW**
YPL086C	ELP3	VER	0	MS	**NEW**
YPL097W	MSY1	VER	HS	HS	**genome**
YPL101W	ELP4	VER	0	HS	**NEW**
YPL104W	MSD1	VER	HS	HS	**genome**
YPL118W	MRP51	VER	HS	HS	**genome**
YPL120W	VPS30	VER	0	MS	**NEW**
YPL132W	COX11	VER	HS	HS	**genome**
YPL148C	PPT2	VER	HS	HS	**genome**
YPL172C	COX10	VER	HS	HS	**genome**
YPL173W	MRPL40	VER	HS	HS	**genome**
YPL174C	NIP100	VER	MS	MS	**genome**
YPL178W	CBC2	VER	0	HS	**NEW**
YPL188W	POS5	VER	MS	HS	**genome**
YPL215W	CBP3	VER	HS	HS	**genome**
YPL259C	APM1	VER	0	LS	**NEW**
YPL262W	FUM1	VER	MS	MS	**genome**
YPL271W	ATP15	VER	HS	HS	**genome**
YPR020W	ATP20	VER	LS	HS	**pet only**
YPR024W	YME1	VER	LS	MS	**genome**
YPR029C	APL4	VER	LS	LS	**NEW**
YPR043W	RPL43A	VER	0	MS	**NEW**
YPR047W	MSF1	VER	HS	HS	**genome**
YPR051W	MAK3	VER	LS	MS	**NEW**
YPR066W	UBA3	VER	HS	HS	**genome**
YPR100W	MRPL51	VER	HS	HS	**genome**
YPR116W	RRG8	VER	HS	HS	**genome**
YPR131C	NAT3	VER	LS	LS	**NEW**
YPR133W-A	TOM5	VER	0	HS	**genome**
YPR134W	MSS18	VER	MS	HS	**genome**
YPR135W	CTF4	VER	LS	LS	**NEW**
YPR173C	VPS4	VER	0	HS	**NEW**

APPENDIX 2: List of 177 candidates with mitochondrial localization, presence of ortholog, original phenotypes, phenotypical classes and respiratory efficiency.

ORF	GENE	MITOC	ORTHOLOG	FILTER	CLASS	RESP EFF%
YPR116W	RRG8	**?**		genome	A	0
YDL157C		**mitoc**		genome	A	0
YDL088C	ASM4			NEW	A	0
YBL031W	SHE1			genome	A	1
YDL012C				genome	A	1
YDL091C	UBX3			genome	A	1
YHR009C				genome	A	1
YLR125W				genome	A	1
YML087C	AIM33	**?**		genome	A	1
YLR091W	GEP5	**mitoc**		genome	A	2
YCL010C	SGF29			genome	A	2
YDR114C				genome	A	2
YBL036C				genome	A	2
YDR458C	HEH2			genome	A	2
YDL129W				genome	A	2
YGR243W	FMP43	**mitoc**	YES	genome	A	2
YHR168W	MTG2	**mitoc**	YES	genome	A	2
YDR244W	PEX5		YES	NEW	A	2
YNL081C	SWS2	**mitoc**		genome	A	2
YDR115W		**mitoc**	YES	genome	A	3
YOL091W	SPO21			NEW	A	3
YLL033W	IRC19			genome	A	3
YER087W	AIM10	**mitoc**	YES	genome	A	3
YDL039C	PRM7			genome	A	3
YDR512C	EMI1			genome	A	4
YOL012C	HTZ1		YES	NEW	A	4
YHR013C	ARD1		YES	NEW	A	4
YLR362W	STE11			NEW	A	6
YJR120W				genome	A	8
YPL101W	ELP4		YES	NEW	A	8
YDL005C	MED2			NEW	A	8
YJR074W	MOG1		YES	NEW	A	9
YPR131C	NAT3		YES	NEW	A	11
YOL087C				NEW	A	12
YJL131C	AIM23	**mitoc**		genome	A	12
YIR024C		**mitoc**		genome	A	13
YDR074W	TPS2			NEW	A	14
YOR275C	RIM20		YES	NEW	A	14
YKL006W	RPL14A		YES	NEW	A	15
YDR332W	IRC3	**mitoc**		genome	A	15
YJL183W	MNN11			NEW	A	16
YGR092W	DBF2		YES	NEW	A	17
YLR087C	CSF1	**mitoc**		NEW	A	18
YIL039W	TED1			NEW	A	21
YDR065W	RRG1	**mitoc**		genome	A	25
YHR021C	RPS27B		YES	NEW	A	26
YLR055C	SPT8			NEW	A	27
YCR051W			YES	NEW	A	28
YHR030C	SLT2			NEW	A	37
YNL199C	GCR2			NEW	A	41
YDR202C	RAV2			genome	A	76

ORF	GENE	MITOC	ORTHOLOG	FILTER	CLASS	RESP EFF%
YDR493W	MZM1	**mitoc**		genome	A	87
YNL136W	EAF7		YES	NEW	B	8
YPL178W	CBC2		YES	NEW	B	11
YGR104C	SRB5			NEW	B	13
YJL189W	RPL39		YES	NEW	B	16
YMR116C	ASC1		YES	NEW	B	18
YHL027W	RIM101			NEW	B	19
YDR207C	UME6			NEW	B	21
YPL084W	BRO1		YES	NEW	B	23
YML030W	AIM31	**mitoc**	YES	genome	B	23
YDR435C	PPM1		YES	NEW	B	23
YLR200W	YKE2		YES	NEW	B	24
YPR051W	MAK3		YES	NEW	B	24
YPR043W	RPL43A		YES	NEW	B	24
YJL095W	BCK1		YES	NEW	B	25
YNL215W	IES2			NEW	B	25
YKL011C	CCE1	**mitoc**		NEW	B	25
YNR052C	POP2		YES	NEW	B	25
YCR077C	PAT1		YES	NEW	B	26
YMR063W	RIM9			genome	B	27
YLR079W	SIC1			NEW	B	29
YMR312W	ELP6			NEW	B	29
YGR200C	ELP2		YES	NEW	B	30
YKL204W	EAP1			NEW	B	31
YOR014W	RTS1		YES	NEW	B	31
YLL002W	RTT109			NEW	B	31
YGL173C	KEM1		YES	NEW	B	32
YKR052C	MRS4	**mitoc**	YES	NEW	B	32
YHR111W	UBA4		YES	NEW	B	33
YIR026C	YVH1		YES	NEW	B	33
YLR021W	IRC25			NEW	B	36
YOR106W	VAM3			NEW	B	37
YLR182W	SWI6			NEW	B	38
YOR030W	DFG16			NEW	B	41
YEL038W	UTR4			NEW	B	41
YPL065W	VPS28		YES	NEW	B	41
YML014W	TRM9			NEW	B	43
YHR029C	YHI9			NEW	B	45
YLL039C	UBI4		YES	NEW	B	46
YDR005C	MAF1		YES	NEW	B	46
YPL086C	ELP3		YES	NEW	B	50
YGL168W	HUR1			genome	B	51
YDR162C	NBP2			NEW	B	51
YBR021W	FUR4			NEW	B	51
YMR164C	MSS11			NEW	B	56
YKL213C	DOA1		YES	NEW	B	57
YCL005W	LDB16	**mitoc**		NEW	B	57
YDR363W-A	SEM1			NEW	B	61
YOR323C	PRO2		YES	NEW	B	62
YLR315W	NKP2			NEW	B	65
YCL008C	STP22		YES	NEW	B	67
YML013W	UBX2			NEW	B	67
YMR142C	RPL13B		YES	NEW	B	70
YKL002W	DID4		YES	genome	B	74
YDR316W	OMS1	**mitoc**		genome	C	17

ORF	GENE	MITOC	ORTHOLOG	FILTER	CLASS	RESP EFF%
YBR095C	RXT2			NEW	C	31
YHR129C	ARP1		YES	NEW	C	32
YLR384C	IKI3		YES	NEW	C	36
YMR216C	SKY1		YES	NEW	C	37
YCR020C-A	MAK31			NEW	C	38
YMR179W	SPT21			NEW	C	38
YDR140W	MTQ2		YES	NEW	C	40
YKL110C	KTI12		YES	NEW	C	41
YMR125W	STO1			NEW	C	43
YHR039C-A	VMA10		YES	NEW	C	44
YMR202W	ERG2		YES	NEW	C	46
YLR417W	VPS36			NEW	C	46
YPL002C	SNF8		YES	NEW	C	49
YJR079W		**mitoc**		NEW	C	49
YDR495C	VPS3			genome	C	50
YDL232W	OST4			NEW	C	50
YGL045W	RIM8			NEW	C	51
YBR267W	REI1		YES	NEW	C	52
YEL007W				NEW	C	53
YGR260W	TNA1			NEW	C	55
YMR275C	BUL1			NEW	C	56
YBR081C	SPT7			NEW	C	57
YKL037W	AIM26	**?**		genome	C	57
YLR357W	RSC2			NEW	C	57
YDL204W	RTN2			NEW	C	57
YMR244C-A			YES	genome	C	58
YJL126W	NIT2		YES	NEW	C	58
YHL012W			YES	NEW	C	59
YGR229C	SMI1			NEW	C	59
YLR042C				NEW	C	61
YGL226W	MTC3	**mitoc**		genome	C	63
YMR238W	DFG5			NEW	C	66
YGL212W	VAM7		YES	NEW	C	66
YNL320W		**mitoc**	YES	NEW	C	68
YPR135W	CTF4			NEW	C	68
YMR154C	RIM13			NEW	C	68
YDR403W	DIT1			NEW	C	70
YOR322C	LDB19			NEW	C	72
YPR029C	APL4		YES	NEW	C	75
YPL051W	ARL3		YES	NEW	C	76
YDR276C	PMP3			NEW	C	78
YKL067W	YNK1		YES	NEW	C	78
YGL213C	SKI8			NEW	C	79
YPR173C	VPS4		YES	NEW	C	79
YLR320W	MMS22			NEW	C	79
YAL021C	CCR4		YES	NEW	C	79
YPL120W	VPS30		YES	NEW	C	83
YNL298W	CLA4		YES	NEW	C	85
YFL025C	BST1		YES	NEW	C	87
YOR286W	RDL2	**mitoc**		genome	D	57
YLR015W	BRE2			NEW	D	65
YBR126C	TPS1			NEW	D	67
YJR033C	RAV1			NEW	D	73
YAL002W	VPS8			NEW	D	76
YGL012W	ERG4		YES	NEW	D	80

ORF	GENE	MITOC	ORTHOLOG	FILTER	CLASS	RESP EFF%
YGL211W	NCS6	**mitoc**	YES	NEW	D	81
YDR368W	YPR1		YES	NEW	D	82
YKR097W	PCK1			NEW	D	82
YOL126C	MDH2		YES	NEW	D	83
YDR443C	SSN2			NEW	D	84
YHR049W	FSH1		YES	NEW	D	86
YJL117W	PHO86			NEW	D	87
YLR119W	SRN2			NEW	D	87
YDR349C	YPS7			NEW	D	87
YKR035W-A	DID2		YES	NEW	D	91
YDL119C		**mitoc**	YES	genome	D	106
YER117W	RPL23B		YES	NEW	D	111
YPL259C	APM1		YES	NEW	D	117
YAL046C	AIM1	**?**	YES	genome	D	121
YCL001W-A				genome	D	129
YOR068C	VAM10			NEW	D	263

APPENDIX 3: List of 10 gene whose deletion caused EtOH specific phenotype.

ORF	GENE	MITOC	ORTHOLOG	FILTER	OXPHOS
YBR298C	MAL31			NEW	EtOH SPECIFIC
YDL203C	ACK1	**mitoc**		NEW	EtOH SPECIFIC
YDR293C	SSD1		YES	NEW	EtOH SPECIFIC
YGL062W	PYC1		YES	NEW	EtOH SPECIFIC
YGR127W			YES	NEW	EtOH SPECIFIC
YJR049C	UTR1		YES	NEW	EtOH SPECIFIC
YKL185W	ASH1			NEW	EtOH SPECIFIC
YMR198W	CIK1			NEW	EtOH SPECIFIC
YOR184W	SER1		YES	NEW	EtOH SPECIFIC
YPL066W				NEW	EtOH SPECIFIC

APPENDIX 4: Total results of GO Term Finder analysis applied total list of 488 genes.

GO TERM	BIOLOGICAL PROCESS	p-value	genes
GO:0007005	mitochondrion organization	6.45E-75	146
GO:0032543	mitochondrial translation	1.84E-56	83
GO:0006996	organelle organization	4.38E-33	220
GO:0071842	cellular component organization at cellular level	7.16E-30	242
GO:0016043	cellular component organization	7.13E-25	256
GO:0097034	mitochondrial respiratory chain complex IV biogenesis	1.71E-16	18
GO:0070271	protein complex biogenesis	2.14E-15	59
GO:0071841	cellular component organization or biogenesis at cellular level	5.10E-15	250
GO:0045333	cellular respiration	7.58E-15	38
GO:0033108	mitochondrial respiratory chain complex assembly	8.80E-15	19
GO:0071840	cellular component organization or biogenesis	1.33E-14	260
GO:0000959	mitochondrial RNA metabolic process	2.27E-13	17
GO:0000002	mitochondrial genome maintenance	1.10E-11	19
GO:0006461	protein complex assembly	1.16E-11	51
GO:0071822	protein complex subunit organization	2.12E-10	53
GO:0006412	translation	3.33E-10	109
GO:0043623	cellular protein complex assembly	3.63E-10	41
GO:0033617	mitochondrial respiratory chain complex IV assembly	3.82E-10	11
GO:0015980	energy derivation by oxidation of organic compounds	6.04E-10	39
GO:0042773	ATP synthesis coupled electron transport	7.98E-10	15
GO:0042775	mitochondrial ATP synthesis coupled electron transport	7.98E-10	15
GO:0006119	oxidative phosphorylation	1.53E-09	15
GO:0019538	protein metabolic process	1.89E-09	204
GO:0044267	cellular protein metabolic process	2.02E-09	194
GO:0070127	tRNA aminoacylation for mitochondrial protein translation	3.65E-09	10
GO:0008535	respiratory chain complex IV assembly	3.92E-09	11
GO:0022904	respiratory electron transport chain	5.05E-09	15
GO:0009060	aerobic respiration	5.81E-09	26
GO:0010821	regulation of mitochondrion organization	5.36E-08	11
GO:0070129	regulation of mitochondrial translation	8.09E-08	10
GO:0044249	cellular biosynthetic process	9.09E-08	241
GO:0017004	cytochrome complex assembly	9.11E-08	8
GO:0010822	positive regulation of mitochondrion organization	1.02E-07	9
GO:0070131	positive regulation of mitochondrial translation	1.02E-07	9
GO:0043038	amino acid activation	1.03E-07	16
GO:0043039	tRNA aminoacylation	1.03E-07	16
GO:0009058	biosynthetic process	1.42E-07	243
GO:0006091	generation of precursor metabolites and energy	3.03E-07	42
GO:0007035	vacuolar acidification	3.51E-07	12
GO:0045851	pH reduction	3.51E-07	12
GO:0051452	intracellular pH reduction	3.51E-07	12
GO:0043162	ubiquitin-dependent protein catabolic process via the MVB pathway	3.96E-07	11
GO:0030641	regulation of cellular pH	5.84E-07	12
GO:0051453	regulation of intracellular pH	5.84E-07	12
GO:0065003	macromolecular complex assembly	2.19E-06	64
GO:0034220	ion transmembrane transport	2.31E-06	18
GO:0000372	Group I intron splicing	2.72E-06	7
GO:0000376	RNA splicing, via transesterification reactions	2.72E-06	7
GO:0097033	mitochondrial respiratory chain complex III biogenesis	2.72E-06	7
GO:0015992	proton transport	3.05E-06	14
GO:0002097	tRNA wobble base modification	3.18E-06	11
GO:0002098	tRNA wobble uridine modification	3.18E-06	11
GO:0006885	regulation of pH	3.46E-06	12
GO:0006818	hydrogen transport	4.23E-06	14

GO:0030004	cellular monovalent inorganic cation homeostasis	4.81E-06	13
GO:0006122	mitochondrial electron transport, ubiquinol to cytochrome c	6.95E-06	7
GO:0006418	tRNA aminoacylation for protein translation	9.37E-06	13
GO:0010557	positive regulation of macromolecule biosynthetic process	1.11E-05	41

GO TERM	CELLULAR COMPONENT	p-value	genes
GO:0044429	mitochondrial part	4.21E-78	191
GO:0005739	mitochondrion	2.78E-58	242
GO:0005759	mitochondrial matrix	2.64E-57	102
GO:0000313	organellar ribosome	3.35E-44	58
GO:0005761	mitochondrial ribosome	3.35E-44	58
GO:0005743	mitochondrial inner membrane	4.43E-32	80
GO:0019866	organelle inner membrane	5.95E-32	82
GO:0005740	mitochondrial envelope	1.61E-28	102
GO:0044444	cytoplasmic part	1.04E-27	349
GO:0000315	organellar large ribosomal subunit	4.27E-26	32
GO:0005762	mitochondrial large ribosomal subunit	4.27E-26	32
GO:0031966	mitochondrial membrane	1.73E-24	92
GO:0043226	organelle	6.04E-21	427
GO:0043229	intracellular organelle	6.04E-21	427
GO:0031967	organelle envelope	9.02E-21	108
GO:0031975	envelope	9.02E-21	108
GO:0043227	membrane-bounded organelle	7.10E-19	406
GO:0043231	intracellular membrane-bounded organelle	7.10E-19	406
GO:0005840	ribosome	8.69E-18	68
GO:0000314	organellar small ribosomal subunit	1.75E-17	23
GO:0005763	mitochondrial small ribosomal subunit	1.75E-17	23
GO:0005737	cytoplasm	8.29E-17	408
GO:0044422	organelle part	1.14E-16	317
GO:0044446	intracellular organelle part	1.14E-16	317
GO:0044455	mitochondrial membrane part	4.84E-16	46
GO:0031974	membrane-enclosed lumen	1.62E-13	155
GO:0015934	large ribosomal subunit	2.39E-12	38
GO:0005746	mitochondrial respiratory chain	1.63E-11	16
GO:0070469	respiratory chain	4.10E-11	17
GO:0043233	organelle lumen	1.05E-10	142
GO:0070013	intracellular organelle lumen	1.05E-10	142
GO:0031090	organelle membrane	1.17E-10	144
GO:0032991	macromolecular complex	1.87E-09	221
GO:0015935	small ribosomal subunit	1.02E-08	27
GO:0005622	intracellular	4.76E-08	457
GO:0044424	intracellular part	1.21E-07	455
GO:0016469	proton-transporting two-sector ATPase complex	1.10E-06	13
GO:0044440	endosomal part	1.25E-06	22
GO:0005758	mitochondrial intermembrane space	1.28E-06	15
GO:0005750	mitochondrial respiratory chain complex III	2.19E-06	7
GO:0045275	respiratory chain complex III	2.19E-06	7
GO:0031970	organelle envelope lumen	5.69E-06	15
GO:0033588	Elongator holoenzyme complex	1.96E-05	5
GO:0005768	endosome	3.69E-05	26
GO:0016602	CCAAT-binding factor complex	4.34E-05	4
GO:0009295	nucleoid	6.26E-05	9
GO:0042645	mitochondrial nucleoid	6.26E-05	9

APPENDIX 5: Total results of GO Slim Mapper analysis applied total list of 488 genes

GOID	GO term		Gene(s)
8150	biological process unknown	34	AIM1, YBL036C, YCL001W-A, LDB16, YCR051W, YDL012C, UBX3, YDL129W, YDL157C, RTN2, YDR114C, OMS1, IRC3, HEH2, MIT1, AIM10, MTC3, FMP43, YHL012W, FSH1, YIR024C, NIT2, AIM23, YJR079W, YLR042C, YLR125W, NKP2, AIM31, AIM33, YMR244C-A, IES2, YNL320W, YOL087C, RDL2
6366	transcription from RNA polymerase II promoter	27	CCR4, RXT2, SGF29, MED2, UME6, SSN2, EMI1, SRB5, ELP2, RIM101, KTI12, RTT109, SPT8, SWI6, RSC2, IKI3, VPS36, MSS11, SPT21, ELP6, EAF7, GCR2, POP2, HTZ1, SNF8, ELP3, ELP4
42221	response to chemical stimulus	16	UME6, YPR1, SSN2, RIM101, YHI9, SLT2, UBA4, BCK1, SWI6, STE11, VPS36, ASC1, SKY1, CLA4, SNF8, BRO1
6605	protein targeting	15	VPS8, STP22, PEX5, VPS3, SLT2, MOG1, DID2, SRN2, VPS36, SKY1, MDH2, SNF8, VPS28, BRO1, VPS30
70271	protein complex biogenesis	12	SPT7, RAV2, PEX5, SEM1, PPM1, MZM1, EMI1, SKI8, RAV1, IRC25, YKE2, VPS4
51603	proteolysis involved in cellular protein catabolic process	12	STP22, SEM1, BST1, DID4, DOA1, SRN2, VPS36, UBX2, SNF8, VPS28, BRO1, VPS30
7005	mitochondrion organization	11	RRG1, YDR115W, MZM1, EMI1, YJR120W, CCE1, GEP5, BUL1, SWS2, RRG8, NAT3
278	mitotic cell cycle	11	CCR4, SHE1, REI1, XRN1, SMI1, ARP1, SIC1, SWI6, CLA4, RTS1, CTF4
43934	sporulation	10	DIT1, EMI1, RIM101, YVH1, IRC19, UBI4, RIM9, SWS2, SPO21, RIM20
5975	carbohydrate metabolic process	9	TPS1, OST4, TPS2, YPR1, MNN11, PCK1, MSS11, GCR2, MDH2
9451	RNA modification	9	NCS6, ELP2, UBA4, KTI12, IKI3, TRM9, ELP6, ELP3, ELP4
16197	endosome transport	9	VPS8, STP22, TDA3, RAV1, DID4, DID2, BRO1, VPS30, VPS4
51321	meiotic cell cycle	9	UME6, RIM8, SKI8, RIM101, YVH1, SWI6, MMS22, SPO21, RTS1
71554	cell wall organization or biogenesis	9	YPS7, DIT1, SMI1, RIM101, SLT2, YVH1, STE11, DFG5, SPO21
8033	tRNA processing	9	NCS6, ELP2, UBA4, KTI12, IKI3, TRM9, ELP6, ELP3, ELP4
43543	protein acylation	9	SPT7, SGF29, MAK31, ARD1, RTT109, SPT8, EAF7, MAK3, NAT3
51726	regulation of cell cycle	8	CCR4, UME6, SEM1, XRN1, SMI1, SIC1, CLA4, RTS1
6325	chromatin organization	8	SPT7, SGF29, ARD1, RTT109, BRE2, SPT8, RSC2, EAF7
6468	protein phosphorylation	8	NBP2, DBF2, SLT2, BCK1, SIC1, STE11, SKY1, CLA4
6401	RNA catabolic process	8	CCR4, PAT1, XRN1, SKI8, IRC25, STO1, POP2, HTZ1
18193	peptidyl-amino acid modification	8	SPT7, SGF29, ARD1, RTT109, BRE2, SPT8, EAF7, NAT3
6873	cellular ion homeostasis	8	RRG1, RAV2, PMP3, VPS3, DBF2, VMA10, RAV1, SKY1
23052	signaling	8	YHI9, SLT2, YVH1, BCK1, SWI6, STE11, ASC1, CLA4
6397	mRNA processing	7	CCR4, SLT2, SWI6, STO1, SKY1, POP2, CBC2

6974	response to DNA damage stimulus	7	YNK1, DOA1, RTT109, MMS22, RSC2, EAF7, CTF4
16570	histone modification	7	SPT7, SGF29, ARD1, RTT109, BRE2, SPT8, EAF7
2181	cytoplasmic translation	7	RPL23B, RPS27B, MTG2, RPL39, RPL14A, RPL13B, RPL43A
1403	invasive growth in response to glucose limitation	7	RXT2, RIM8, UBA4, STE11, ASC1, MSS11, RIM20
70647	protein modification by small protein conjugation or removal	7	NCS6, ELP2, UBA4, UBI4, BUL1, ELP6, BRO1
6281	DNA repair	6	DOA1, RTT109, MMS22, RSC2, EAF7, CTF4
6629	lipid metabolic process	6	UME6, BST1, ERG4, ERG2, VPS30, VPS4
51169	nuclear transport	6	REI1, ASM4, SEM1, SLT2, MOG1, SKY1
7124	pseudohyphal growth	6	UME6, UBA4, STE11, MSS11, DFG5, DFG16
48193	Golgi vesicle transport	6	BST1, TED1, PHO86, ARL3, APM1, APL4
10324	membrane invagination	5	RIM8, VAM7, VAM3, LDB19, VPS30
7033	vacuole organization	5	VPS3, VAM7, CLA4, VAM10, VAM3
7059	chromosome segregation	5	PAT1, MMS22, RSC2, RTS1, CTF4
16050	vesicle organization	5	BST1, VAM7, DID4, VAM3, VPS4
7031	peroxisome organization	5	PEX5, SLT2, BCK1, MDH2, VPS30
8380	RNA splicing	4	MRS4, STO1, SKY1, CBC2
55085	transmembrane transport	4	FUR4, SLT2, SKY1, CLA4
746	conjugation	4	SPT7, RXT2, PRM7, STE11
6310	DNA recombination	4	SKI8, IRC19, MMS22, CTF4
6260	DNA replication	4	CCR4, HUR1, MMS22, CTF4
7114	cell budding	4	REI1, UBA4, DFG5, CLA4
48308	organelle inheritance	4	VPS3, BUL1, CLA4, NAT3
15931	nucleobase-containing compound transport	4	FUR4, ASM4, SEM1, TNA1
51604	protein maturation	4	RIM8, RIM13, DFG16, RIM20
6417	regulation of translation	4	PAT1, MTQ2, EAP1, ASC1
7010	cytoskeleton organization	3	SHE1, ARP1, NAT3
31399	regulation of protein modification process	3	NBP2, SIC1, STE11

6970	response to osmotic stress	3	NBP2, STE11, STO1
42594	response to starvation	3	SIC1, VAM3, VPS30
910	cytokinesis	3	RIM101, SLT2, CLA4
8213	protein alkylation	3	MTQ2, PPM1, BRE2
6091	generation of precursor metabolites and energy	3	YJR120W, CSF1, GCR2
6811	ion transport	3	PMP3, PHO86, MRS4
6354	transcription elongation, DNA-dependent	3	CCR4, RSC2, POP2
51049	regulation of transport	3	SLT2, PHO86, SKY1
9408	response to heat	3	ASM4, NBP2, STE11
61025	membrane fusion	3	VAM7, VAM10, VAM3
6352	transcription initiation, DNA-dependent	2	MED2, SRB5
6869	lipid transport	2	YJR120W, CLA4
6486	protein glycosylation	2	OST4, MNN11
6520	cellular amino acid metabolic process	2	UTR4, PRO2
70925	organelle assembly	2	RPS27B, YVH1
6979	response to oxidative stress	2	YPR1, UBA4
32196	transposition	2	RTT109, STE11
6457	protein folding	2	PHO86, YKE2
42255	ribosome assembly	2	RPS27B, YVH1
32543	mitochondrial translation	2	YDR115W, SWS2
9311	oligosaccharide metabolic process	2	TPS1, TPS2
6470	protein dephosphorylation	2	YVH1, RTS1
6364	rRNA processing	2	XRN1, RPS27B
6897	endocytosis	2	RIM8, LDB19
48285	organelle fission	2	DBF2, CTF4
42273	ribosomal large subunit biogenesis	2	REI1, YVH1
48284	organelle fusion	2	VAM7, VAM3
6413	translational initiation	1	PAT1
42274	ribosomal small subunit biogenesis	1	RPS27B
6997	nucleus organization	1	ASM4
6887	exocytosis	1	SEM1

45333	cellular respiration	1	YJR120W
6383	transcription from RNA polymerase III promoter	1	MAF1
51052	regulation of DNA metabolic process	1	CCR4
55086	nucleobase-containing small molecule metabolic process	1	YNK1
32200	telomere organization	1	BRE2

APPENDIX 6: Primer used in *YIR024C* characterization

Primer	Sequence 5'-3'	Used For
FWYIR024c	GGGCGAATTCGCCGTCTAGTAACTGACTGGCTG	cassette transf.
RVYIR024c	GGGCGGATCCCCCTCTAATACATCTTCACCAAG	cassette transf.
A1YIR024c	CCTTCCGCGTTTTGAGCTCGTG	cassette transf.
K3	GGAGAAAACTCACCGAGGC	cassette transf.
Y024CFWBam	CGCGGGATCCCGTGCTGCCTGAAGTCTTCCTC	tagging
Y024CHA3RVPst	GCGCCTGCAGTCAAGCGTAATCTGGAACATCGTATGGGTAAGC GTAATCTGGAACATCGTATGGGTAAGCGTAATCTGGAACATCGT ATGGGTATAGAAATTTTGGGATTTTATCATGTTCTTTGGC	tagging